GROUP CONTRIBUTION WITH ASSOCIATION EQUATION OF STATE FOR RAPID EXPANSION OF SUPERCRITICAL SOLUTION OF DOXORUBICIN BY USING MODIFIED CO-SOLVENT

MISS PLOYPETCH PRISSAWONG

A SPECIAL RESEARCH PROJECT SUBMITTED IN PARTIAL FULFILLMENT OF
THE REQUIREMENTS FOR THE DEGREE OF MASTER OF ENGINEERING
FACULTY OF ENGINEERING
KING MONGKUT’S UNIVERSITY OF TECHNOLOGY THONBURI
2011

Group Contribution with Association Equation of State for Rapid Expansion of Supercritical Solution of Doxorubicin by using modified co-solvent

Miss Ploypetch Prissawong B.Eng. (Chemical Engineering)

A Special Research Project Submitted in Partial Fulfillment of the Requirements for
the Degree of Master of Engineering (Chemical Engineering)
Faculty of Engineering
King Mongkut's University of Technology Thonburi
2011

Special Research Project Committee

………………………………………………….. Chairman of special Research Project
(Assoc. Prof. Apichai Therdthianwong, Ph.D.)

………………………………………………….. Member and Special Research Advisor
(Assoc. Prof. Thongchai Srinophakun, Ph.D.)

………………………………………………….. Member
(Asst. Prof. Kwanchanok Pasuwat, Ph.D.)

Copyright reserved

Special Research Project Title	Group Contribution with Association Equation of State for Rapid Expansion of Supercritical Solution of Doxorubicin by using modified co-solvent
Special Research Project Credits	6
Candidate	Miss Ploypetch Prissawong
Special Research Project Advisor	Assoc. Prof. Dr. Thongchai Srinophakun
Program	Master of Engineering
Field of Study	Chemical Engineering
Department	Chemical Engineering
Faculty	Engineering
B.E.	2554

Abstract

Rapid Expansion of Supercritical Solution (RESS) is a recently developed micronization technique in pharmaceutical industries. The mathematical process model was developed to consider solubility Doxorubicin (DOX) in supercritical carbon dioxide with methanol as a modified co-solvent and particle formation. Group Contribution with Association Equation of State (GCA-EoS) is used to predict the solubility of DOX because of the complex of molecular structures. The additional 3, 4, and 5 mole percentage of methanol were mixed into pure supercritical carbon dioxide. The solubility of DOX was determined at the extraction temperature and pressure range of 308.15 – 323.15 K, and 80 – 300 bar due to the limitation of DOX degradation temperature and GCA-EoS model. Results from the mathematical model indicated that the solubility of DOX in modified co-solvent is much higher than that in pure supercritical carbon dioxide. For the particle formation section, the mathematical model of flow field in expansion section consists of mass, momentum, and energy balance correlated to an extended generalized Bender equation of state (egB-EoS). The flow was assumed to be steady state, one-dimensional, and adiabatic. In addition, the assumption of flow model considered only the solvent phase as a vapor phase of mixed carbon dioxide and methanol. The model considers the effect of pre-expansion temperature (333.13 – 343.15 K), pre-expansion pressure (175 – 225 bar), and co-solvent concentration (3 – 5 mole percentage of methanol) which are chosen from extraction condition. However, the pre-expansion temperature should be higher than the extraction temperature in order to prevent phase changes of the solution and plugging due to precipitation along the capillary nozzle region. The results show that particle formation mainly occurs in supersonic free jet. The results of 338.15 K, 200 bar, and 3 percentage mole of methanol indicate that the nucleation rate of DOX is about 10^{24} particles/cm^{3}s, whereas the number of concentration of critical nuclei is about 10^{22} particles/cm^3 with the nanometer scale of particle at approximately 1.7 nanometer.

Keywords: RESS process/ Doxorubicin (DOX)/ Group Contribution with Association Equation of State (GCA-EoS)/ Micronization/ Particle formation

หัวข้อโครงการศึกษาวิจัย	การศึกษากระบวนการขยายตัวอย่างรวดเร็วของด๊อกโซรูบิซินในสารละลายผสมเหนือวิกฤตโดยใช้สมการสภาวะการกระจายตัวและการรวมตัวแบบกลุ่ม
หน่วยกิต	6
ผู้เขียน	นางสาวพลอยเพชร ปริศวงศ์
อาจารย์ที่ปรึกษา	รศ.ดร.ธงไชย ศรีนพคุณ
หลักสูตร	วิศวกรรมศาสตรมหาบัณฑิต
สาขาวิชา	วิศวกรรมเคมี
ภาควิชา	วิศวกรรมเคมี
คณะ	วิศวกรรมศาสตร์
พ.ศ.	2554

บทคัดย่อ

ปัจจุบันแบบจำลองกระบวนการขยายตัวอย่างรวดเร็วของสารละลายเหนือวิกฤต (RESS) เป็นเทคนิคที่พัฒนาขึ้นสำหรับการทำอนุภาคให้มีขนาดเล็กระดับไมครอนในอุตสาหกรรมยา แบบจำลองกระบวนการทางคณิตศาสตร์ถูกพัฒนาขึ้นเพื่อพิจารณาการละลายของด๊อกโซรูบิซิน (DOX) ในสารละลายร่วมเหนือวิกฤตคาร์บอนไดออกไซด์กับเมทานอลและการเกิดอนุภาค สมการสภาวะการกระจายตัวและการรวมตัวแบบกลุ่ม (GCA-EoS) ได้ถูกนำมาใช้ในการประมาณค่าการละลายของด๊อกโซรูบิซินอันเนื่องมาจากความซับซ้อนของโครงสร้างโมเลกุล เมทานอลในอัตราส่วน 3, 4 และ 5 เปอร์เซ็นต์โมล ถูกผสมในสารละลายบริสุทธิ์ของคาร์บอนไดออกไซด์เหนือวิกฤต ค่าการละลายของด๊อกโซรูบิซินถูกคำนวณที่อุณหภูมิและความดันของการสกัดในช่วง 308.15 ถึง 323.15 เคลวิน และ 80 - 300 บาร์ เนื่องจากขีดจำกัดของอุณหภูมิการสลายตัวของด๊อกโซรูบิซินและรูปแบบของสมการสภาวะการกระจายตัวและการรวมตัวแบบกลุ่ม ผลการศึกษาแบบจำลองทางคณิตศาสตร์พบว่าการละลายของด๊อกโซรูบิซินในตัวทำละลายร่วมมีค่ามากกว่าการละลายในสารละลายคาร์บอนไดออกไซด์บริสุทธิ์เหนือวิกฤต และ แบบจำลองทางคณิตศาสตร์ของการไหลในบริเวณที่เกิดการขยายตัวเพื่อศึกษาประบวนการเกิดอนุภาคขนาดเล็ก จะประกอบไปด้วยสมการดุลมวลสาร, ดุลโมเมนตัม และดุลพลังงานที่สัมพันธ์กับรูปแบบสมการสภาวะโดยทั่วไปของเบ็นเดอร์ (egB-EoS) โดยการไหลถูกศึกษาภายใต้สมมติฐานที่สภาวะคงตัว, การไหลในทิศทางเดียว และสภาวะที่ไม่มีการสูญเสียความร้อน นอกจากนี้สมมติฐานของการไหลจะถูกพิจารณาเฉพาะตัวทำละลายในสภาวะไอของสารผสมระหว่างคาร์บอนไดออกไซด์และเมทานอล แบบจำลองนี้ได้ศึกษาผลของอุณหภูมิในช่วงก่อนการขยายตัว (333.13 – 343.15 เคลวิน), ความดันในช่วงก่อนการขยายตัว (175 - 225 บาร์), และความเข้มข้นของตัวทำละลายร่วม (3 – 5 เปอร์เซ็นต์โมลของเมทานอล) ที่ได้จากการสกัด

อย่างไรก็ตามอุณหภูมิในช่วงก่อนการขยายตัวควรจะมีค่ามากกว่าอุณหภูมิที่ใช้ในการสกัดเพื่อป้องกันการเปลี่ยนสถานะของสารละลายและการเกิดอนุภาคภายในหัวฉีด ผล การทดลองพบว่าการเกิดอนุภาคส่วนใหญ่เกิดขึ้นในช่วงความเร็วเหนือเสียง ที่สภาวะ 338.15 เคลวิน, 200 บาร์ และ 3 เปอร์เซ็นต์โมลของเมทานอล ชี้ให้เห็นว่าอัตราการเกิดอนุภาคของด๊อกโซรูบิซิน มีค่าประมาณ 10^{24} อนุภาคต่อลูกบาศก์เซนติเมตรต่อวินาที ในขณะที่ความเข้มข้นของนิวเคลียสมีค่าเท่ากับ 10^{22} อนุภาคต่อลูกบาศก์เซนติเมตร โดยสามารถสร้างขนาดอนุภาคระดับนาโนเมตรได้ประมาณ 1.7 นาโนเมตร

คำสำคัญ: กระบวนการขยายตัวอย่างรวดเร็วของสารละลายเหนือวิกฤต/ ด๊อกโซรูบิซิน/ สมการสภาวะการกระจายตัวและการรวมตัวแบบกลุ่ม/ การทำอนุภาคให้มีขนาดเล็กลงระดับไมครอน/ การเกิดอนุภาค

ACKNOWLEDGEMENTS

This special research project would not have been finished without the effort of many people. Foremost, the author pleasure to express gratitude to Assoc. Prof. Dr. Thongchai Srinophakun, advisor, for technical support, suggestion, valuable guidance, and encouragement which enabled me to complete the special research project in the right direction. In addition, I would like to take this opportunity to give special regards to the oversea advisor, Prof. Suresh Batia, for offering this research topic and valuable experience at Department of Chemical Engineering, The University of Queensland, his guidance and suggestion. Besides, I would like to take this opportunity to give special regards to Assoc. Prof. Apichai Therdthianwong and Asst. Prof. Kwanchanok Pasuwat, special research project committees, for any suggestion and recommendation. Furthermore, I really appreciate Mr. Kanokphong Phongtummaruk, for his help and kindness without him the author would not accomplish this special research project.

Also, the author is grateful to Chemical Engineering Practice School (ChEPS), King Mongkut's University of Technology Thonburi (KMUTT), who provided the scholarship which lots of excellent opportunity. Additional, the author would like to thank my family for the great encouragement that is all supports to make this special research complete. Moreover, I would like to thank Mr. Vorrapat Ketkrai, Ms. Dusadee Yoocha, Mr. Sirisuk Khemdee, and Mr. Thanin Saengkaew, my best friend and good audience, for their comfort, spirit, and great cheer. My classmates ChEPS 14, especially Mr. Piroon Samanot, Mr. Apirut Kuhavichanun, Mr. Pisut Veerahong, and Mr. Thanawat Upienpong, for their assistance, support, and suggestion.

Last but not least, the author offers my regard to all of those who supported me in any respect during the competition of this special project. Without help of the particular mentioned above, the author would face difficulties while during the special research

CONTENTS

PAGE

ENGLISH ABSTRACT ii
THAI ABSTRACT iii
ACKNOWLEDGEMENTS v
CONTENTS vi
LIST OF TABLES viii
LIST OF FIGURES x
NOMENCLATURES xiv

CHAPTER

1. INTRODUCTION **1**
- 1.1 Background 1
- 1.2 Objectives 2
- 1.3 Scopes of work 2
- 1.4 Expected results 2

2. THEORIES AND LITERATURE REVIEWS **3**
- 2.1 Theories 3
- 2.1.1 History of Doxorubicin 3
- 2.1.2 Mechanism of action 3
- 2.2 Supercritical Fluid Extraction 3
- 2.3 Co-solvent or Modifier 6
- 2.4 Estimation the pure component properties 7
- 2.4.1 First-order groups 8
- 2.4.2 Second-order groups 8
- 2.4.3 Third-order groups 9
- 2.4.4 Proposed model 9
- 2.5 GCA-EoS model 11
- 2.5.1 Repulsive term 11
- 2.5.2 Attractive term 12
- 2.5.3 Association term 13
- 2.6 Rapid expansion of super critical solution (RESS) process 14
- 2.7 Particle formation 16
- 2.7.1 Mass, Momentum and Energy Conservation 16
- 2.7.2 Particle formation model 16

3. METHODOLOGY **18**
- 3.1 Methodology 18
- 3.1.1 Studying the overview of supercritical technology specified on the RESS process 19

CONTENTS (CONT.)

PAGE

3.1.2 Formulating mathematical model to solve the solubility of DOX in modified supercritical phase using GCA-EoS model 19
3.1.3 Formulating and developing mathematical model in the RESS process to predict particle formation in precipitation unit 20
3.2 The requirements of parameter in GCA-EOS model 22
3.2.1 Repulsive parameters 22
3.2.2 Attractive parameters 22
3.2.3 Association parameters 27
3.3 Modeling of particle formation 31
3.3.1 Modeling of flow field in subsonic region 32
3.3.2 Modeling of flow field in supersonic free jet region 36
3.3.3 Modeling of particle formation in supersonic free jet region 37

4. RESULTS AND DISCUSSION **39**
4.1 Validation of Group-Contribution base estimate method 39
4.2 GCA-EoS in extraction unit 40
4.2.1 The compressibility factor of system (z) 41
4.2.2 Fugacity coefficient of DOX in supercritical phase (ϕ_i) 43
4.2.3 Solubility of DOX in supercritical phase 46
4.3 Results of the flow model in the precipitation unit 49
4.3.1 Physical properties of the supercritical fluid in subsonic and supersonic free jet region 50
4.4 Sensitivity analysis 56
4.4.1 Pre-expansion temperature 56
4.4.2 Pre-expansion pressure 61
4.4.3 Co-solvent concentration (methanol) 67

5. CONCLUSIONS AND RECOMMENDATIONS **72**
5.1 Conclusions 72
5.2 Recommendations 73

REFERENCES **74**

APPENDIX

A. Comparison of estimation method **78**
B. Validdation of estimation properties between previous and this work **82**
C. Parameters estimation **88**

CURRICULUM VITAE **94**

LIST OF TABLES

TABLE **PAGE**

2.1 Physical and transport properties of gases, liquids and SCFs 5
2.2 Critical condition for carious solvents 5
2.3 Modifier in pure supercritical carbon dioxide 6
2.4 Selected function for each property 10
2.5 Value of the additional adjustable parameters 10
3.1 The critical properties parameters of DOX, carbon dioxide, and methanol using the method of Marrero and Gani 22
3.2 The GCA-EOS pure-group parameters of this system 23
3.3 The GCA-EOS binary interaction parameters (k_{kj}^{*}) 25
3.4 The GCA-EOS binary interaction parameters (k_{kj}'') 25
3.5 The GCA-EOS binary interaction parameters (α_{kj}) 26
3.6 Associating groups, their active sites, and type of association effect in DOX and methanol molecule 30
3.7 Energy ($\varepsilon^{A_k B_j}$) and volume ($\kappa^{A_k B_j}$) of association parameters for self- and cross- association in both systems of DOX in pure supercritical carbon dioxide and supercritical carbon dioxide with methanol as a modifier 30
3.8 Critical temperature (T_c), critical pressure (P_c), critical density (ρ_c), molecular weight, acentric factor (ω), and polar factor (χ) of both carbon dioxide and methanol [37] 35
4.1 Comparing the accuracy between two widely-used group contribution prediction methods for normal melting point 39
4.2 Comparing the accuracy of normal melting point (T_m) estimation between the previous work of Phongtummaruk and this work. 40
4.3 Assumption of flow model along the sub-sonic and supersonic free jet region 50
A.1 The property function, group contribution term and adjustable parameter of normal melting point estimation 79
A.2 First level group of estimation by using method of Marrero and Gani 79
A.3 Second level group of estimation by using method of Marrero and Gani 79
A.4 Third level group of estimation by using method of Marrero and Gani 80
A.5 Estimation of normal melting point of method of Joback and Reid 81
B.1 Group contribution parameters of first level of estimation of the previous work of Phongtummaruk 84
B.2 Group contribution parameters of first level of estimation of this work 84
B.3 Group contribution parameters of second level of estimation of the previous work of Phongtummaruk 86
B.4 Group contribution parameters of second level of estimation of this work 86

LIST OF TABLES (CONT.)

TABLE **PAGE**

B.5 Group contribution parameters of third level of estimation of this work 87
C.1 The property function, group contribution term and adjustable parameter of normal boiling point, critical temperature, and critical pressure estimation 88
C.2 First level group of estimation normal boiling point critical temperature, and critical pressure by method of Marrero and Gani 88
C.3 Second level group of estimation normal boiling point, critical temperature, and critical pressure by method of Marrero and Gani 89
C.4 Third level group of estimation normal boiling point, critical temperature, and critical pressure by using method of Marrero and Gani 89
C.5 Estimated normal boiling point, critical temperature, and critical pressure by using method of Marrero and Gani 89
C.6 Simple group, number of each group in DOX molecule, and volume increment (ΔV) for estimating solid density based on Lyman method 90
C.7 Molecular feature, number of each feature in DOX molecule, and incremental values (V_b) for estimating molar volume based on Schroeder's method 92
C.8 Simple groups for Parachoe estimation, number of each group in DOX molecule, and Parachor incremental for estimating molar volume based on Schroeder's method 93

LIST OF FIGURES

FIGURE **PAGE**

2.1 Chemical structure of Doxorubicin 3
2.2 Pressure-temperature diagram of a pure substanc 4
2.3 T_c-x_c, P_c-x_c, and P_c-T_c diagrams of the supercritical carbon dioxide and methanol system 7
2.4 RESS equipment concept 15
3.1 Schematic diagrams of methodology 18
3.2 Classification and numbering of DOX into pure chemical group 23
3.3 Functional group specification in DOX molecule (a) the seventh and eighth simple functional group based on Figure 3.2, (b) lack functional group, and (c) excess functional group 24
3.4 Associated hydroxyl (OH) and ketone (CO) groups of DOX molecule in pure supercritical carbon dioxide 27
3.5 Schematic of self- and cross- association DOX molecule in pure supercritical carbon dioxide 28
3.6 Schematic of self- and cross- association of DOX in supercritical carbon dioxide and methanol as a modifier 29
3.7 Schematic drawing of the rapid expansion parts 31
4.1 Calculated compressibility factor (z) of the system of DOX in pure supercritical carbon dioxide correlated with pressure (bar) at various temperatures 41
4.2 Calculated compressibility factor (z) of the system of DOX in supercritical carbon dioxide with added methanol as a modified co-solvent (a) 3, (b) 4, and (c) 5 mole percentage correlated with pressure (bar) at various temperatures 42
4.3 Calculated compressibility factor (z) of the system of DOX in modified co-solvent of supercritical carbon dioxide and methanol at constant temperature (308.15 K) correlated with pressure (bar) at various ratio of modified co-solvent 43
4.4 Calculated fugacity coefficient (ϕ_i) of DOX in (a) pure supercritical carbon dioxide, (b) modified co-solvent of supercritical carbon dioxide and methanol (x_{CO_2} = 0.97) correlated with pressure (bar) at various temperature 44
4.5 Calculated fugacity coefficient (ϕ_i) of DOX in pure supercritical carbon dioxide and modified co-solvent at constant temperature (a) 308.15 K, (b) 313.15 K., (c) 318.15 K, and (d) 323.15 K correlated with pressure (bar) at various ratio of methanol as a modified co solvent 46
4.6 Solubility of DOX in pure supercritical carbon dioxide correlated with pressure (bar) at various extraction temperatures 47

LIST OF FIGURES (CONT.)

FIGURE **PAGE**

4.7 Solubility of DOX in modified co-solvent of supercritical carbon dioxide and 3 mole percentage of methanol correlated with pressure (bar) at various extraction temperatures 47
4.8 Solubility of DOX in pure supercritical carbon dioxide and modified co-solvent at constant temperature (a) 308.15 K, (b) 313.15 K, (c) 318.15 K, and (d) 323.15 K correlated with pressure (bar) at various ratio of methanol as a modified co-solvent 49
4.9 Calculated velocity profile (cm/s) correlated with expansion distance (cm) when expanding saturated modified supercritical solution through expansion paths (a) subsonic and (b) supersonic free jet region with pre-expansion condition 338.15 K and 200 bar (methanol 3 mole percentage) 51
4.10 Calculated density profile (g/cm^3) correlated with expansion distance (cm) when expanding saturated modified supercritical solution through expansion paths (a) subsonic and (b) supersonic free jet region with pre-expansion condition 338.15 K and 200 bar (methanol 3 mole percentage) 52
4.11 Calculated temperature profile (K) correlated with expansion distance (cm) when expanding saturated modified supercritical solution through expansion paths (a) subsonic and (b) supersonic free jet region with pre-expansion condition 338.15 K and 200 bar (methanol 3 mole percentage) 53
4.12 Calculated pressure profile (bar) correlated with expansion distance (cm) when expanding saturated modified supercritical solution through expansion paths (a) subsonic and (b) supersonic free jet region with pre-expansion condition 338.15 K and 200 bar (methanol 3 mole percentage) 54
4.13 Calculated supersaturation ratio in supersonic free jet region correlated with expansion distance (cm) when expanding saturated modified supercritical solution through expansion path with pre-expansion condition 338.15 K and 200 bar (methanol 3 mole percentage) 54
4.14 Calculated nucleation rate (particles/cm^{3}s) in supersonic free jet region correlated with expansion distance (cm) when expanding saturated modified supercritical solution through expansion path with pre-expansion condition 338.15 K and 200 bar (methanol 3 mole percentage) 55
4.15 Calculated critical radius (nm) in supersonic free jet region correlated with expansion distance (cm) when expanding saturated modified supercritical solutionthrough expansion path with pre-expansion condition 338.15 K and 200 bar (methanol 3 mole percentage) 55

LIST OF FIGURES (CONT.)

FIGURE **PAGE**

4.16 Calculated number concentration of critical nuclei (particles/cm^3) in supersonic free jet region correlated with expansion distance (cm) when expanding saturated modified supercritical solution through expansion path with pre-expansion condition 338.15 K and 200 bar (methanol 3 mole percentage) 56
4.17 Velocity profile (cm/s) of modified saturated solution when expanding through (a) subsonic (b) supersonic free jet region correlated with expansion distance (cm) at various pre-expansion temperatures 57
4.18 Density profile (g/cm^3) of modified saturated solution when expanding through (a) subsonic (b) supersonic free jet region correlated with expansion distance (cm) at various pre-expansion temperatures 58
4.19 Temperature profile (K) of modified saturated solution when expanding through (a) subsonic (b) supersonic free jet region correlated with expansion distance (cm) at various pre-expansion temperatures 58
4.20 Pressure profile (bar) of modified saturated solution when expanding through (a) subsonic (b) supersonic free jet region correlated with expansion distance (cm) at various pre-expansion temperatures 59
4.21 Supersaturation ratio in supersonic free jet region correlated with expansion distance (cm) at various pre-expansion temperatures 60
4.22 Nucleation rate (particles/cm^{3}s) in supersonic free jet region correlated with expansion distance (cm) at various pre-expansion temperatures 60
4.23 Critical radius (nm) in supersonic free jet region correlated with expansion distance (cm) at various pre-expansion temperatures 60
4.24 Number concentration of critical nuclei (particles/cm^3) in supersonic free jet region correlated with expansion distance (cm) at various pre-expansion temperatures 61
4.25 Velocity profile (cm/s) of modified saturated solution when expanding through (a) subsonic (b) supersonic free jet region correlated with expansion distance (cm) at various pre-expansion pressures 62
4.26 Density profile (g/cm^3) of modified saturated solution when expanding through (a) subsonic (b) supersonic free jet region correlated with expansion distance (cm) at various pre-expansion pressures 63
4.27 Temperature profile (K) of modified saturated solution when expanding through (a) subsonic (b) supersonic free jet region correlated with expansion distance (cm) at various pre-expansion pressures 64
4.28 Pressure profile (bar) of modified saturated solution when expanding through (a) subsonic (b) supersonic free jet region correlated with expansion distance (cm) at various pre-expansion pressures 64
4.29 Supersaturation ratio in supersonic free jet region correlated with expansion distance (cm) at various pre-expansion pressures 65

LIST OF FIGURES (CONT.)

FIGURE **PAGE**

4.30 Nucleation rate (particles/cm^{3}s) in supersonic free jet region correlated with expansion distance (cm) at various pre-expansion pressures 66

4.31 Critical radius (nm) in supersonic free jet region correlated with expansion distance (cm) at various pre-expansion pressures 66

4.32 Number concentration of critical nuclei (particles/cm^3) in supersonic free jet region correlated with expansion distance (cm) at various pre-expansion pressures 66

4.33 Velocity profile (cm/s) of modified saturated solution when expanding through (a) subsonic (b) supersonic free jet region correlated with expansion distance (cm) at various ratios of methanol modified co-solvent 67

4.34 Density profile (g/cm^3) of modified saturated solution when expanding through (a) subsonic (b) supersonic free jet region correlated with expansion distance (cm) at various ratios of methanol modified co-solvent 68

4.35 Temperature profile (K) of modified saturated solution when expanding through (a) subsonic (b) supersonic free jet region correlated with expansion distance (cm) at various ratios of methanol modified co-solvent 69

4.36 Pressure profile (bar) of modified saturated solution when expanding through (a) subsonic (b) supersonic free jet region correlated with expansion distance (cm) at various ratios of methanol modified co-solvent 69

4.37 Supersaturation ratio in supersonic free jet region correlated with expansion distance (cm) at various ratios of methanol modified co-solvent 70

4.38 Nucleation rate (particles/cm^{3}s) in supersonic free jet region correlated with expansion distance (cm) at various ratios of methanol modified co-solvent 70

4.39 Critical radius (nm) in supersonic free jet region correlated with expansion distance (cm) at various ratios of methanol modified co-solvent 70

4.40 Number concentration of critical nuclei (particles/cm^3) in supersonic free jet region correlated with expansion distance (cm) at various ratio of methanol modified co-solvent 71

B.1 Defined simple functional groups in first level of estimation of DOX molecule (a) previous work of Phongtummaruk and (b) this work 83

B.2 Defined polyfunctional groups in second level of estimation of DOX molecule (a) previous work of Phongtummaruk and (b) this work 85

B.3 Defined in polycyclic groups in third level of estimation of DOX molecule in this work 87

C.1 Estimation of molar volume of pure solid base on Lyman method 90

NOMENCLATURES

A = Helmholtz energy (J)
= Area (flow model)
a = Coefficients of the Bender equation of state
B, C, D, E, F, G, and H = Temperature dependent coefficients (egB-EoS)
$B^*, C^*, D^*, E^*, F^*, G^*$, and H^* = Reduced function (egB-EoS)
C = Heat capacity
C, D, E = Contribution of first- , second-, and third- order group (Estimation method)
d = Hard sphere diameter
D = Diameter
f = Fanning friction factor (flow model)
Conversion factor (egB-EoS)
g = Attractive energy parameter for interaction (GCA-EoS)
Constant (egB-EoS)
h = Heat transfer coefficient
H = Specific enthalpy
k = Boltzmann’s constant (particle formation)
Attractive energy parameter for interaction (GCA-EoS)
L = Length
= Avogadro number (particle formation)
M = Number of associating sites
n = Number of moles of component
N = Fluid phase concentration
N, M, O = Times occurred in component (estimation method)
P = Pressure (bar, MPa)
q = Surface parameter
Q = Heat loss by convection
r = Radius of conical shape in supersonic free jet region
R = Universal gas constant (cm^3 bar/mol K)
s = Surface area
S = Supersaturation ratio
T = Temperature (K)
v = Number of groups in molecule (GCA-EoS model)
Velocity (flow model)
V = Total volume
w = Sonic velocity
x = Mole fraction of component
Distance (flow model)
X = Mole fraction of group not associate

NOMENCLATURES (CONT.)

y = Solute solubility (mole fraction basis)
z = Compressibility factor
NC = Number of components in the mixture
NGA = Number of associating functional groups in the mixture
MW = Molecular weight
$\tilde{q}$ = Total number of surface segments
θ_k = Surface fraction
α = NRTL non-randomness parameter
ε = Characterizes the association energy
κ = Associating volume
ρ = Density
σ = Solid-fluid interfacial tension
ϕ = Fugacity
ω = Acentric factor
υ = Solute molar volume (solubility expression)
χ = Polar factor
τ = Reduced temperature
δ = Reduced density
$\xi,\ \eta$ = Binary parameters for interaction between species (egB-EoS)

Subscripts

$*$ = Referent state (GCA-EoS model)
Prevailing condition (particle formation)
0 = Adjustable value
2 = Solute phase
b = Boiling point
c = Critical
i, j, k = Type, molecule
m = Melting point (estimation method)
Mach (flow model)
Mixed (egB-EoS)
$nozzle$ = Nozzle region
pre = pre-expansion condition
$post$ = post-expansion condition

NOMENCLATURES (CONT.)

Superscripts

att = Attractive term
assoc = Association term
E = Extraction condition
out = Outlet
p = Constant pressure
res = Residual Helmholtz energy
rep = Repulsive term
sat = Saturated
v = Constant volume

CHAPTER 1 INTRODUCTION

1.1 Background

Rapid Expansion of Supercritical Solution (RESS) is an application of supercritical fluid (SCF) techniques in a wide range of pharmaceutical industries for producing the small and uniform particles without purification unit. Supercritical fluid extraction has been developed for natural product extraction especially in food and pharmaceutical industries during the last two decades [1]. The pharmaceutical extraction processes are currently limited by safety constraints of the toxicant of contaminated organic solvent in the drugs [2]. Therefore, carbon dioxide is an excellent alternative supercritical solvent due to low critical temperature, low critical pressure, non-flammability, non-toxicity, and low cost [3]. Moreover, the carbon dioxide has a number of limitations resulted from its polarity and capacity for specific solvent-solute interaction especially in non-volatile organic, and high polar compound. Here the solubility is quite low in pure supercritical carbon dioxide. As a consequence, additional of polar-compound as a modified co-solvent assisted to enhance the solubility for increasing the polarity of non-polar solvent.

Traditional thermodynamic cubic equation of state cannot be used for predicting solubility of solute in any solvent without some experimental data due to the requirement of interaction parameter between solute and solvent. On the other hand, only accessible thermodynamic properties such as critical temperature and pressure, and their group contribution parameters are required Group contribution Equation of State (GC-EoS) of Skjold Jørgensen [4]. The GC-EoS model is not accurate for predicting equilibria phase in the system consisting of association and salvation effect and major role of hydrogen bond. As a result, the GC-EoS was developed into Group Contribution with Association Equation of State (GCA-EoS) which was explicitly taken into account in these two effects [5].

A procedure of the RESS process, saturating supercritical fluid with substrate, is suddenly depressurized through a heated nozzle into a low pressure chamber causing fast nucleation and fine particle formation. Mathematical model of RESS process accounts for particle formation mechanisms in both subsonic and supersonic regions. The mathematical model is derived to complete supersaturation ratio and critical nucleus size profiles under the simplifying assumption throughout expansion range [6].

Doxorubicin (DOX) is a common chemotherapy drug which has been given to treat a wide range of cancer [7]. Thermodynamic properties of DOX from the experiment are hard to obtain because of highly complex molecular structure and toxicant side effect of DOX. Estimation method or mathematical model is necessary to estimate thermodynamic properties. A recent work of prediction thermodynamic properties and solubility of DOX in supercritical carbon dioxide was given by Phongtummaruk [8].

However, the result indicated that the solubility of DOX in supercritical carbon dioxide was quite low.

Therefore, in this study the solubility of DOX in supercritical carbon dioxide which mixed with methanol as a modified co-solvent for increasing the solubility of DOX in the pure non-polar supercritical fluid using Group Contribution with Association Equation of States (GCA-EoS) has been focused under limitation of experimental data in the co-solvent available, different sizes between solvents and solute, and association effects. Moreover, flow model in both subsonic and supersonic free jet region by using an extended generalized Bender Equation of State (egB-EoS) would be emphasized. The effect of pre-expansion temperature, pre-expansion pressure and mole percentage of methanol as a modified co-solvent were used to study thermodynamic properties, velocity, density, temperature, and pressure of supercritical solution in both regions. However, particle formation parameters, nucleation rate, number of concentration of critical nuclei, and critical radius, were investigated in supersonic free jet region only.

1.2 Objectives

1.2.1 To improve the solubility of Doxorubicin (DOX) by adding methanol into supercritical carbon dioxide as a modified co-solvent

1.2.2 To perform the sensitivity analysis of precipitation variables, pre-expansion temperatures, pre-expansion pressures, and mole percentages of methanol on particle formation

1.3 Scopes of work

The scopes of this work are as follows:

1.3.1 The estimation of thermodynamic properties of DOX is based on Group Contribution method of Marero and Gani estimation method of Lyman.

1.3.2 The prediction of solubility of DOX in modified supercritical carbon dioxide and methanol is performed by Group Contribution with Association Equation of State (GCA-EoS).

1.3.3 There are the sensitivity of 3 precipitation variables including pre-expansion temperatures, pre-expansion pressures, and mole percentages of methanol for studying thermodynamic properties of supercritical solution in precipitation unit (subsonic and supersonic region).

1.3.4 The particle formation in supersonic free jet region is based only on the 3 precipitation variables.

1.4 Expected results

The expected results of this work are that the GCA-EoS model could predict the solubility of DOX in both pure supercritical carbon dioxide and supercritical carbon dioxide with methanol as a modified co-solvent. Mathematical model will predict particle formation of RESS process throughout the precipitation unit

CHAPTER 2 THEORIES AND LITERATURE REVIEWS

2.1 Theories

2.1.1 History of Doxorubicin

Doxorubicin (DOX) is the most effective chemotherapeutic is used for treatment of cancers by slowing or stopping the growth of cancer cells in your body [9]. The length of treatment depends on the types of drugs and cancer that being treated. Moreover, patient's health of is the most important factor [10]. It is an anthracycline antibiotic that is related to the natural product and daunomycin. DOX was discovered in the 1950's by Castel del Monte when he isolated the found bacteria in the soil samples [7]. The molecular structure of DOX is shown in Figure 2.1.

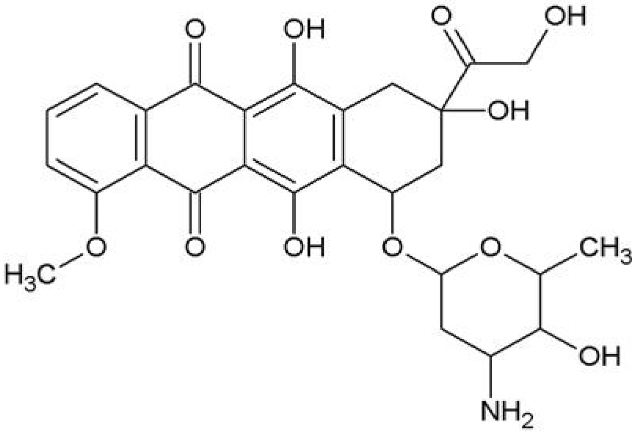

Figure 2.1 Chemical structure of Doxorubicin [7]

2.1.2 Mechanism of action

The real mechanism of DOX is complex and unclear. Interacting with DNA by intercalation and inhibition of macromolecular biosynthesis is the recent knowledge of DOX. This inhibits the progression of enzyme topoisomerase II, which relaxes supercoils in DNA transcription. DOX stabilizes the topoisomerase II complex after it has broken the DNA chain for replication. Preventing the DNA doubles helix from being resealed and stopping process of replication are significant function of DOX [7].

2.2 Supercritical Fluid Extraction

Supercritical fluid extraction (SFE) is carried out by contraction between solids and supercritical solvent [11]. This technique resembles Soxhlet extraction except the solvent. Supercritical fluid, substance above its critical temperature and pressure, is the distinguished of this method. The supercritical fluid not only exploits the solvent power but also inherent physical properties of a pure compound or mixture at temperatures and pressures at or near its critical point in phase equilibrium [12].

One main advantage of SFE technique is the reduction of the problems of organic solvents in the lipidologist laboratory due to the legislative protocols. Several studies have shown that SFE is a replacement method for traditional gravimetric techniques. Carbon dioxide is the most adopted supercritical fluid due to its advantage such as low cost, non-toxic, and nonflammable [13]. Many green industries used SFE for removal of impurities from polymer, cleaning of electronic parts, binder removal from ceramics, waste and environmental remediation as well [14].

The condition of a pure supercritical fluid (SCF) is at the temperature and pressure above its critical point, where the gas and liquid phases merge to form a single homogeneous fluid phase. SCF is described as intermediate of two phases as shown in Figure 2.2. [15]

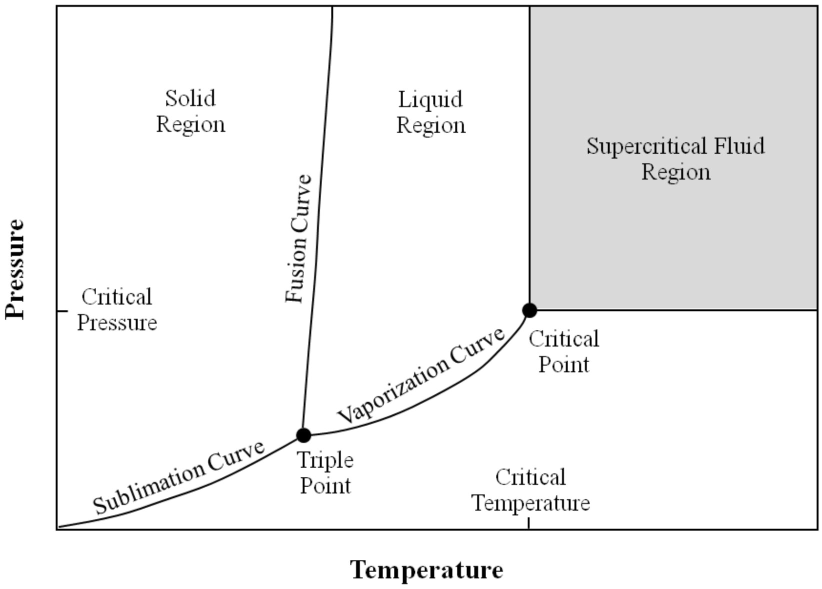

Figure 2.2 Pressure-temperature diagram of a pure substance [12]

According to this figure, the location of the critical point of a pure compound on its pressure-temperature phase diagram lies at the end of the vaporization curve [12]. However, at a very high pressure the fusion line can rise into the supercritical fluid regions and both solid and supercritical phases can exist. For analytical scale extraction, the term supercritical generally refers to the conditions above the critical temperature and close to the critical pressure.

The transportation properties of SCF phase is approximating as gases, on the other hand, this phase has abilities to dissolve like a liquid. A comparison of typical values for density, viscosity and diffusivity of gases, liquids, and SCFs is presented in Table 2.1.

Table 2.1 Physical and transport properties of gases, liquids and SCFs [15]

Properties	Density (kg/m^3)	Viscosity (cP)	Diffusivity (mm^2/s)
Gases	1	0.01	1-10
Supercritical fluids	100-1000	0.05-0.1	0.01-0.1
Liquids	1000	0.5-1.0	0.001

Supercritical fluids are characterized by high densities, low viscosities, and diffusivities intermediate between gases and liquids, according to this table. The high density values enable appreciable salvation power, while the diffusivity of solutes facilitates mass transfer. These unusual properties make supercritical fluids potentially very good solvents. The solubility of a compound in a supercritical solvent is dependent on the density of the solvent, as well as on the physicochemical affinity of the solute for the solvent [12]. On the contrary, the solubility power of supercritical fluids is sensitive to small changes in operating conditions, and is possible to fine tune of the pressure and temperature to tailor the solvent capacity of supercritical fluids for a particular process [16]. The commonly used of supercritical fluid is carbon dioxide because of its low critical temperature and pressure, inert to reaction, non-flammable, low cost and safety. The critical temperature and pressure of common supercritical solvent are listed in Table 2.2.

Table 2.2 Critical condition for carious solvents [16-18]

Solvents	Critical Temperature (°C)	Critical pressure (bar)
Carbon dioxide [16]	31.1	73.8
Ethane [16]	32.2	48.8
Ethylene [16]	9.3	50.4
Propane [16]	96.7	42.5
Propylene [16]	91.9	46.2
Cyclohexane [16]	280.3	40.7
Isopropanol [16]	235.2	47.6
Benzene [16]	289.0	48.9
Toluene [16]	318.6	41.1
p-Xylene [16]	343.1	35.2
Chlorotrifluoromethane [16]	28.9	39.2
Trichlrofluoromethane [16]	198.1	44.1
Ammonia [16]	132.5	112.8
Water [16]	374.2	220.5
Methanol [17]	240.1	80.9
Nitrous oxide [17]	36.6	72.4
Xenon [17]	16.7	58.4
Ethanol [18]	243	63.8
n-Hexane [18]	234	29.7

2.3 Co-solvent or Modifier

The low solubility of polar substance in non-polar supercritical fluid, carbon dioxide, is an obstacle to the development of operating condition of supercritical solvents. Addition of small amounts of polar co-solvents such as methanol, ethanol, and water etc. into non-polar supercritical fluid, results in a higher polarity of supercritical co-solvent. Due to the increasing of density of mixture from adding polar compound, the magnitude of physical interactions such as dipole–dipole, dipole–induced dipole and induced dipole–induced dipole interactions between solute and solvent molecules are increased. Moreover, the addition of co-solvent also increases the critical point, the difference between the local density and the bulk density. It also increases the interactions, hydrogen bonding between the solute and co-solvent molecules. The effect results in a large enhancement of solubility than obtained with non-specific interactions alone [19]. The polar modifiers usually added to the pure supercritical carbon dioxide are listed in Table 2.3.

Table 2.3 Modifier in pure supercritical carbon dioxide [14]

Modifier	T_C (^oC)	P_C (atm)	Molecular mass	Dielectric Constant at 20 ^oC	Polarity index
Methanol	239.4	79.9	32.04	32.70	5.1
Ethanol	243.0	63.0	46.07	46.07	4.3
Propan-1-ol	263.5	51.0	60.10	20.33	4.0
Propan -2-ol	235.1	47.0	60.10	19.30	3.9
Hexan-1-ol	336.8	40.0	102.18	13.30	3.5
2-Methoxyethahanol	302.0	52.2	76.10	16.93	5.5
Tetrahydrofuran	267.0	51.2	72.11	7.58	4.0
1,4-Dioxane	314.0	51.4	88.11	2.25	4.8
Acetonitrile	275.0	47.7	41.05	37.50	5.8
Dichloromethane	237.0	60.0	84.93	8.93	3.1
Chloroform	263.2	54.2	119.38	4.81	4.1
Propylene carbonate	352.0	-	102.09	69.00	6.1
N,N-Dimethaylacetamide	384.0	-	87.12	37.78	6.5
Dimethyl sulphoxide	465.0	-	78.13	46.68	7.2
Formic acid	307.0	-	46.02	58.50	-
Water	374.1	217.6	18.01	80.1	10.2
Carbon disulphide	279.0	78.0	76.13	2.64	-

From the mid-l980s, supercritical carbon dioxide and alcohol systems have received increased attention due to low molecular weight of alkanols for extraction biomaterials and medicines. Therefore, it is necessary to define critical regions for this system.

Scott and Konynenburg [20] have classified critical curves based on Van der Waals equation for non-polar components. Schneider and Rowlinson [20] have published comprehensive discussions of classification of critical curves. Moreover, Brunner et al. [20] has measured the critical curve of the CO_2-methanol system with a high-pressure view-cell.

In addition, Neichel and Franck [20] calculated the critical curves of binary systems from water-methane to water-hexane and water-dodecane by means of the Heiligs Franck Equation of State (EoS). This EoS contains a hard-sphere repulsion term and square-well attraction term. It has been successfully used at high pressures and temperatures and has even been used for component partners with high polarity differences. Many Equation of States have been proposed and applied in the past [20]. The critical curves of binary fluid mixtures carbon dioxide and methanol is shown in Figure 2.3

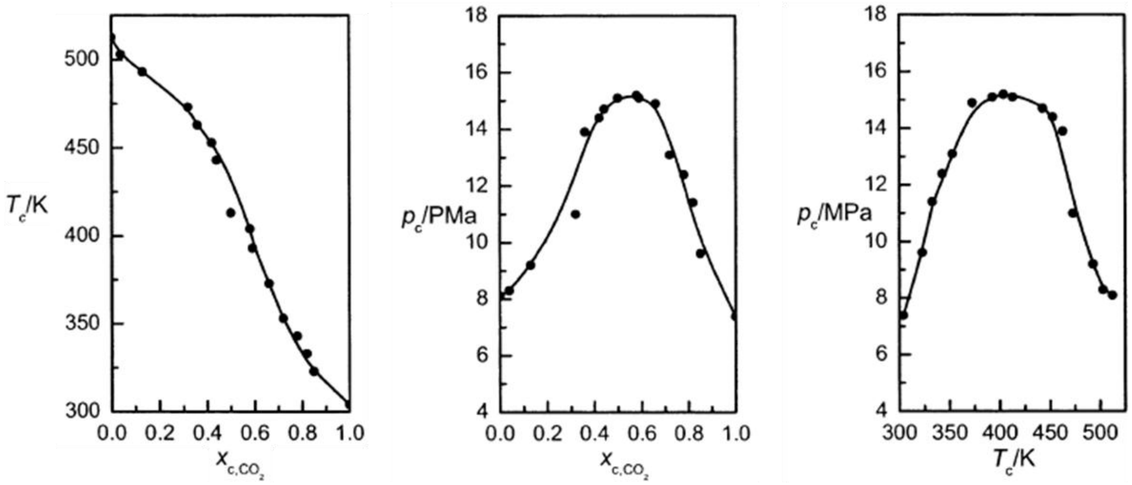

Figure 2.3 T_c-x_c, P_c-x_c, and P_c-T_c diagrams of the supercritical carbon dioxide and methanol system [20]

2.4 Estimation the pure component properties

A set of physical and thermodynamic properties of any compound is the most basis for the design and simulation of many chemical processing. However, most of toxic and reactive compounds are hard to measure as the need arises. Therefore, estimation method from mathematical model is generally investigated. For the estimation of properties of pure compounds, group-contribution methods have been widely used. In this method, the property of a compound is a function of structurally-dependent parameters, which are determined by summing the frequency of each group occurring in the molecule times of its contribution. The method allows to the estimations of the following properties like normal boiling point, critical temperature, critical pressure, standard enthalpy of formation, standard enthalpy of vaporization, and standard enthalpy of fusion. In addition, this technique provides accurate estimations of several properties of pure compounds and allows capturing the differences among isomers.

The estimation is performed at 3 levels consisting of a large set of simple groups that describe any variety of organic compounds. However, these groups capture only partially the proximity effects and are unable to distinguish among isomers [21].

2.4.1 First-order groups

The primary level of estimation has a large set of simple groups that allows describing a wide variety of organic compounds while the higher levels involve poly-functional and structural groups that provide more information about molecular fragments that is negligible. The assumption follows these criteria.

(1) The first-order groups including both aromatic and aliphatic hydrocarbons, alcohols, phenols, ketones, aldehydes, acids, esters, ethers, amines, anilines and many other different classes of organic compounds should be small as possible entire molecule. However, any atom should not overlap to any other first-order groups. These groups should be independent of the molecule in which the group occurs.

(2) Aromatic compounds should be provided at this level in order to describe a large number of different aromatic substituents. The 3 different corrections of the form aC have been defined to differentiate among those as follows.
   (a) Carbon atoms shared by different aromatic rings in a same fused system
   (b) Carbon atoms shared by both aromatic and non-aromatic rings in the same fused system
   (c) Any other substituted aromatic carbon that does not fall in the above categories

(3) Two specific groups, aN and aCH, have been specified in order to describe pyridines and other nitrogen-containing aromatics and the aromatic carbon without substitution, respectively.

(4) Cyclic and acyclic structures should be determined in this level by using separate ring and non-ring groups.

2.4.2 Second-order groups

The second level involves groups that permit a better description of polyfunctional compounds, polar or nonpolar compounds of medium size (C_3 – C_6), aromatic or cycloaliphatic compounds with only one ring and several substituents, and differentiation among isomers. The following criteria have been considered in order to identify the second-order groups.

(1) At the second level, the properties of simple and monofuntional groups are estimated after a first level of approximation.

(2) Molecular fragments including alicyclic substituents that could not completely be described by first-order groups are described and improved in this level in order to provide a better description of polyfunctional groups which usually results in poor estimates at a first level of approximation.

(3) The differentiation between isomers is specified in this order. The groups in this level allow the distinction of isomers not only in alkenes, alkenes and other open-chain structures, but also in aromatic compounds in special groups.

(4) A specific atom of the molecule may be included or many overlap in more than one group. This is contrary to the first-order groups in order to prevent a situation that one group overlaps completely to another group. However, it would lead to a redundant description of a same molecular fragment.

However, the second-order groups are unable to provide a good representation of compounds containing more than one ring as well as, in some case, open-chain polyfunctional compounds with more than four carbon atoms in the main chain. For this reason, a further level is required to allow a better description of these types of compounds.

2.4.3 Third-order groups

The third-order level has been described in more structural information about molecular fragments in polycyclic compounds since the first and second level description is insufficient. The groups in this level allows the estimation of complex systems consisting of fused aromatic rings, fused aromatic and nonaromatic rings, and non-fused rings joined by chains that can occur in different functional groups.

2.4.4 Proposed model

The property-estimation model has the form of the following equation:

$$f(x) = \sum_i N_i C_i + w \sum_j M_j D_j + z \sum_k O_k E_k \tag{2.1}$$

Where C_i is the contribution of the first-order group of type-*i* that occurs N_i times, D_j is the contribution of the second-order group of type-*j* that occurs M_j times, and E_k is the contribution of the third-order group of type-*k* that has O_k occurrences in a compound.

In the first level of estimation, the constants w and z are assigned zero values because only first-order groups are employed. In the second level, the constants w and z are assigned unity and zero values respectively because only first- and second-order groups are involved while in the third level both w and z are set to unity values.

The left-hand side of Equation (2.1) is a simple function $f(x)$ of the target property X. The target properties as well as their corresponding estimation functions are listed in Table 2.4.

Table 2.4 Selected function for each property [21]

Property (*X*)	**Function *f(x)* of Equation (2.1)**	**Right hand side of Equation (2.1) (group-contribution terms)**
Normal melting point (T_m)	$exp\left(T_m/T_{m0}\right)$	$\sum_i N_i T_{m1i} + \sum_j M_j T_{m2j} + \sum_k O_k T_{m3k}$
Normal boiling point (T_b)	$exp\left(T_b/T_{b0}\right)$	$\sum_i N_i T_{b1i} + \sum_j M_j T_{b2j} + \sum_k O_k T_{b3k}$
Critical temperature (T_c)	$exp\left(T_c/T_{c0}\right)$	$\sum_i N_i T_{c1i} + \sum_j M_j T_{c2j} + \sum_k O_k T_{c3k}$
Critical pressure (P_c)	$\left(P_c - P_{c1}\right)^{-0.5} - P_{c2}$	$\sum_i N_i P_{c1i} + \sum_j M_j P_{c2j} + \sum_k O_k P_{c3k}$

According to this table, the symbols T_{m1i}, T_{b1i}, T_{c1i}, and P_{c1i}, represent the contributions (C_i) of the first-order groups for the corresponding properties. Similarly, T_{m2i}, T_{b2i}, T_{c2i}, P_{c2i}, and T_{m3i}, T_{b3i}, T_{c3i}, and P_{c3i}, represent the contributions (D_j) and (E_k) of the second and third-order groups, respectively. Moreover, the T_{m0}, T_{b0}, T_{b0}, and P_{c0} are additional adjustable parameters of the estimation models or universal constants. The determination of the adjustable parameters of the models that is the contributions C_i, D_j, and E_k have been divided into a 3 steps regression procedure.

(1) Regression is carried out to determine the contributions (C_i) of the first-order groups and the universal constants of the models while w and z are set to zero.

(2) Then w is set to unity, z is set to zero and another regression, is performed using the C_i, and the universal constants are calculated in the previous step to determine the contributions (D_j) of the second-order groups.

(3) Finally, both w and z are assigned to unity and, using the universal constants of the models (C_i and D_j obtained as results of the previous steps), the contributions (E_k) of the third-order groups are determined.

The universal constants determined in the first step of the regression scheme are listed in Table 2.5.

Table 2.5 Value of the additional adjustable parameters [21]

Adjustable parameters (Universal constants)	**Value**	**Unit**
T_{m0}	147.450	K
T_{b0}	222.543	K
T_c	231.239	K
P_{c1}	5.9827	bar
P_{c2}	0.108998	$\text{bar}^{-0.5}$

2.5 GCA-EoS model

In order to predict the phase equilibrium in supercritical system of Doxorubicin that contains a wide variety of organo-oxygenated compounds, hydrocarbons and aromatic rings, the existence appropriate thermodynamic model is required. Due to the presence of association effect, size differences between solvents and solutes, and experimental limitation, Group Contribution with Association Equation of State (GCA-EoS) is the desirable thermodynamic model. Additional of Group-Contribution Association term to the GC-EoS model results in the GCA-EoS model. The GC-EoS is suitable for the modeling of non-polar or slightly polar mixtures, on the other hand, some limitation of MHV2 and PSRK Equation of State in the GC-EoS models such as low-molecular weight, similar size and very asymmetric mixtures are the obstacles in this work [5].

Several Equations of State-excess Gibbs or Helmholtz function models such as MHV1 and LCVM were applied to the GCA-EoS model for the prediction fluid–liquid equilibrium in this system. The GCA-EoS model takes explicit account of association effects with Wertheim's perturbation theory which has been used in Equation of State like the statistical associating fluid theory (SAFT), the Cubic Plus Association Equation of State (CPA), and the group contribution with association GCA -EoS equation [22].

There are 3 contributions to the residual Helmholtz energy in the GCA-EoS model consisting of repulsive, attractive, and associating. The repulsive and attractive contributions are based on Carnahan–Starling and NRTL models, respectively, and keep the same form as the original (GC-EoS) of Skjold Jørgensen.

$$A^{res} = A^{rep} + A^{att} + A^{assoc} \tag{2.2}$$

2.5.1 Repulsive term

In repulsive term, the important assumption is hard a sphere behavior of each substance in the mixture that is characterized by its critical hard sphere diameter of the pure compound molecular size, d_{ci}. Moreover, there is no need binary or higher-order parameter in other assumption of the hard sphere theorem. Carnahan–Starling follows the expression which is developed by Mansoori and Leland for mixtures of hard spheres [5].

$$\left(\frac{A}{RT}\right)^{rep} = 3\left(\frac{\lambda_1\lambda_2}{\lambda_3}\right)(Y-1)+\left(\frac{\lambda_2^3}{\lambda_3^2}\right)\left(Y^2-Y-lnY\right)+n\left(lnY\right) \tag{2.3}$$

With

$$Y = \left(1-\frac{\pi\lambda_3}{6V}\right)^{-1} \tag{2.4}$$

$$\lambda_k = \sum_{i=1}^{NC} n_i d_i^k \tag{2.5}$$

where n_i is the number of moles of component *i*, *NC* presents the number of components in the mixture, *n* the total number of moles, *V* the total volume and d_i the hard-sphere diameter per mol of species *i*. The following generalized expression is assumed for the hard-sphere diameter temperature dependence.

$$d_i = 1.065655 d_{ci}\left(1 - 0.12 exp\left(\frac{-2T_{ci}}{3T}\right)\right) \tag{2.6}$$

where d_{ci} and T_{ci} are the critical hard-sphere diameter and critical temperature of component *i*, respectively. The critical diameter d_{ci} is determined from the critical properties:

$$d_{ci} = \left(\frac{0.08943 RT_{ci}}{P_{ci}}\right)^{1/3} \tag{2.7}$$

2.5.2 Attractive term

For the evaluation of the attractive contribution to the residual Helmholtz energy, this accounts for dispersive forces between functional groups. It is a van der Waals type contribution combined with a density-dependent, local-composition expression based on a group contribution version of the NRTL-type expression. The attractive interactions are derived as follow [5]:

$$\left(\frac{A}{RT}\right)^{att} = -\frac{z}{2}\sum_{i}^{NC} n_i \sum_{j}^{NG} \upsilon_j^i q_j \sum_{k}^{NG} \frac{\left(\dfrac{\theta_k g_{kj} \tilde{q} \tau_{kj}}{RTV}\right)}{\sum_{k}^{NG} \theta_k \tau_{kj}} \tag{2.8}$$

with
$$\tilde{q} = \sum_{i}^{NC} n_i \sum_{j}^{NG} \upsilon_j^i q_j \tag{2.9}$$

$$\theta_k = \left(\frac{q_j}{\tilde{q}}\right)\sum_{i}^{NC} n_i \upsilon_k^i \tag{2.10}$$

$$\tau_{kj} = exp\left(\frac{\alpha_{kj} \Delta g_{kj} \tilde{q}}{RTV}\right) \tag{2.11}$$

$$\Delta g_{kj} = g_{kj} - g_{jj} \tag{2.12}$$

where *z* is coordination number (set equal to 10), υ_j^i is number of groups of type *j* in molecule *i*, q_j represents surface parameter of group *j*, $\tilde{q}$ denotes total number of surface segments, θ_k is surface fraction of group *k*, g_{kj} is attractive energy parameter for interaction between group *k* and *j*, and α_{kj} is NRTL non-randomness parameter.

The parameter for interactions between unlike groups is calculated from those between like groups:

$$g_{kj} = k_{kj}\left(g_{kk}g_{jj}\right)^{1/2} \tag{2.13}$$

where the binary interaction parameter k_{kj} is symmetrical ($k_{kj}=k_{jk}$). In addition, the attractive energy between like segments and the binary interaction parameter are temperature dependent:

$$g_{kk} = g_{kk}^{*}\left(1 + g_{kk}'\left(\frac{T}{T_k^{*}} - 1\right) + g_{kk}'' ln\frac{T}{T_k^{*}}\right) \tag{2.14}$$

$$k_{kj} = k_{kj}^{*}\left(1 + k_{kj}'' ln\left(\frac{2T}{T_k^{*} + T_j^{*}}\right)\right) \tag{2.15}$$

where g_{kk}^{*}, g_{kk}', g_{kk}'' are the pure-group attractive energy and k_{kj}^{*} and k_{kj}'' are the binary interaction parameter at the referent temperature T_k^{*} and $\left(T_k^{*} + T_j^{*}\right)/2$, respectively.

2.5.3 Association term

In the multi-component mixture that contained water, hydroxyl, carboxyl, ketone, and ester groups; the association effect is the third necessary contribution in the original Group Contribution Equation of State (GC-EoS). A well-known concept in association model is the chemical theory which defines the different of chemical species in the solution. Moreover statistical theory of Wertheim's theory that provides a relation between the residual Helmholtz function is the most widely-used concept for association effect. Several literatures have shown that Wertheim's expression for the Helmholtz function can be combined with the repulsive dispersion and attractive interactions in order to generate Equations of State for representing thermodynamic properties of associating systems. Therefore, the group contribution with association derived from Wertheim's statistical theory can combine with the original Group Contribution Equation of State (GC-EOS) of Skjold-Jorgensen [23].

In this work, the Helmholtz function due to the association is calculated with a modified form of the expression used in the Statistical Association Fluid Theory (SAFT) [5]:

$$\left(\frac{A}{RT}\right)^{assoc} = \sum_{k=1}^{NGA} n_k^{*}\left(\sum_{k=1}^{M_k}\left(lnX^{A_k} - \frac{X^{A_k}}{2}\right) + \frac{M_k}{2}\right) \tag{2.16}$$

The *NGA* represents the number of associating functional groups in the mixture, n_k^{*} the total number of moles of associating group *k*, M_k the number of associating sites assigned to associating group *k* and X^{A_k} is the mole fraction of group *k* that does not associate at site *A*. The total number of moles of associating group *k* expression is:

$$n_k^* = \sum_{m=1}^{NC} \upsilon_{assoc}^{(k,m)} n_m \tag{2.17}$$

where $\upsilon_{assoc}^{(k,m)}$ is the number of time associating group, *k* present in molecule m, n_m is the total number of moles of species *m*, and *NC* as total components in the mixture.

The expression of the mole fraction of group *k* that is not bound through the site *A* is determined by:

$$X^{A_k} = \left(1 + \sum_{k=1}^{NGA} \sum_{j=1}^{M_j} \rho_k^* X^{B_j} \Delta^{A_k B_j}\right)^{-1} \tag{2.18}$$

where the summation includes all number of associating groups in the mixture and M_j site. The mole fraction of group *j* is not bonded through the site *A*, X^{A_k} depends on the molar density of the associating group *k*, ρ_k^* and on the association strength, and $\Delta^{A_k B_j}$ between site *A* of group *k* and site *B* of group *j*:

$$\rho_k^* = \frac{n_k^*}{V} \tag{2.19}$$

$$\Delta^{A_k B_j} = \kappa^{A_k B_j} \left(exp\left(\frac{\varepsilon^{A_k B_j}}{kT} \right) - 1 \right) \tag{2.20}$$

The association strength is a function of temperature T (K) and the characteristic association parameters, ε and κ. These parameters have been proposed for a square-well model of specific interactions between the two sites *A* and *B*. The parameter ε characterizes the association energy (well depth) and κ (cm^3/mol) the associating volume (well width). The energy association, and hence the association strength between two like-sites from the same or different associating group are set equal to zero.

2.6 Rapid expansion of super critical solution (RESS) process

Several conventional techniques such as crushing, grinding, milling, spray-drying, freeze-drying, and re-crystallization have been utilized for particle size reduction in pharmaceutical industry. On the other hand, these conventional techniques are not environmental friendly due to the thermal and chemical degradation of products, large amounts of solvent use, associated disposal problems, particle size distributions, and solvent residues [18].

Rapid Expansion of Supercritical Solutions (RESS) is a promising new process for the production of small and uniform particles. Saturating supercritical fluid with the substrate rapidly depressurize through a heated nozzle into a low pressure chamber. This phenomena cause an extremely rapid nucleation of the substrate to small particles and uniform shape [24]. The main advantage of the RESS process is producing solvent free product. Moreover, this process needs no the purification unit, after expansion the solvent in gas phase can be recovered and recycled [18]. On the other hand, this concept can be implemented in simple equipment although particle collection from the gaseous stream is not easy. The applications are limited due to the soluble of substrates in the supercritical fluid that leads to profitable processes. Polar co-solvent may be added into non polar supercritical fluid for improving the solubility of substrate [24].

An equipment concept for the RESS process is represented schematically in Figure 2.4. According to Figure 2.4, the equipment comprises of two main sections: the extraction and the precipitation units. Solvent is pumped and preheated to the desired extraction pressure and temperature, respectively. Then the supercritical fluid is sent to the extraction unit. The substrate will dissolve for extracting the substrate until being saturated. After that the saturated supercritical solution with substrate is expanded through a capillary nozzle and expansion chamber. The capillary nozzle must be reheated to avoid plugging by substrate precipitation. The morphology of particle depends on the RESS parameters consisting of temperature, pressure, nozzle geometry, and distance of supersonic free jet region [24].

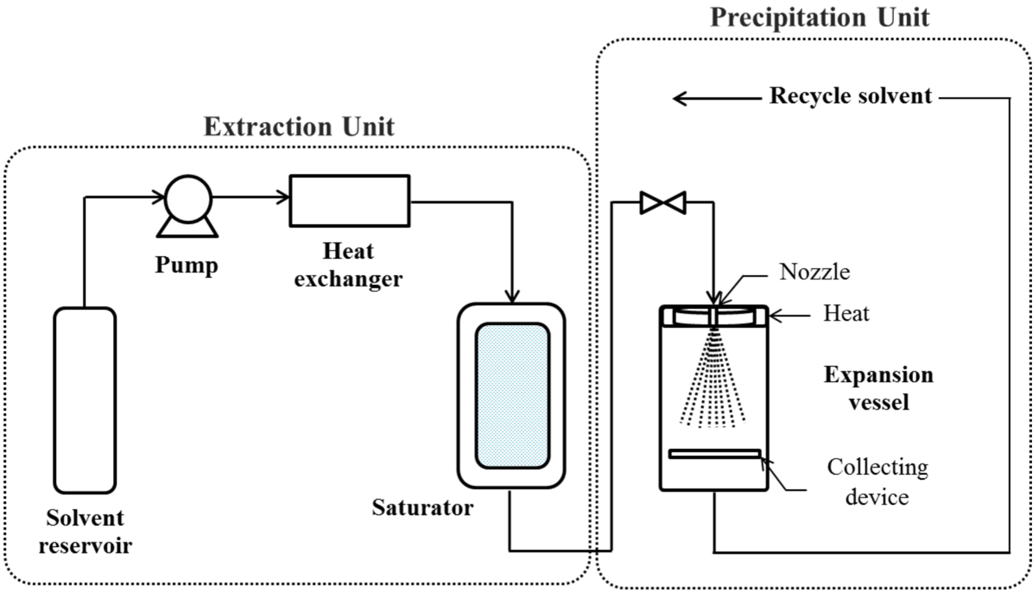

Figure 2.4 RESS equipment concept [24]

2.7 Particle formation

2.7.1 Mass, Momentum and Energy Conservation

Kwauk and Debenedetti [26] presented a mathematical model consisting of mass, momentum, and energy balances of dilute supercritical solution for particle formation during the expansion path. The flow is assumed to be steady, one-dimensional and invicid.

$$\frac{1}{\rho_1}\frac{d\rho_1}{dx}+\frac{1}{U}\frac{dU}{dx}+\frac{1}{\alpha}\frac{d\alpha}{dx}=0 \tag{2.21}$$

$$\frac{1}{\rho_2}\frac{d\rho_2}{dx}+\frac{1}{U}\frac{dU}{dx}+\frac{1}{\alpha}\frac{d\alpha}{dx}=-\frac{J}{U\rho_2} \tag{2.22}$$

$$\frac{1}{\rho_3}\frac{d\rho_3}{dx}+\frac{1}{U}\frac{dU}{dx}+\frac{1}{\alpha}\frac{d\alpha}{dx}=\frac{J}{U\rho_3} \tag{2.23}$$

where ρ_1, ρ_2 and ρ_3 are mass densities per unit total volume, U the velocity, α, the cross-sectional area of the nozzle, x the distance along the nozzle, and J the total condensation rate, that is to say, the mass of solute precipitating out of the fluid phase per unit total volume per unit time. The linear momentum equation reads

$$(\rho_1+\rho_2+\rho_3)U\frac{dU}{dx}+\frac{dP}{dx}=0 \tag{2.24}$$

The energy equation is given by

$$\frac{\rho_1}{m_1}\frac{d\bar{h}_1}{dx}+\frac{\rho_2}{m_2}\frac{d\bar{h}_2}{dx}+\frac{\rho_3}{m_2}\frac{dh_3}{dx}+\frac{J(h_3-\bar{h}_2)}{Um_2}+(\rho_1+\rho_2+\rho_3)U\frac{dU}{dx}=0 \tag{2.25}$$

where m_1 and m_2 are the solvent and solute molecular weights, $\bar{h}_1$ and $\bar{h}_2$ are the partial molar enthalpies of the solvent and solute, and h_3, is the molar enthalpy of the solid.

2.7.2 Particle formation model

Particle formation via the RESS process is considered in terms of initial homogeneous nucleation and subsequent growth phenomena. According to classical nucleation theory, the formation rate for stable critical-sized solute nuclei during homogeneous nucleation is strongly dependent on the degree of solute supersaturation. Specifically, the rate of nuclei formation (particle $s^{-1}cm^{-3}$) is given by Kwauk and Debenedetti [26].

$$I_t = a\left[\frac{P}{kT}\right]^2\left[\frac{2\sigma^{1/2}\upsilon}{(2\pi m)^{1/2}}\right]exp\left[\frac{-16\pi}{3}\left(\frac{\sigma}{kT}\right)^3\left(\frac{\upsilon}{lnS}\right)^2\right] \tag{2.29}$$

where a is the condensation coefficient (assumed to be unity for low vapor pressure solutes); P is the partial temperature in the gas phase of the solute, T is the absolute temperature; k is the Boltzmann constant. Moreover σ, υ, and m are the surface tension, molecular volume, and molecular mass of the condensed solute; and S is the ratio of solute concentration at a given point in the expansion to the saturation concentration under identical conditions.

CHAPTER 3 METHODOLOGY

3.1 Methodology

The propose of this work is the identification of the solubility of Doxorubicin (DOX) in modified co-solvent between carbon dioxide and methanol to predict the nucleation rate of particle formation in Rapid Expansion of Supercritical Solution (RESS) process by using mathematical model. The method of this work was derived into two main parts which were predicting the solubility of DOX in supercritical solution from Group Contribution with Association Equation of State (GCA-EoS) and nucleation rate from classical nucleation in precipitation unit. The schematic of this work is summarized in Figure 3.1 below:

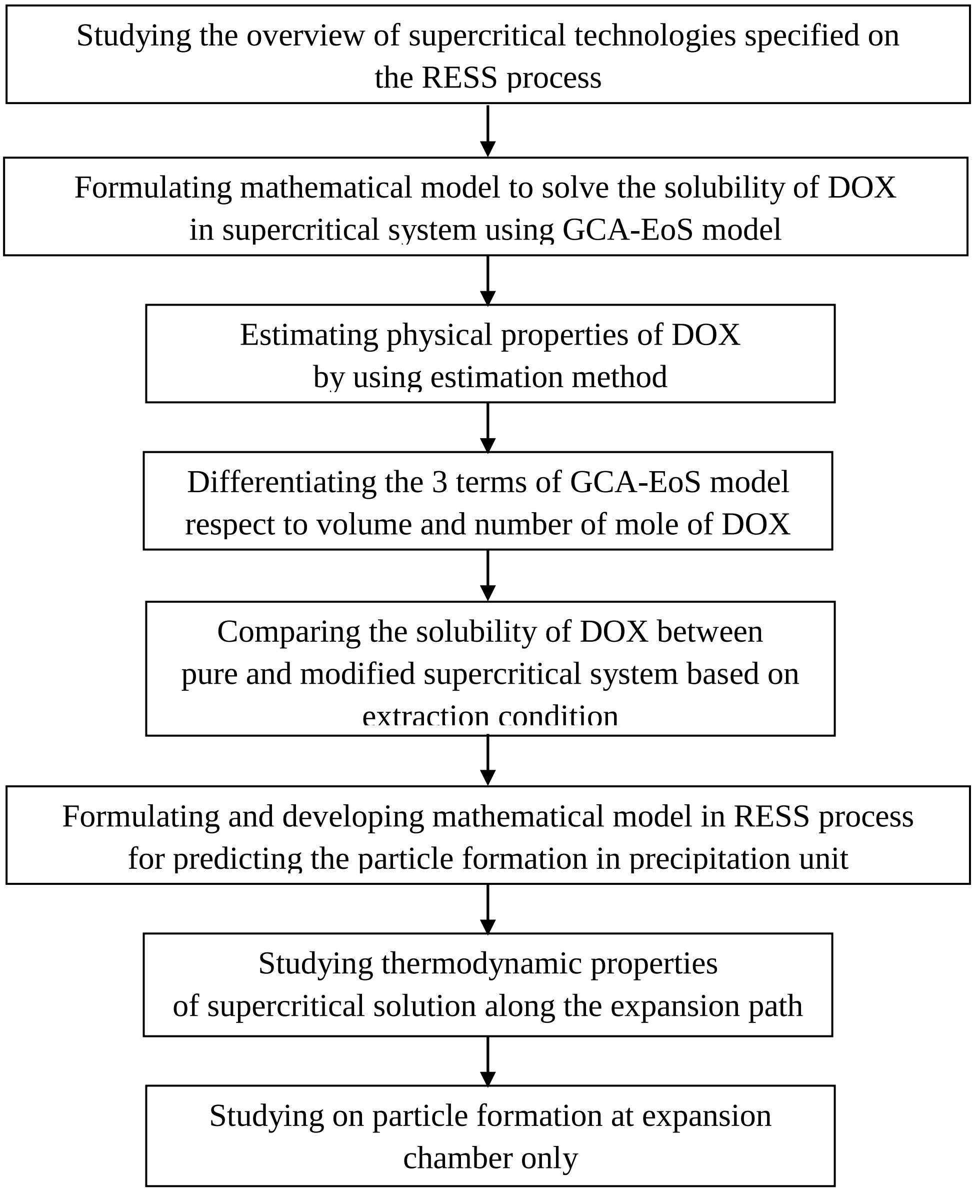

Figure 3.1 Schematic diagrams of methodology

3.1.1 Studying the overview of supercritical technology specified on the RESS process

First of all, overview of supercritical technology and RESS process was studied from international and local literature in order to understand the overall process. There were two main sections in the RESS process which are solubility of DOX in supercritical solution and particle formation. Moreover, gathering the information of RESS process including equipment, operating factor, and mathematical model were necessary.

3.1.2 Formulating mathematical model to solve the solubility of DOX in modified supercritical phase using GCA-EoS model

In this step, Group Contribution with Association Equation of State (GCA-EoS) was used as thermodynamic model for predicting the solubility of DOX in supercritical system. The solubility expression is shown Equation 3.1 below [28].

$$y_2 = \frac{P_2^{sat}\left(T\right) exp\left(\dfrac{\upsilon_2^{sat}\left(P - P_2^{sat}\left(T\right)\right)}{RT}\right)}{\phi_2 P} \tag{3.1}$$

where y_2 is equilibrium mole fraction of DOX in the supercritical phase, $P_2^{sat}(T)$ is solid-saturated vapor pressure at temperature, υ_2^{sat} is solute molar volume, and ϕ_2 is solute fugacity coefficient, and P is the operating pressure.

According to Equation 3.1, the solid-saturated vapor pressure and solute molar volume were obtained from estimation method of Lyman [29], whereas the solute fugacity and operating pressure were obtained from the GCA-EoS model, as described below.

3.1.2.1 Estimating physical properties of DOX from estimation method

The GCA-EoS was written as the summation of 3 residual Helmholtz energy (A^R) consisting of repulsive, attractive and association terms as shown in Equations (2.2 – 2.20). In addition, the repulsive term required critical properties of DOX as input parameters; therefore, estimation method was necessary to complete the predicting. Group Contribution estimation method of Marrero and Gani [21] was applied in this work because of high accuracy of the 3 levels of estimation. In this estimation step, the author validated the estimation results with the normal melting point of DOX, a validating point comparing with the previous work of Phongtummaruk [8]. Moreover, there are also many requirement parameters for attractive and association terms which are gathered from literatures and listed in this chapter.

3.1.2.2 Differentiating the 3 terms of GCA-EoS model respect to volume and number of mole of DOX

After estimating step, all of 3 terms of the Helmholtz energy consisting of repulsive, attractive, and association are differentiated with respect to volume of system and number of moles in order to investigate the solute fugacity coefficient and compressibility factor (*z*) following these equations.

$$ln\ \phi_i = \frac{\partial}{\partial n_i}\left[\frac{A^R}{RT}\right] \tag{3.2}$$

$$z = \frac{\partial}{\partial V}\left[\frac{A^R}{RT}\right] \tag{3.3}$$

where ϕ_i is solute fugacity coefficient, n_i is number of mole of component *i* in the system, A^R is residual Helmholtz energy, *R* is universal gas constant (cm^{3}bar mol^{-1}K^{-1}), *T* is extraction temperature (K), *z* is compressibility factor, and *V* is volume of extraction chamber (cm^3). The compressibility factor was applied to the thermodynamic equation for calculation pressure of system.

3.1.2.3 Comparing the solubility of DOX between pure and modified supercritical system based on extraction condition

After that the solubility of DOX in pure supercritical carbon dioxide and modified co-solvent were computed and compared when adding methanol 3, 4, and 5 mole percentages by using Equation (3.1). All of required parameters in GCA-EoS model were under the same extraction condition. The extractions of temperatures and pressures were studied in the range of 308.15 – 323.15 K, and 80 – 300 bar due to the limitation of DOX degradation temperature and GCA-EoS model.

3.1.3 Formulating and developing mathematical model in the RESS process to predict particle formation in precipitation unit

After that, the flow model equations can be formulated when the properties of supercritical solution are sufficient. The flow model through precipitation unit including subsonic and supersonic regions for predicting the particle formation was presented in form of mass, momentum and energy balance correlated to an extended generalized Bender Equation of State (egB-EoS). However, there were some assumptions used in this work in order to simplify mathematical model as described in this chapter.

3.1.3.1 Studying thermodynamic properties of supercritical solution along the expansion path

The thermodynamic properties of fluid; for example, velocity, density, temperature and pressure, were investigated along expansion path (subsonic and supersonic regions) under chosen pre-expansion temperature and pre-expansion pressure from extraction condition which were focusing on the range of 343.15 – 353.15 K, and 175 – 225 bar, respectively. However, the pre-expansion temperature should be higher than the extraction temperature in order to prevent phase changes of the solution and plugging due to precipitation along the subsonic region.

3.1.3.2 Studying on particle formation at expansion chamber only

The studied of crystallized DOX particle such as critical radius, concentration of critical nuclei, and nucleation rate were also investigated in the supersonic free jet region only. All of these predicting in each step will be solved by MATLAB^{TM}.

3.2 The requirements of parameter in GCA-EOS model

According to the mentioned repulsive, attractive, and association terms in Group Contribution with Association Equation of State (GCA-EoS) in Chapter 2, the requirements of parameter in the system such as critical temperature (T_c), critical pressure (P_c), pure group parameters, binary interaction parameters, and association parameters should be specific. In general, these parameters are obtained from the literature.

3.2.1 Repulsive parameters

The two requirements of parameter that were used in repulsive term were critical temperature and critical pressure of each component in the system. The high complication and toxic of DOX molecule caused the most important obstacle for getting the experimental thermodynamic data. Therefore, mathematical model of estimation will be used as the alternative method in order to estimate the two requirements of thermodynamic properties. In this work, two widely used estimation method are Joback and Reid [30], and Marrero and Gani [21] which were selected for the suitable one. The calculation detail of each method was shown in Appendix A.

Table 3.1 The critical properties parameters of DOX, carbon dioxide, and methanol using the method of Marrero and Gani [21]

Components	Critical properties	
	T_c (K)	P_c (bar)
DOX	1,083.01	12.95
CO_2[31]	304.13	73.75
Methanol [32]	513.15	79.54

**The critical properties of carbon dioxide and methanol were obtained from Hazardous Substances Data Bank (HSDB)

3.2.2 Attractive parameters

The attractive term is a group contribution version of NRTL model consisting of 5 pure group parameters and 3 binary interaction parameters. The two pure group of parameters, reference temperature (T^*) was assumed to be equal to 600 K and critical temperature for paraffinic or hydrocarbon groups, and coincided groups respectively. Moreover the surface parameter (q) was obtained as a UNIFAC model. While the other 3 energy parameters (g^*, g', and g'') in Equation (2.14) were adjustable parameters that estimated from vapor pressure data of pure compounds. The binary interaction parameters of each component consist of temperature dependence (k_{kj}^* and k_{kj}'') and the asymmetric non-randomness parameters (α_{kj}) in Equations 2.15 and 2.11, respectively.

In this work, the classification of pure group parameters was followed the two recent literatures which were Fornari [4] and Sanchez et al. [33]. This system consisted of one large solid component (DOX) and two kinds of solvent (carbon dioxide and methanol). Due to the size differences between DOX, carbon dioxide and methanol; DOX could be classified into simple functional groups in order to study attractive force in the system. DOX molecule could be classified into 9 simple functional groups which were paraffin, aromatic ether, phenol, primary alcohol, secondary alcohol, tertiary alcohol, ketone, ether, and primary amines as shown in Figure 3.2 below. However, both of the solvents are specified the functional group by its molecule. Therefore, there are eleven pure groups parameter in this work.

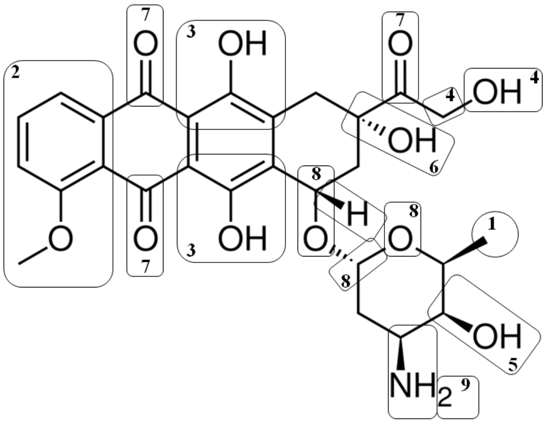

Figure 3.2 Classification and numbering of DOX into pure chemical group

Figure 3.2, represented the nine simple functional group in DOX molecule which were labeled the number of each group. The attractive parameters of the 5 pure group parameters (T^*, q, g^*, g', and g'') and the 3 binary parameters (k^*_{kj}, k''_{kj}, and α_{kj}) in GCA-EoS for this work were listed and numbered in Tables 3.2-3.5.

Table 3.2 The GCA-EOS pure-group parameters of this system [4, 33]

Group	**T^*(K)**	**q**	**g^* (atm cm^6 mol^{-2})**	**g'**	**g''**
1) -CH_3 [4]	600	0.848	316,910	-0.9274	0
2) ≥aC-OCH_3 [4]	600	1.208	514,800	-0.9771	0
3) ≥aC-OH [4]	600	0.680	1,336,000	0.7042	-1.2295
4) -CH_2OH [4]	512.6	1.124	1,207,500	-0.6441	0
5) >CHOH [4]	512.6	0.908	1,207,500	-0.6441	0
6) >COH [4]	512.6	0.714	1,207,500	-0.6441	0
7) -CH_2CO- [4]	600	1.180	888,410	-0.7081	0
8) -CH_2O- [4]	600	0.780	503,700	-0.9821	0
9) -$CHNH_2$ [33]	430.05	0.942	768,254	-0.4510	-0.0581
10) CO_2 [4]	304.2	1.261	531,890	-0.5780	0
11) CH_3OH [4]	512.6	1.432	1,109,600	-0.9474	0

The functional group of DOX is defined into 9 groups, showed and labeled the number in Figure 3.2 and Table 3.2 above. On the other hand, there were many excess and lack functional groups represented in Figure 3.3 below.

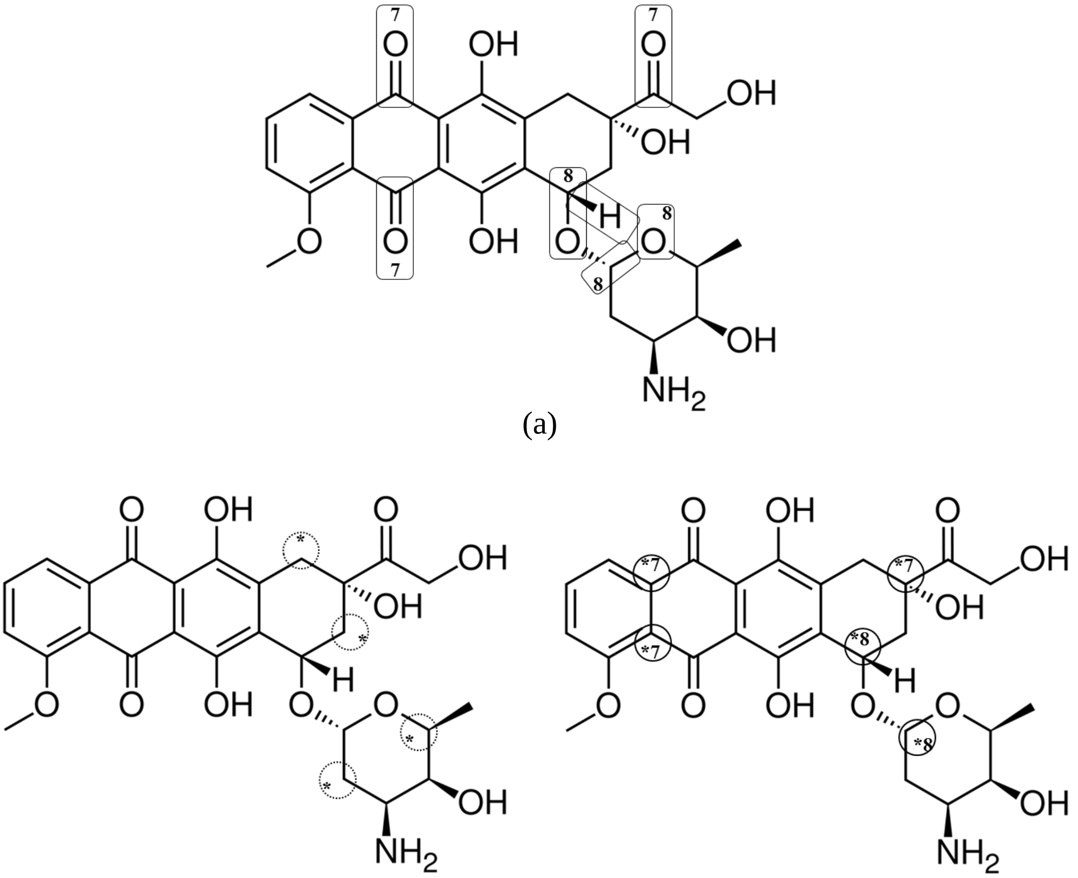

(a)

(b)

(c)

Figure 3.3 Functional group specification in DOX molecule (a) the seventh and eighth simple functional group based on Figure 3.2, (b) lack functional group, and (c) excess functional group

According to Figure 3.3 (a) – (c), the excess and lack functional groups were represented in a solid circle and dash circle, respectively. The 3 excess carbon atoms and 6 hydrogen atoms resulted from the definition of the seventh functional group (CH_2-CO) as shown in Figure 3.3 (a). The definition of this group includes the atom in the solid circle with number as seven in Figure 3.3 (c). The support reasons are; firstly, aromatic ether in the second functional group (≥aC-OCH_3) in Figure 3.2 was completely defined 6 carbon atoms in aromatic ring. Moreover, there are only 2 classifications of ketone functional group, primary ketone (-CH_3CO) and secondary ketone (-CH_2CO-). Therefore, the suitable one was the secondary ketone which included a carbon atom and 2 hydrogen atoms. Furthermore, the eighth functional group (-CH_2O-) or ether group specified 2 excess hydrogen atoms. These excess molecules were compensated to the lack 4 carbon atoms, and 7 hydrogen atoms were shown in the dash circle in Figure 3.3 (b).

Table 3.3 The GCA-EOS binary interaction parameters (k^{*}_{kj}) [4, 33]

Group	**1**	**2**	**3**	**4**	**5**	**6**	**7**	**8**	**9**	**10**	**11**
1[4]		0.940	0.894	0.715	0.715	0.715	0.834	0.924	0.8608	0.892	0.811
2[4]	0		1.075	NA	NA	NA	NA	NA	NA	1.047	NA
3[4]	0	0		NA	NA	NA	NA	NA	NA	1.094	NA
4[4]	0	NA	NA		1	1	0.953	NA	NA	0.985	0
5[4]	0	NA	NA	0		1	0.953	NA	NA	0.985	0
6[4]	0	NA	NA	0	0		0.953	NA	NA	0.985	0
7[4]	0.084	NA	NA	0	0	0		NA	NA	1.025	0
8[4]	-0.056	NA	NA	NA	NA	NA	NA		NA	1.042	NA
9[33]	-0.0219	NA	NA	NA	NA	NA	NA	NA		NA	NA
10[4]	0	0	0	0	0	0	0.108	0	NA		0.009
11[4]	0	NA	NA	1.016	1.016	1.085	0.959	NA	NA	0.945	

Table 3.4 The GCA-EOS binary interaction parameters (k''_{kj}) [4, 33]

Group	**1**	**2**	**3**	**4**	**5**	**6**	**7**	**8**	**9**	**10**	**11**
1[4]		0	0	0	0	0	0.084	-0.056	-0.0219	0	0
2[4]	0.940		0	NA	NA	NA	NA	NA	NA	0	NA
3[4]	0.894	1.075		NA	NA	NA	NA	NA	NA	0	NA
4[4]	0.715	NA	NA		0	0	0	NA	NA	0	1.016
5[4]	0.715	NA	NA	1		0	0	NA	NA	0	1.016
6[4]	0.715	NA	NA	1	1		0	NA	NA	0	1.085
7[4]	0.834	NA	NA	0.953	0.953	0.953		NA	NA	0.108	0.959
8[4]	0.924	NA	NA	NA	NA	NA	NA		NA	0	NA
9[33]	0.8608	NA	NA	NA	NA	NA	NA	NA		NA	NA
10[4]	0.892	1.047	1.094	0.985	0.985	0.985	1.025	1.042	NA		0.945
11[4]	0.811	NA	NA	0	0	0	0	NA	NA	0.009	

Table 3.5 The GCA-EOS binary interaction parameters (α_{kj}) [4, 33]

Group	**1**	**2**	**3**	**4**	**5**	**6**	**7**	**8**	**9**	**10**	**11**
1[4]		0	0	1.471	1.471	1.471	0.854	0	1	3.369	0.836
2[4]	0		0	NA	NA	NA	NA	NA	NA	0	NA
3[4]	0	0		NA	NA	NA	NA	NA	NA	0	NA
4[4]	10.220	NA	NA		0	0	0	NA	NA	-0.390	0
5[4]	10.220	NA	NA	0		0	0	NA	NA	-0.390	0
6[4]	10.220	NA	NA	0	0		0	NA	NA	-0.390	0
7[4]	5.146	NA	NA	0	0	0		NA	NA	0.170	0.576
8[4]	0	NA	NA	NA	NA	NA	NA		NA	0	NA
9[33]	1	NA	NA	NA	NA	NA	NA	NA		NA	NA
10[4]	3.369	0	0	0.468	0.468	0.468	0.170	0	NA		0.130
11[4]	2.335	NA	NA	0	0	0	0.576	NA	NA	0.205	

3.2.3 Association parameters

Association effect is a kind of attractive force which is strong and high. In this effect, hydrogen bonding of any compound in the mixtures is the major role of this effect. In order to describe the association effect in this work, the following associating groups were considered: alcohol or hydroxyl group (-OH), primary amine group (-NH_2), and ketone group (-CO-) that has two, one, and one associating sites in its molecule, respectively. The two sites of hydroxyl group (2B) consisting of electronegative and one electropositive site, while the one site (1A) of primary amine and ketone group is electronegative site. Moreover, the capable of two hydroxyl group can self- and cross-associate with any group that has electronegative or electropositive site. On the other hand, the negative site of both primary amine and ketone group cannot be self-associated but can be cross-associated with any group that was electropositive site like hydroxyl group.

However, the effect of self-association is normally dominated in determining the value of a coefficient activity at infinite dilution. The previous work of Phongtummaruk [8] of DOX in pure supercritical carbon dioxide only took an interest in self-association effect of hydroxyl groups in DOX molecule. As a result of this work, addition of another associating group in DOX molecule (primary amine and ketone group) was concentrated. Nevertheless, steric hindrance is the limitation of self-association even with the existence of co-solvent molecule like methanol.

The following assumptions of the modified systems of DOX in pure supercritical carbon dioxide (base case) have been considered:

(1) Due to the fact that steric effect is complicated and, only four hydroxyl groups (OH), one primary amine, and one ketone (CO) group in DOX molecule are the associating groups in the systems of DOX in pure supercritical carbon dioxide as shown in the Figure 3.4 below.

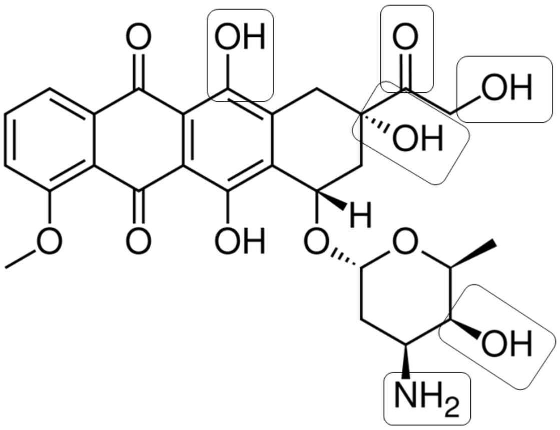

Figure 3.4 Associated hydroxyl (OH) and ketone (CO) groups of DOX molecule in pure supercritical carbon dioxide

(2) This system is full of excess carbon dioxide molecules as a supercritical solvent is up to 300 times comparing to the DOX. In addition, the molecular size of DOX is very large. Therefore, selectivity of the 3 associating group forming hydrogen bonding between DOX molecules is not significant. In this case, DOX molecule will associate each other in specified arrangement. As a consequence, each of associating groups which are hydroxyl, primary amine, and ketone has the same probability to form hydrogen bonding.

The schematic of self- and cross- association between DOX molecules in pure supercritical carbon dioxide is shown in Figure 3.5. The probability of the less hydroxyl group (aromatic ring) to form the hydrogen bonding with the other associating groups is quite low because it is the same plane with oxygen atom from ketone group and ether group. Electronegative force from the two neighbor oxygen atoms will force with the hydrogen atom in the less hydroxyl group. That means the electronegative and electropositive forces of the less hydroxyl group are not strong enough comparing to the four hydroxyl group. Then the less hydroxyl group cannot be the associating group.

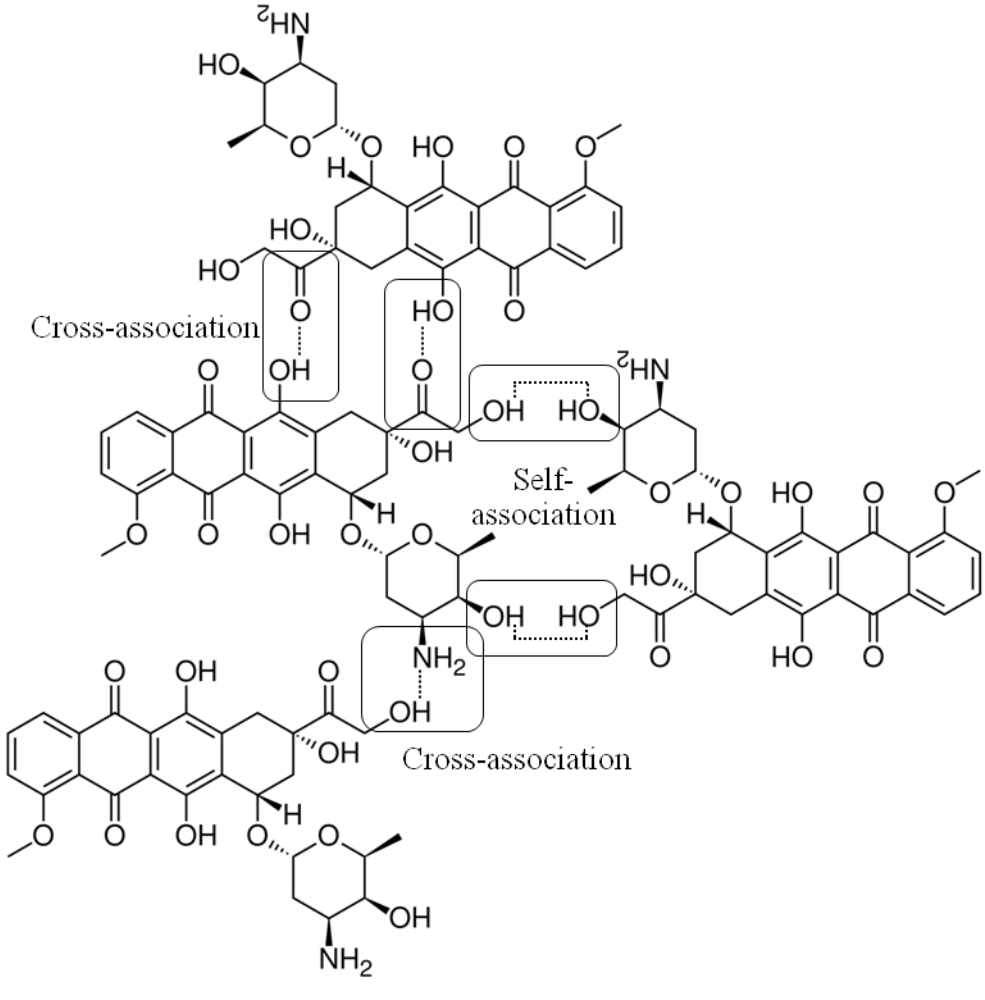

Figure 3.5 Schematic of self- and cross- association DOX molecule in pure supercritical carbon dioxide

Furthermore, in the assumptions of the modified systems of DOX in supercritical carbon dioxide and methanol as a modifier (modified case) these following things are taken into consideration.

(1) The associating groups in DOX molecule in this system is considered as well as pure supercritical carbon dioxide system. In this case, the reactivity of the 3 associating groups is the determination to form hydrogen bond.
(2) Due to a large number of reactive molecule of methanol comparing to DOX molecule (up to 5.5 times), methanol becomes the main selected molecule in order to form hydrogen bond with the 3 associating groups in DOX molecule and its molecule.
(3) The priority of association groups from the highest to the lowest are hydroxyl, primary amine, and ketone group, respectively.
(4) Therefore, the first to the fourth hydroxyl group in methanol modified co-solvent will associate with the fourth hydroxyl groups in DOX molecule~~,~~ first.
(5) Then the less hydroxyl group in methanol modified co-solvent will associate with the primary amine, and ketone groups in DOX molecule will be followed by group of priority.

The schematic of self- and cross- association of DOX in supercritical carbon dioxide and methanol as a modifier is shown in Figure 3.6 below.

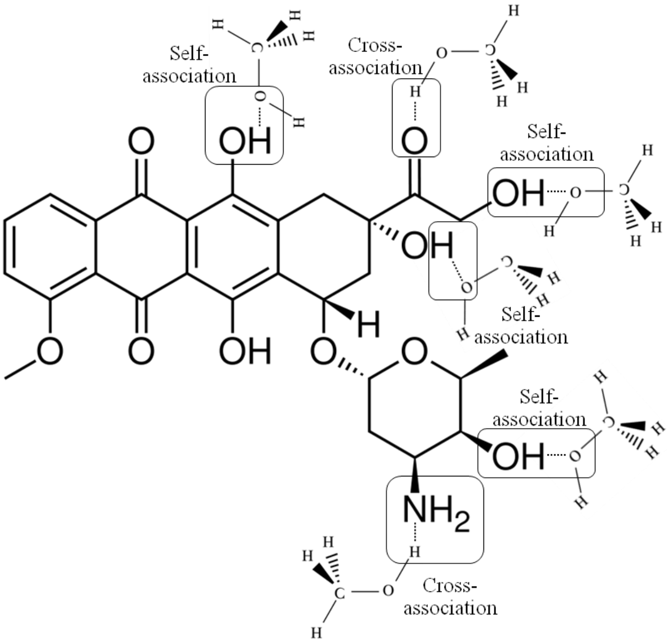

Figure 3.6 Schematic of self- and cross- association of DOX in supercritical carbon dioxide and methanol as a modifier

In order to model the association effect in Group Contribution with Association Equation of State (GCA-EoS), it is necessary to determine number of associating groups, number of active sites in each associating group and the value of the corresponding association strength. The associating group in the two system of DOX in pure supercritical carbon dioxide and supercritical carbon dioxide with methanol as a modifier are summarized in Table 3.6.

Table 3.6 Associating groups, their active sites, and type of association effect in DOX and methanol molecule [34]

Molecule	**Associating Groups**		**Number of active sites**	**Kind of active sites**	
				Electronegative	**Electropositive**
DOX	Hydroxyl (-OH)	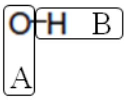	2	1 (A)	1 (B)
	Primary amine (-NH_2)	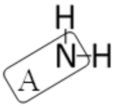	1	1 (A)	-
	Ketone (CO)	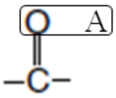	1	1 (A)	-
Methanol	Hydroxyl (-OH)	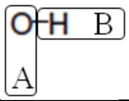	2	1 (A)	1 (A)

The corresponding association strengths consist of energy ($\varepsilon^{A_kB_j}$) and volume ($\kappa^{A_kB_j}$) of association parameters which follow the Wertheim's theory in statistical associating fluid theory (SAFT) equation. The association strengths were obtained by reproducing the fraction of non-bounded molecules predicted by SAFT equation. The corresponding self- and cross- association parameters are shown in Table 3.7.

Table 3.7 Energy ($\varepsilon^{A_kB_j}$) and volume ($\kappa^{A_kB_j}$) of association parameters for self- and cross- association in both systems of DOX in pure supercritical carbon dioxide and supercritical carbon dioxide with methanol as a modifier [33, 34]

Associating Site *A*	**Associating Groups *k***	**Associating Site *B***	**Associating Groups *j***	**Energy ($\frac{\varepsilon^{A_kB_j}}{k}$) (K)**	**Volume ($\kappa^{A_kB_j}$) (cm^3/mol)**
A	OH	B	OH	2,700 [34]	0.8621[34]
B	OH	A	OH	2,700 [34]	0.8621[34]
		A	NH_2	3,049 [33]	0.5418 [33]
		A	CO	2,485 [34]	0.5000 [34]

3.3 Modeling of particle formation

In the following part, saturated solution of supercritical fluid with dissolved solute was sent to expansion device consisting of capillary nozzle and expansion chamber as shown in Figure 3.7. This work, the expansion path was considered only in 2 regions, subsonic (capillary nozzle) and supersonic free jet (expansion chamber) region. The expanding fluid was accelerated from the pre-expansion condition to a supersonic free jet in the expansion chamber, negligible the inlet region. Due to the low solute solubility in the supercritical phase, solid mole fraction around 10^{-11}, the thermodynamic model would be performed considering the mixture of supercritical fluid between carbon dioxide and methanol only along the expansion path. Moreover, over the distance, x along the expansion path, the flow was described by conservation of mass, momentum, and energy correlated to an extended generalized Bender Equation of State (egB-EoS). Since the diameter of capillary nozzle is very small, the property of the supercritical fluid can be approximated as one dimensional flow. In addition, the simplifying assumptions, such as steady state, adiabatic and inviscid are applied in this model.

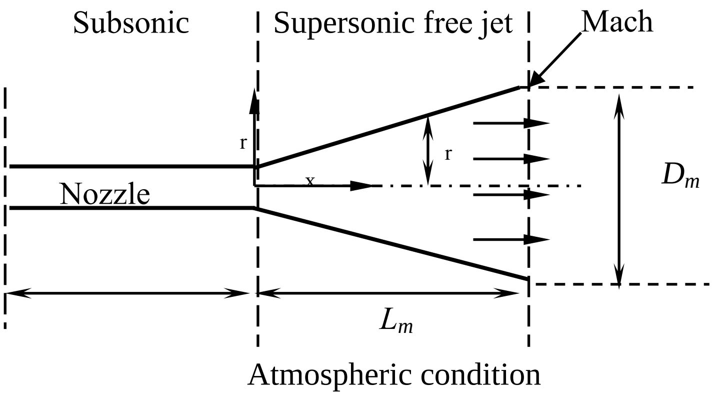

Figure 3.7 Schematic drawing of the rapid expansion parts

In this work, mathematical model was used for investigating the physical properties of supercritical fluid inside the capillary nozzle and expansion chamber and also predicting the particle formation. According to Figure 3.7, the inlet started as capillary nozzle as well as connecting with atmospheric pre-expansion chamber where supersonic free jet region occur. The capillary nozzle had a centimeter and 50 micrometers diameter. The shape of supersonic free jet was assumed to be conical whereas the boundary of supersonic free jet was characterized by the distance of Mach disk from capillary nozzle exit as shown in Equation 3.4. [35]

$$L_m = 0.67 D_{nozzle} \sqrt{\frac{P_{pre}}{P_{post}}} \tag{3.4}$$

$$D_m = 0.5625 L_m \tag{3.5}$$

where L_m is a Mach distance or length of supersonic free jet region (cm), D_{nozzle} is a diameter of capillary nozzle (cm), P_{pre} is a pre-expansion pressure (MPa), P_{post} is pressure inside expansion chamber (MPa), and D_m denotes diameter of Mach (cm).

3.3.1 Modeling of flow field in subsonic region

The governing equation used to calculate the flow field in both capillary nozzle and expansion chamber regions is the mass, momentum, and energy balances along the axial (x) distance. In both regions, the flow was performed for mixed solution between carbon dioxide and methanol due to the dilute solid soluble in mixed solution. In addition, the flow is assumed to be steady state and one dimensional flow along the x distance due to micro scale of capillary nozzle diameter.

For the subsonic (capillary nozzle) region, the main assumptions are followed.

(1) Adiabatic
(2) Friction lost between fluid and capillary nozzle wall
(3) Mach number at the end of capillary nozzle equals to unity
(4) Estimating the properties of fluid along the subsonic region by mixing rules
(5) No phase change and particles forming during the expansion

The set of governing equation following these assumptions [35]:

$$\rho \frac{dv}{dx} + v \frac{d\rho}{dx} = 0 \tag{3.6}$$

$$\rho v \frac{dv}{dx} + \frac{dP}{dx} = \frac{-2 f \rho v^2}{D_{nozzle}} \tag{3.7}$$

$$\frac{dH}{dx} + v \frac{dv}{dx} = 0 \tag{3.8}$$

where, ρ is density (g cm^{-3}), v is velocity (ms^{-1}), P is pressure (MPa), f is the fanning friction factor (assumed to be 0.005), H is the specific enthalpy, and x is the distance along the nozzle (cm).

According to Equations (3.7) – (3.8), two parameters consisting of pressure (P) and specific enthalpy (H) have to be rearranged in density (ρ) and temperature dependent form following these expressions [36]:

$$\frac{dH}{dx}=\left[C_v+RT\left(\frac{\partial z}{\partial T}\right)_\rho+Rz\right]\frac{dT}{dx}+\left[RT\left(\frac{\partial z}{\partial \rho}\right)_T-RT^2\left(\frac{\partial z}{\partial T}\right)_\rho\right]\frac{d\rho}{dx} \quad (3.9)$$

$$\frac{dP}{dx}=\left(\frac{\partial P}{\partial \rho}\right)_T\frac{d\rho}{dx}+\left(\frac{\partial P}{\partial T}\right)_\rho\frac{dT}{dx} \quad (3.10)$$

where C_v is heat capacity at constant volume, R is gas constant, and z is compressibility factor. The compressibility factor and pressure expression are derived from generalized Bender Equation of State (egB-EoS) expression that is also particularly accurate near the critical region [37].

$$P(\rho,T)=\rho T\left(R+B\rho+C\rho^2+D\rho^3+E\rho^4+F\rho^5+\left(G+H\rho^2\right)\rho^2 exp\left(-a_{20}\rho^2\right)\right) \quad (3.11)$$

where ρ is the solvent density (g/cm^3), P is the pressure (MPa), T is the temperature (K), and R is the universal constant for gases considered on a weight basis. The *B, C, D, E, F, G,* and *H* coefficients are defined by means of polynomial expressions which are temperature dependent and also are correlated with 20 coefficients of the Bender Equation of State a_1-a_{20}.

$$B=a_1-\frac{a_2}{T}-\frac{a_3}{T^2}-\frac{a_4}{T^3}-\frac{a_5}{T^4} \quad (3.12)$$

$$C=a_6+\frac{a_7}{T}+\frac{a_8}{T^2} \quad (3.13)$$

$$D=a_9+\frac{a_{10}}{T} \quad (3.14)$$

$$E=a_{11}+\frac{a_{12}}{T} \quad (3.15)$$

$$F=\frac{a_{13}}{T} \quad (3.16)$$

$$G=\frac{a_{14}}{T^3}+\frac{a_{15}}{T^4}+\frac{a_{16}}{T^5} \quad (3.17)$$

$$H=\frac{a_{17}}{T^3}+\frac{a_{18}}{T^4}+\frac{a_{19}}{T^5} \quad (3.18)$$

The expression of compressibility factor (z) is derived by normalizing density and temperature with their corresponding critical properties ρ_C and T_C respectively. Moreover, the parameter a_{20} is also approximated from $1/\rho_C^2$ [37].

$$Z=1+B^*\delta+C^*\delta^2+D^*\delta^3+E^*\delta^4+F^*\delta^5+\left(G^*+H^*\delta^2\right)\delta^2 exp\left(-\delta^2\right) \quad (3.19)$$

With the temperature functions:

$$B^* = e_1 - \frac{e_2}{\tau} - \frac{e_3}{\tau^2} - \frac{e_4}{\tau^3} - \frac{e_5}{\tau^4} \tag{3.20}$$

$$C^* = e_6 + \frac{e_7}{\tau} + \frac{e_8}{\tau^2} \tag{3.21}$$

$$D^* = e_9 + \frac{e_{10}}{\tau} \tag{3.22}$$

$$E^* = e_{11} + \frac{e_{12}}{\tau} \tag{3.23}$$

$$F^* = \frac{e_{13}}{\tau} \tag{3.24}$$

$$G^* = \frac{e_{14}}{\tau^3} + \frac{e_{15}}{\tau^4} + \frac{e_{16}}{\tau^5} \tag{3.25}$$

$$H^* = \frac{e_{17}}{\tau^3} + \frac{e_{18}}{\tau^4} + \frac{e_{19}}{\tau^5} \tag{3.26}$$

where B^*, C^*, D^*, E^*, F^*, G^*, and H^* are functions of the generalized Bender Equation of State depending on the reduced temperature, $e_1 - e_{19}$ is the generalized parameter of the Bender Equation of State while δ and τ are the normalized parameters ($\delta = \rho / \rho_C$ and $\tau = T / T_C$). The generalized parameter of the Bender Equation of State (e_i) and the coefficients of the Bender Equation of State ($a_1 - a_{19}$) are a function of acentric factor (ω) and polar factor (χ).

$$e_i = e_i(\omega, \chi) \tag{3.27}$$

$$e_i = g_{4,i} + g_{1,i}\omega + g_{2,i}\chi + f^{res}(\omega, \chi) \tag{3.28}$$

$$f^{res}(\omega, \chi) = g_{3,i}\omega\chi + g_{5,i}\chi^2 \tag{3.29}$$

and $$a_i = e_i f_i \tag{3.30}$$

The expression of acentric factor and polar factor mixing rule are shown below [37].

$$\omega_m = \sum_k x_k \omega_k \tag{3.31}$$

$$\chi_m = \sum_k x_k \chi_k \tag{3.32}$$

The critical properties of mixture are investigated from mixing rules for the pseudo-pure parameters following these equations [37].

$$T_{cm} = \frac{1}{v_{cm}^{\eta_m}} \sum_k \sum_j x_k x_j v_{c_{kj}}^{\eta_m} T_{c_{kj}} \tag{3.33}$$

$$T_{c_{kj}} v_{c_{kj}}^{\eta_m} = \sqrt{\left(T_{c_k} T_{c_j}\right)\left(v_{c_k} v_{c_j}\right)^{\eta_m}}\, k_{kj} \tag{3.34}$$

$$v_{cm} = \sum_k \sum_j x_k x_j v_{c_{kj}} \tag{3.35}$$

$$v_{c_{kj}} = \frac{1}{8}\left(v_{c_k}^{1/3} + v_{c_j}^{1/3}\right)^3 \xi_{kj} \tag{3.36}$$

$$\eta_m = \frac{1}{1/2N(N-1)} \sum_k \sum_{j>k} \left(x_k + x_j\right)\eta_{kj} \tag{3.37}$$

where x is mole fraction, v is molar volume, and N is umber of component, while k_{kj}, ξ_{kj}, and η_{kj} are binary parameters for interaction between species k and j.

Table 3.8 Critical temperature (T_c), critical pressure (P_c), critical density (ρ_c), molecular weight, acentric factor (ω), and polar factor (χ) of both carbon dioxide and methanol [37]

Component	**Critical properties**			**Molecular Weight**	**Acentric factor**	**Polar factor**
	Temperature (K)	**Pressure (MPa)**	**Density (g/cm^3)**			
Carbon dioxide	304.21	7.38610	0.4743	44.010	0.21304	0.003971
Methanol	512.580	8.10300	0.2720	32.000	0.56520	0.037655

Sonic condition, where Mach number at the exit of capillary nozzle equals to unity, is used as criteria to determine the initial velocity of saturated supercritical solvent due to the unmeasured initial velocity. Mach number is the velocity divided by sonic velocity (w_s), and the expression of sonic velocity is given below [35]:

$$w_s = \sqrt{\frac{C_p}{C_v}\left(\frac{dP}{d\rho}\right)_T} \tag{3.38}$$

where C_p and C_v are heat capacity at constant pressure and volume, respectively. The expression of C_v relates to the C_p following Equation (3.39) below [38]:

$$C_v = C_p - T\left(\frac{\partial V}{\partial T}\right)_P \left(\frac{\partial P}{\partial T}\right)_P \tag{3.39}$$

The heat capacity at constant pressure (J/mol K) of pure carbon dioxide and methanol in gas phase can be expressed in a function of temperature following these expressions [39].

$$C_{p,CO_2} = 27.437 + 4.2315\times10^{-2}T - 1.9555\times10^{-5}T^2 + 3.9968\times10^{-9}T^3 - 2.9872\times10^{-13}T^4 \quad (3.40)$$

$$C_{p,MeOH} = 40.046 - 3.8287\times10^{-2}T + 2.4529\times10^{-4}T^2 - 2.1679\times10^{-7}T^3 + 5.9909\times10^{-11}T^4 \quad (3.41)$$

3.3.2 Modeling of flow field in supersonic free jet region

The governing equation for investigating the flow field in expansion chamber regions is similar to the governing equation in the capillary nozzle. The saturated supercritical fluid will expand along the Mach distance which is estimated from Equation (3.4) under atmospheric condition. Moreover, the extended generalized Bender Equation of State (egB-EoS) is also used to estimate physical properties of the supercritical solution between carbon dioxide and methanol along the expansion path by differentiation of pressure and compressibility expression with respect to density and temperature. The main assumptions are followed.

(1) Steady-state
(2) One-dimensional flow (axial direction)
(3) No drag force
(4) The expansion shape is assumed to be conical in horizontal direction
(5) Non adiabatic
(6) Initial conditions are the condition at the exit of capillary nozzle.
(7) Estimating the properties of fluid along the subsonic region by mixing rules
(8) Estimating the height of horizontal conical (*r*) from the middle by using linear law following the expression below in centimeter scale.

$$r = \frac{D_{nozzle}}{2} + \frac{\left(D_m - D_{nozzle}\right)}{2L_m}x \quad (3.41)$$

where D_{nozzle} is the diameter of capillary nozzle, D_m and L_m are Mach diameter and Mach distance obtained from Equations (3.4 - 3.5). Moreover, *x* is the distance from the capillary nozzle exit (starting at zero value).

The set of governing equations following above assumptions [35]:

$$\rho\frac{dv}{dx} + v\frac{d\rho}{dx} + \frac{\rho v}{A}\frac{dA}{dx} = 0 \quad (3.42)$$

$$\rho v\frac{dv}{dx} = -\frac{dP}{dx} \quad (3.43)$$

$$\frac{dH}{dx} + v\frac{dv}{dx} = \frac{dQ}{dx} \quad (3.44)$$

where *A* is flow area (πr^2) and *Q* is heat loss by convection as shown below [35]:

$$Q = h(T - T_{out})s \tag{3.45}$$

Where h is heat transfer coefficient (assumed to be 1.0×10^{7} W/m^{2}K), T_{out} is the temperature in expansion chamber (ambient temperature), and s is surface area of supersonic free jet $\left(\pi r\sqrt{r^2+x^2}\right)$.

3.3.3 Modeling of particle formation in supersonic free jet region

The driving force for particle formation growth is a supersaturation ratio (S) of the expanding solution. The supersaturation ratio is a measure of the phase saturation level. That means the supersaturation level can be considered as the potential of particle formation in the system. The expression of supercritical ratio is defined as follows [35]:

$$S = \frac{y_E(T_E, P_E)}{y^*(T, P)} \tag{3.45}$$

where $y_E(T_E, P_E)$ is the solute equilibrium mole fraction at extraction temperature which is calculated from Equation (3.3) and pressure whereas, $y^*(T, P)$ is the solute equilibrium mole fraction at prevailing temperature and pressure of the fluid during the expansion.

The classical nucleation rate is expressed following the expression below [26]:

$$I = 2N_2 \frac{Py_2}{\sqrt{2\pi MW_2 L^{-1} kT}} \sqrt{\frac{\sigma\left(\upsilon_2^{sat}\right)^2}{kT}}\, exp\left\{-\frac{16\pi}{3}\left(\frac{\sigma\left(\upsilon_2^{sat}\right)^{2/3}}{kT}\right)^3 \left(\frac{1}{lnS}\right)^2\right\} \tag{3.46}$$

where I represents nucleation rate (particle/cm^{3}s), N_2 is fluid phase solute concentration, P is the pressure of system (MPa), y_2 is solid solubility (mole fraction), σ is solid-fluid interfacial tension (N/m), υ_2^{sat} is solid molecular volume, MW_2 is solid molecular weight, L is Avogadro number (1/mol), k is Boltzmann's constant (J/K), T is temperature (K), and S is supersaturation ratio.

The fluid phase solute concentration is a function of solute liquid density (ρ_l), which is calculated from the following equation [36]:

$$N_2 = \frac{L\rho_l}{MW_2} \tag{3.47}$$

The liquid density (ρ_l) and solid-fluid interfacial tension (σ) ware estimated by Grain's method.

The critical nucleus size and the number concentration of critical nuclei are given by Equations (3.48 - 3.49), respectively. These equations serve for a system composed of homogeneous nucleation and supersaturation ratio larger than unity [36].

$$r^* = \frac{2\sigma\upsilon_2^{sat}}{kT(lnS)} \tag{3.48}$$

where r^* is critical size of nucleus (m).

$$N^* = N_2 exp\left\{-\frac{16\pi}{3}\left(\frac{\sigma\left(\upsilon_2^{sat}\right)^{2/3}}{kT}\right)^3\left(\frac{1}{lnS}\right)^2\right\} \tag{3.49}$$

where N^* is number concentration of critical nuclei (particle cm^{-3}).

CHAPTER 4 RESULTS AND DISCUSSION

4.1 Validation of Group-Contribution base estimate method

Due to the lack of critical properties data for Doxorubicin (DOX), a suitable estimation method is required. Group contribution base estimate method is a new method performed at 3 levels of estimation for significantly improving both of accuracy and applicability. After the estimate method has been performed, the validation of result with the experimental data is necessary to verify the accuracy of the model.

However, the normal melting point is the only one property of DOX which has been obtained from many sources such as experimental, literature, or medical handbook, etc. Moreover, another substance with molecular weight and molecule structure close to DOX, for instance, normally Daunorubicin, Cytochalasin D, also lacks critical properties data. As a result, the normal melting point of DOX is used to validate the model of estimation. The validation is divided into 2 main sections which are validation with another widely-used prediction method of Joback and Reid [30], and the previous work of Phongtummaruk [8]. In the validation of previous work, consideration is given to the efficiency of estimation method, Marerro and Gani [21], with the other molecule in which the DOX molecule is not considered. In this work, the efficiency of the Marerro and Gani method with the experimental normal melting point data of DOX will be focused. The results of the model validation with the widely-used method and the previous work are shown in Tables 4.1 and 4.2, respectively.

Table 4.1 Comparing the accuracy between two widely-used group contribution prediction methods for normal melting point

Estimation method	Normal melting point (K) (referent data)	Estimation value (K)	%Error
1. Group contribution (Marrero and Gani)	503.15	556.23	10.55
2. Joback and Reid method	503.15	1,309.99	160.36

According to Table 4.1, the referenced normal melting point is obtained from *Handbook of Chemistry and Physics 88th Edition 2007-2008*. The estimated normal melting points of DOX from the method of Marrero and Gani [21] and Joback and Reid [30] method were approximately 556.23, and 1,309.99 K, respectively. The error between the referenced and estimation values indicates that the method of Marrero and Gani has a significant higher reliability than that of Joback and Reid. According to the assumption of Joback and Reid method, neglected intermolecular interaction and molecular symmetry lead to high error of estimation. The detail and procedure of each estimation method is shown in Appendix A. Thus, the Marrero and Gani method was more applicable to estimate the normal boiling point and the critical properties in this work.

Table 4.2 Comparing the accuracy of normal melting point (T_m) estimation between the previous work of Phongtummaruk [8] and this work.

Estimation level	**Summation of group contribution normal melting point (T_m) parameters in each level**	
	Previous work	**This work**
First (1^{st})	63.5060	44.4791
Second (2^{nd})	4.2261	1.8094
Third (3^{rd})	-	-3.2068
Total	**67.5844**	**43.4817**

According to Table 4.2, it shows that the level of estimation is quite different between the previous work and this work, especially in the first and the third level of estimations. The details and the procedure of each estimation method are shown in Appendix B. In the group contribution, estimation method of Marrero and Gani was performed in 3 levels. In the first level, sets of simple groups to describe a large variety of complex organic compounds will be specified while in the second and the third level of estimation, the substituent group on aromatic or cycloaliphatic compound, and polyfunctional compound will be described respectively. Therefore, DOX compound needs all of the 3 levels of estimation in order to be more accurate due to the complicated polyfunctional group in DOX molecule.

The summation of 3 levels estimation is the value on the right hand side of the Equation (2.1) in order to convert this value into normal melting point by using the left hand site equation in Table 2.4. Finally, the result indicates that the normal melting points are about 621.58 K, and 556.23 K for the previous work and this work, respectively. Comparing with validating point, the result from this work is perceived as being better with 10.55% errors.

4.2 GCA-EoS in extraction unit

In the extraction unit, the most important parameter is solubility of DOX in pure supercritical carbon dioxide and the modified co-solvent with methanol. Group Contribution with Association Equation of State (GCA-EoS) is the suitable equation of state for predicting the compressibility factor (z) and fugacity coefficient of DOX in supercritical phase (ϕ_i), since GCA-EoS is not necessary to be conducted in this experiment in order to identify binary parameters. On the other hand, the binary parameters in most cubic equations of states such as Peng-Robinson and Soave modification of Redlich-Kwong etc can be done by fitting the experimental data curve. The compressibility factor and fugacity coefficient expression are derived from differentiating 3 terms of residual Helmholtz energy in GCA-EoS with respect to volume and numbers of mole, respectively.

In this work, the extracting temperature is varied from 308.15 to 323.15 K depending on the extraction temperature of Taxol, a chemotherapy drug which has a normal melting point close to DOX, in pure supercritical carbon dioxide for preventing thermal degradation of solute compound. Furthermore, the general encapsulation temperature of DOX is about 343.15 – 353.15 K which is acceptable with the extraction temperature and the boiling point of methanol co-solvent (337.85 K). In addition, the extracting pressure is also varied from supercritical pressure pure of carbon dioxide to 300 bars due to the limitation of GCA-EoS.

4.2.1 The compressibility factor of system (*z*)

The compressibility factor (*z*) of system includes 3 components: DOX, supercritical carbon dioxide and methanol (modified co-solvent system) at various temperature and pressure ranges between 308.15 to 323.15 K, and 80 to 300 bar, respectively. The calculated compressibility factor from repulsive, attractive, and association effect in residual Helmholtz energy expression are shown in Figures 4.1 - 4.3 below.

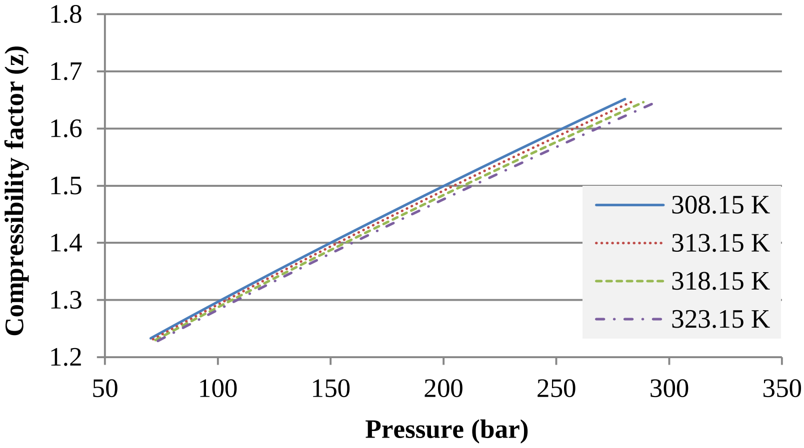

Figure 4.1 Calculated compressibility factor (*z*) of the system of DOX in pure supercritical carbon dioxide correlated with pressure (bar) at various temperatures

According to Figure 4.1, Group Contribution with Association Equation of State (GCA-EoS) gives the compressibility factor trend of DOX in the system of pure supercritical carbon dioxide at various temperatures and pressures in form of straight line. On the other hand, the compressibility factor is the inverse proportion with the temperature. While there is a slight change in a small value of pressure, the compressibility factor is sharply increased. This means that increasing pressure will affect the volume of fluid more than temperature.

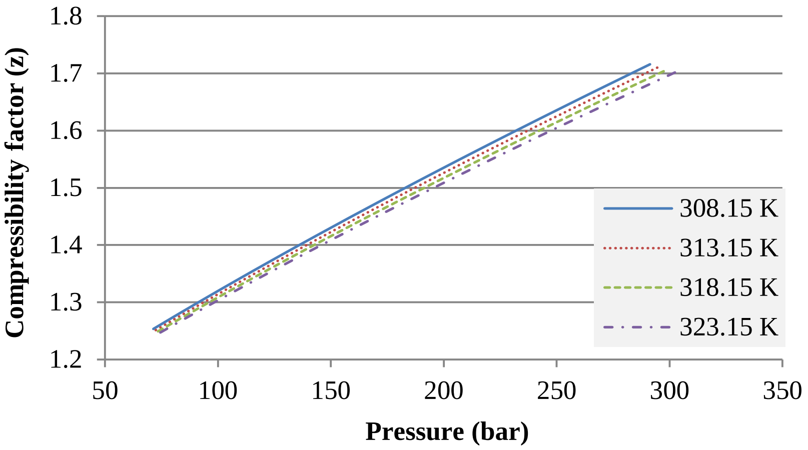

(a)

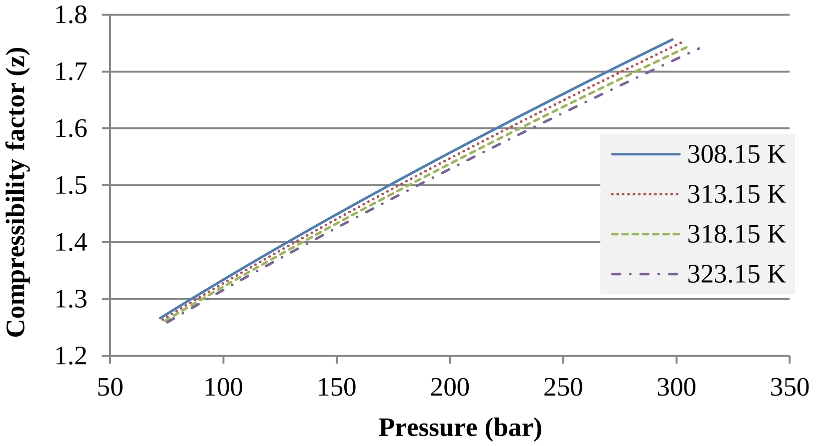

(b)

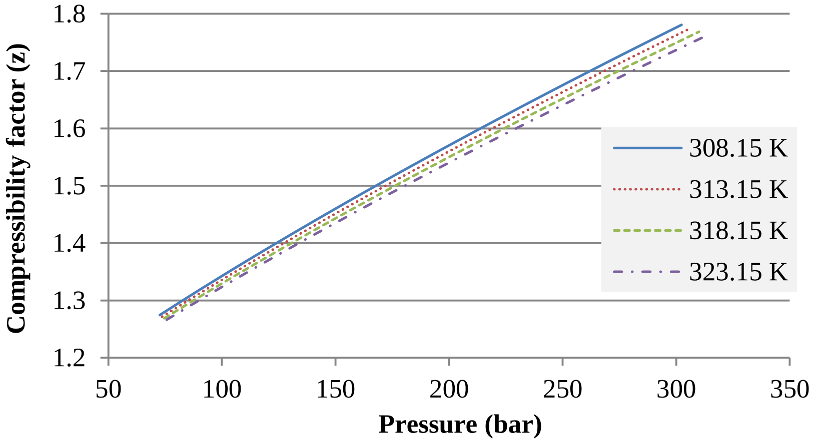

(c)

Figure 4.2 Calculated compressibility factor (z) of the system of DOX in supercritical carbon dioxide with added methanol as a modified co-solvent (a) 3, (b) 4, and (c) 5 mole percentage correlated with pressure (bar) at various temperatures

Figure 4.2 (a) – (c), shows the trend of compressibility factor for 3 ratios of methanol (3, 4, and 5 percent mole) as a modified co-solvent in the supercritical carbon dioxide. The trend is the same as the pure supercritical carbon dioxide. However, adding polar compound as modified co-solvent makes the compressibility of the system higher than the pure supercritical carbon dioxide system due to the interaction between methanol, carbon dioxide, and DOX as shown in Figure 4.3 below. The interaction makes the modified co-solvent system move further from ideal system with no interaction between molecules.

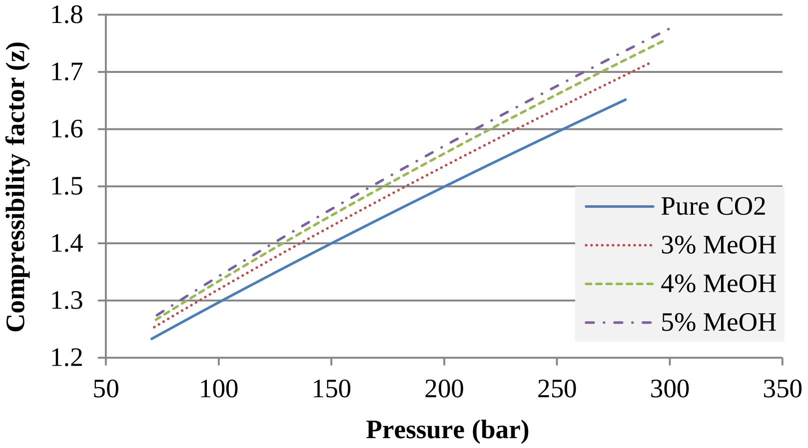

Figure 4.3 Calculated compressibility factor (z) of the system of DOX in modified co-solvent of supercritical carbon dioxide and methanol at constant temperature (308.15 K) correlated with pressure (bar) at various ratio of modified co-solvent

According to this figure, adding the polar compound as a modified co-solvent in the supercritical non-polar compound at constant temperature causes the compressibility factor to be higher than the ideal compressibility (z equal to unity). As shown in this figure, the increase of compressibility factor in every one mole percent of methanol from 3 to 4 percent is more significant than 4 to 5 percent. Moreover, the trend of the increment is the same with any temperature.

4.2.2 Fugacity coefficient of DOX in supercritical phase (ϕ_i)

The fugacity of DOX in supercritical phase is one of the most important properties which are calculated from the expression of residual Helmholtz function by differentiating the Helmholtz energy with respect to number of mole of that component at constant volume and the other component. This parameter is used for calculating solubility of DOX in both systems of supercritical phase: pure carbon dioxide and modified co-solvent between methanol and carbon dioxide.

In the system of pure supercritical carbon dioxide, the differentiated result indicates that the variation trend of fugacity coefficient of DOX in supercritical phase inverses to the pressure significantly. The decrease of fugacity coefficient is dominant when the pressure of the system increases from 80 to 125 bar. After that, the fugacity decreasing effect is not dominant comparing from the lower pressure to the pressure reaching 200 bar. On the contrary, fugacity coefficient is the direct proportion to the temperature, but the increment of fugacity coefficient is not dominant comparing with the pressure effect. However, after 200 bar both of the temperature and the pressure do not affect the fugacity coefficient. As demonstrated in Figure 4.4 (a), the value of fugacity coefficient is less than unity, which means that the behavior of supercritical fluid is different from the ideal gas.

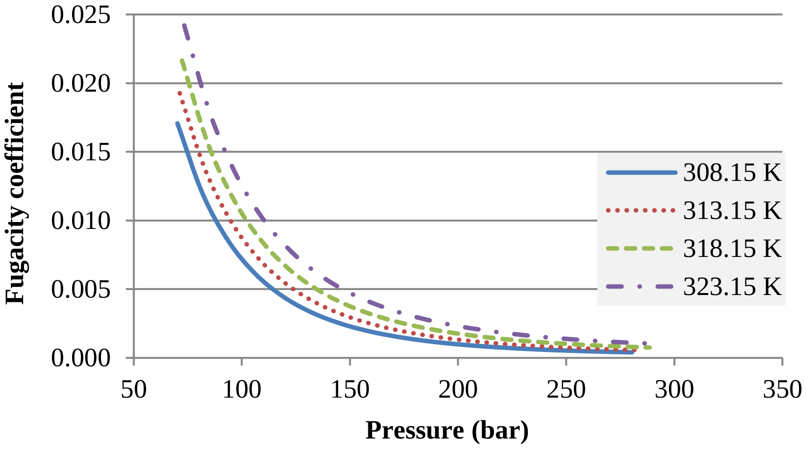

(a)

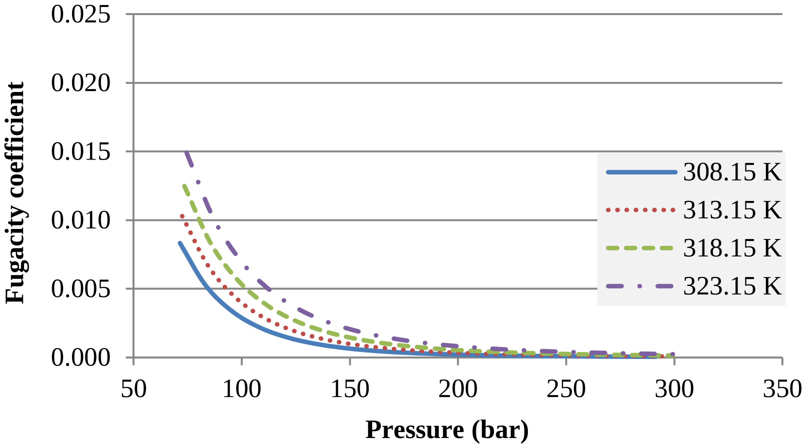

(b)

Figure 4.4 Calculated fugacity coefficient (ϕ_i) of DOX in (a) pure supercritical carbon dioxide, (b) modified co-solvent of supercritical carbon dioxide and methanol (x_{CO_2} = 0.97) correlated with pressure (bar) at various temperature

According to Figure 4.4 (b), when adding polar compound as a modified co-solvent into supercritical non-polar solvent, the trend of fugacity coefficient is the same as the pure supercritical solvent. Due to the interaction between molecules, especially DOX and polar modified co-solvent, adding polar compound at the same extraction condition will make the system become further from the ideal system as shown in the Figure 4.5 (a) – (d) below. Moreover, the trend of fugacity coefficient of DOX in supercritical phase at any ratio of polar compound is the same as that in Figure 4.4 (b).

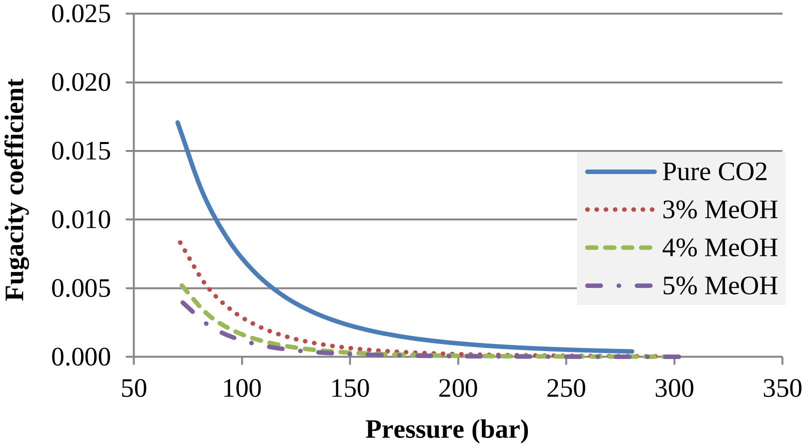

(a)

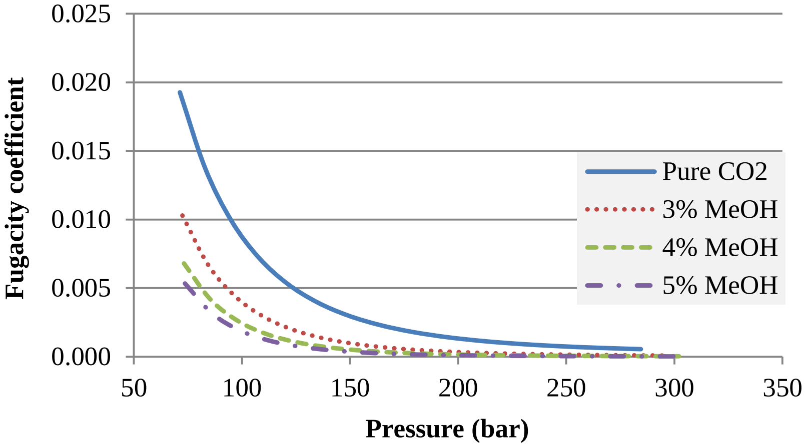

(b)

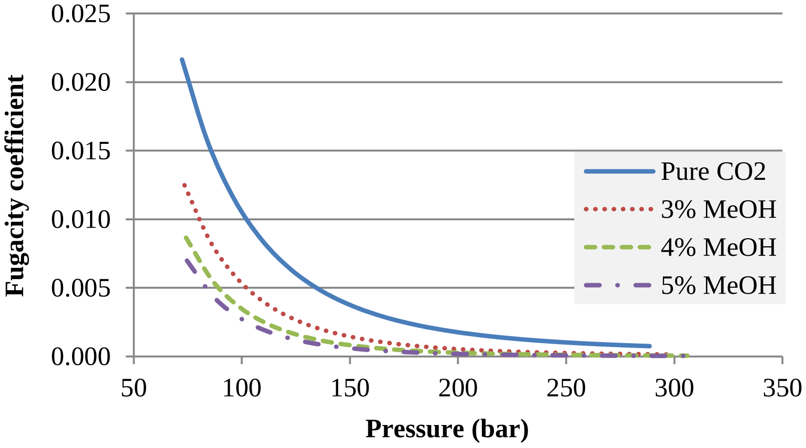

(c)

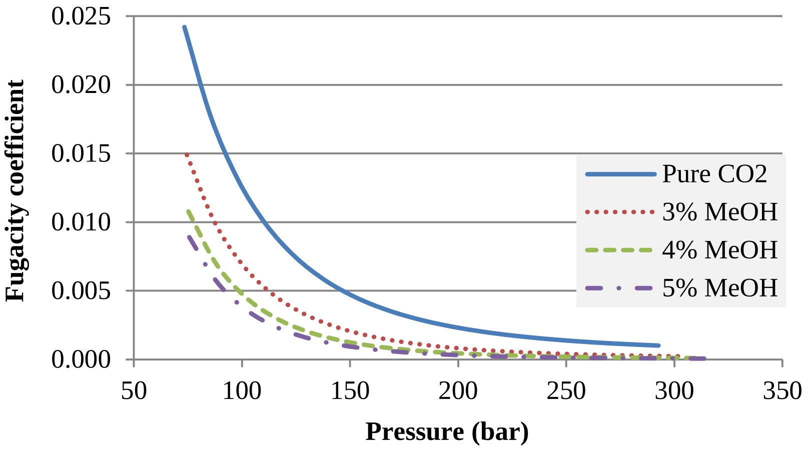

(d)

Figure 4.5 Calculated fugacity coefficient (ϕ_i) of DOX in pure supercritical carbon dioxide and modified co-solvent at constant temperature (a) 308.15 K, (b) 313.15 K., (c) 318.15 K, and (d) 323.15 K correlated with pressure (bar) at various ratio of methanol as a modified co solvent

Figure 4.5 (a) – (d) shows the trend of fugacity coefficient of DOX in two systems of supercritical phase: pure carbon dioxide and modified co-solvent between methanol and carbon dioxide at any temperature. As illustrated in these figures, the 3 values of mole percentage of modified co-solvent are not significant when the extraction pressure reach more than 150 bar at any temperature. The increasing of modified co-solvent increment from 3 to 4 mole percentage is more significant than 4 to 5 mole percentage.

4.2.3 Solubility of DOX in supercritical phase

In the solubility equation as shown in equation 3.1, two important estimation parameters which are molar volume of pure solid and saturated vapor pressure should be estimated by using the method of Lyman [29]. The detail and procedure of this estimation of the two parameters are shown in Appendix A. Moreover, there are two important required parameters from Group Contribution with Association Equation of State (GCA-EoS) which are fugacity coefficient of DOX in supercritical phase and pressure of system that is calculated from compressibility factor. Finally, the solubility is reported in the mole fraction of solute in the system.

In this part, we will consider about the effect of adding polar compound as a modified co-solvent into non-polar supercritical fluid comparing with the pure non-polar supercritical alone at any extraction condition will be considered. Moreover, validation of GCA-EoS model and estimation method is investigated by using the solubility of DOX in water as a validating point due to the lack of experimental data if DOX is in supercritical fluid.

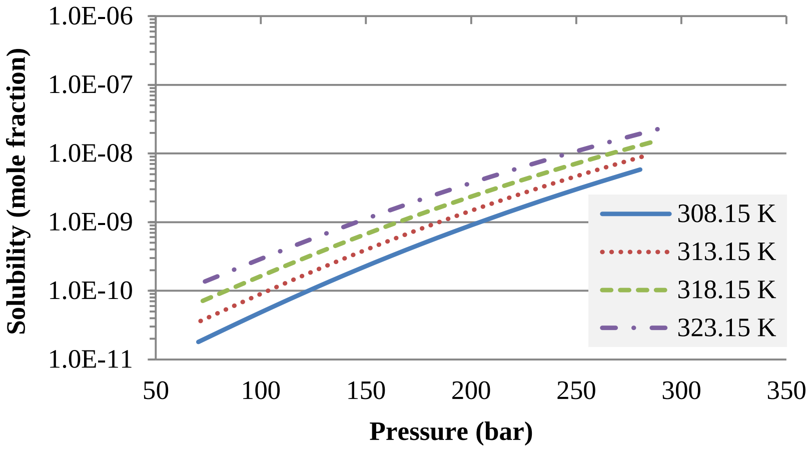

Figure 4.6 Solubility of DOX in pure supercritical carbon dioxide correlated with pressure (bar) at various extraction temperatures

According to Figure 4.6, the solubility range of DOX in pure supercritical carbon dioxide is varied from 10^{-11} to 10^{-8} along with the extraction temperature and pressure due to more polar functional groups. As represented in this figure, the effect extraction temperature is significantly higher than extraction pressure. As every 5 degree temperature increased, the increasing of solubility is doubled. In contrast, the times increased are lower when increasing operating pressure up to 300 bar. This phenomenon indicates that the heat from extraction temperature will break down the holding bond such as hydrogen bonding between solute molecules. Moreover, when the pressure increases, the supercritical solvent molecule will close to the solute molecule more than it is at low pressure. Therefore, the solute will dissolve in supercritical solvent easier.

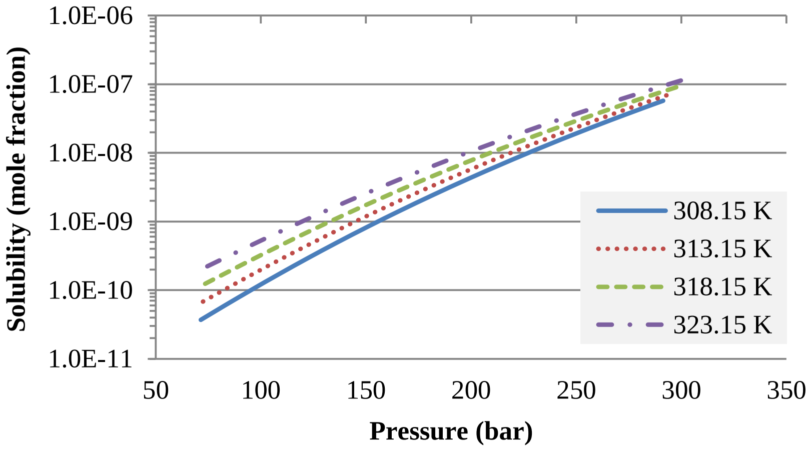

Figure 4.7 Solubility of DOX in modified co-solvent of supercritical carbon dioxide and 3 mole percentage of methanol correlated with pressure (bar) at various extraction temperatures

According to Figure 4.7 solubility of DOX in modified co-solvent varies from 10^{-11} to 10^{-6} along the extraction temperature and pressure. As every 5 degree temperature increase, the increasing of solubility in modified co-solvent system will be reduced comparing with the system of pure supercritical carbon dioxide. Moreover when the pressure reaches to 250 bar, the solubility of DOX in supercritical phase with modified co-solvents is not affected by the extraction temperature.

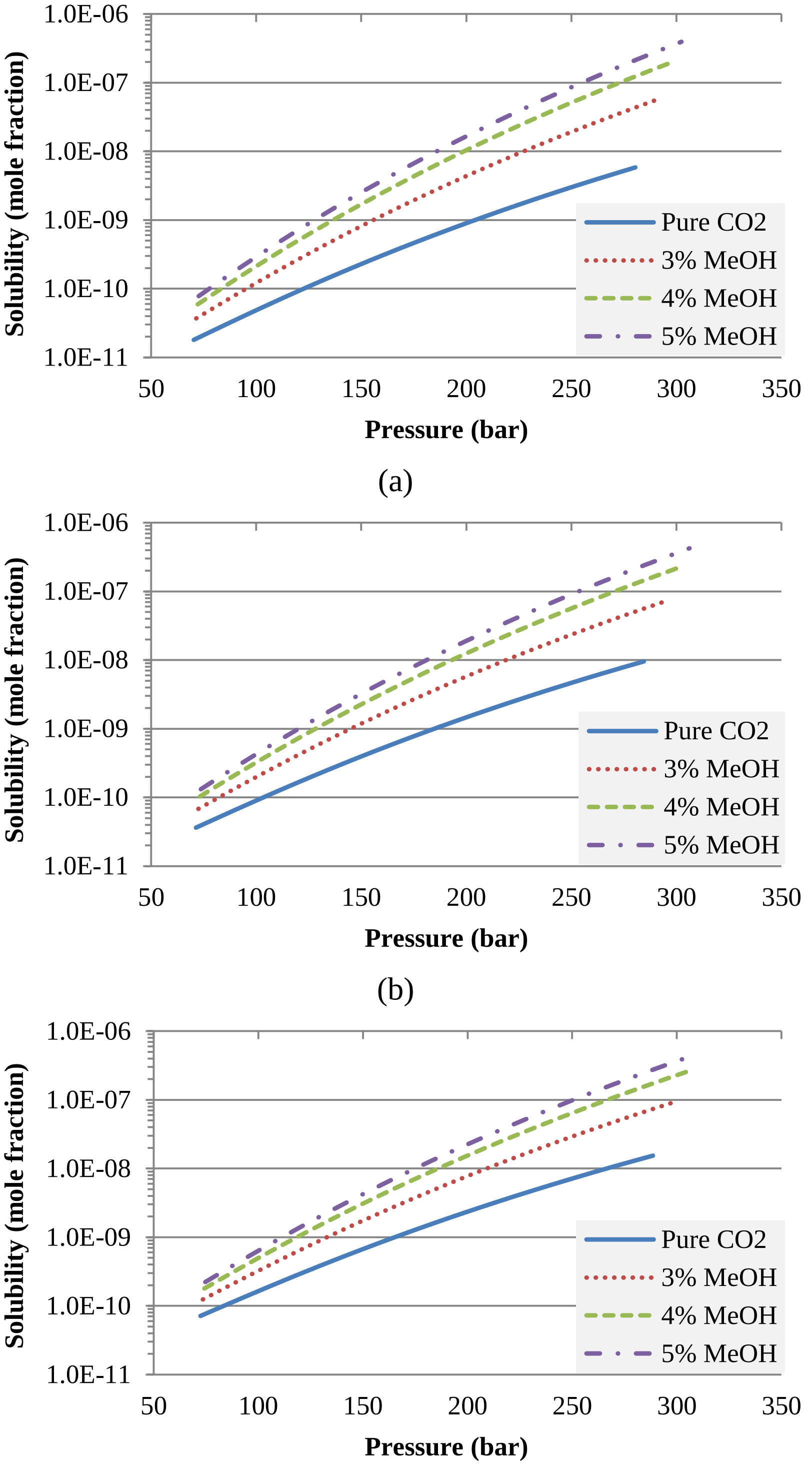

(a)

(b)

(c)

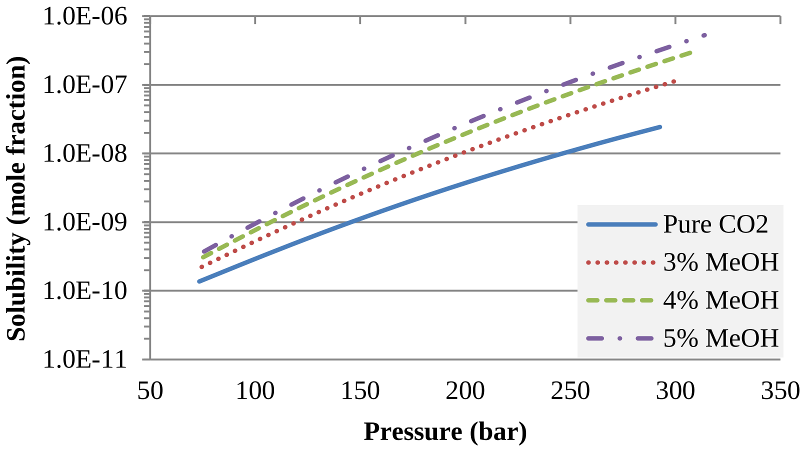

(d)

Figure 4.8 Solubility of DOX in pure supercritical carbon dioxide and modified co-solvent at constant temperature (a) 308.15 K, (b) 313.15 K, (c) 318.15 K, and (d) 323.15 K correlated with pressure (bar) at various ratio of methanol as a modified co-solvent

As represented in Figure 4.8, at any temperature the solubility of DOX in supercritical phase with modified co-solvent is significantly higher than the pure supercritical carbon dioxide system. When adding the polar compound into non-polar supercritical compound, the polar compound will break down the attractive forces between solute molecules like hydrogen bonding. This effect will support the effect of temperature for breaking molecule bonding down. As shown in these figures, more amounts of modified co-solvent are added into nonpolar supercritical phase and more solubility is increased at the same extraction temperature and pressure. At the low extraction temperature, the effect of adding polar modified co-solvent into non-polar supercritical system is more significant than the extraction temperature at the same extraction pressure. This phenomenon indicates that the effect of extraction temperature is more important than polar modified co-solvent effect for breaking down the intermolecular force. In addition, the effect of extraction pressure to the methanol as a co-solvent is dominant in high pressure because the solute and solvent molecule will be closer. The modified co-solvent will break down the intermolecular force between solute molecules easier.

The solubility of DOX, pressure and temperature are used as the initial conditions of the flow model in the rapid expansion section.

4.3 Results of the flow model in the precipitation unit

After the extraction unit, the saturated supercritical fluid with solid solute is sent to the precipitation unit by rapid depressurizing through sub-sonic (capillary nozzle) and supersonic free jet (expansion chamber) region where the Mach umber, the ratio of fluid velocity and sound velocity at the capillary nozzle exit equal to unity and the atmosphere temperature is constant at 298.15 K.

Due to the low solubility of DOX in supercritical solvent, the flow model will be considered only as the supercritical binary mixer between carbon dioxide and methanol in vapor phase. The fluid flow is assumed to be steady state, one-dimensional flow, and adiabatic. In this part, the thermodynamic properties of fluid; for example, velocity, density, temperature and pressure, were investigated along the capillary nozzle and expansion chamber under chosen pre-expansion temperature and pressure from extraction condition. The solubility of DOX in modified supercritical phase between carbon dioxide and methanol is very sensitive with a high operated pressure at any temperature. On the other hand, pre-expansion temperature should be higher than extraction temperature in order to prevent phase changes of the solution and plugging due to a precipitation along the capillary nozzle region. Therefore, the chosen pre-expansion temperature and pressure are 348.15 K and 200 bar with 3 moles percentage of adding methanol in pure supercritical carbon dioxide respectively. Moreover, in this work there has been a focus on the range of pre-expansion temperature, pre-expansion pressure, and mole percentage of methanol from 343.15 – 353.15 K, 175 – 225 bar, and 3 – 5, respectively. In addition, the morphology of DOX particle such as critical radius, concentration of critical nuclei, and nucleation rate are also investigated in the supersonic free jet region only.

4.3.1 Physical properties of the supercritical fluid in subsonic and supersonic free jet region

The assumptions of flow model is simplified and summarized in the Table 4.3 below.

Table 4.3 Assumption of flow model along the sub-sonic and supersonic free jet region

Assumptions	Expansion region	
	Sub-sonic region	**Supersonic free jet**
Steady state	✓	✓
One-dimensional flow	✓	✓
Adiabatic	✓	✗ (Atmosphere temperature is constant at 298.15 K)
Mach number	✓ (Mach umber at the capillary nozzle exit equal to unity)	✗
Precipitation process	✗	✓

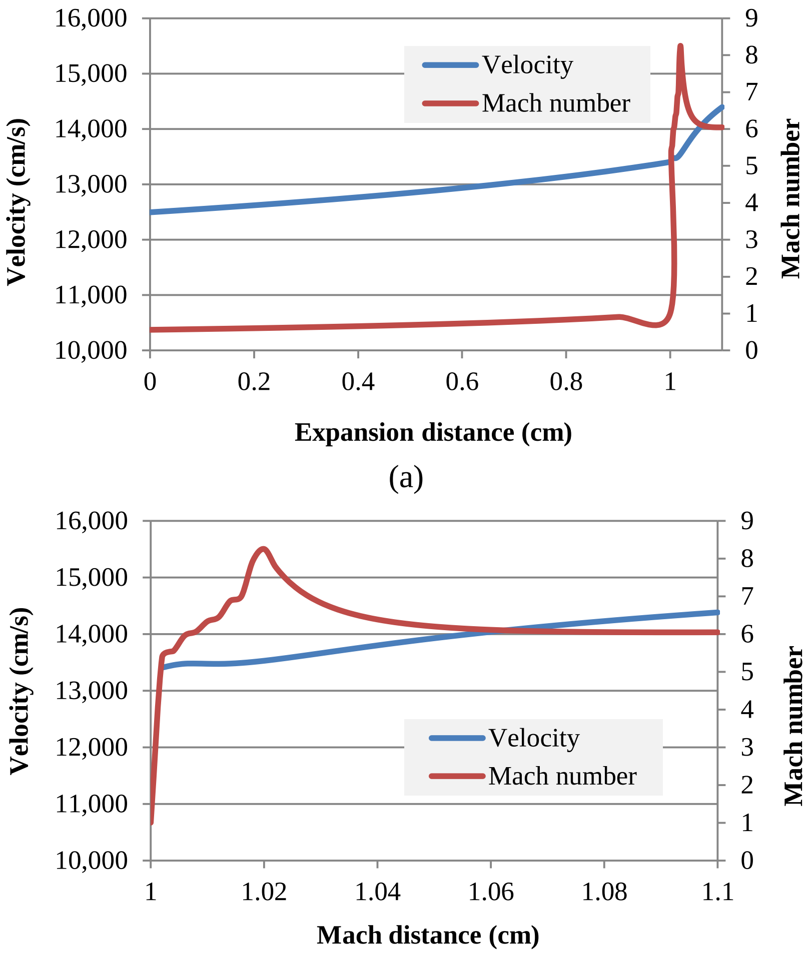

(a)

(b)

Figure 4.9 Calculated velocity profile (cm/s) correlated with expansion distance (cm) when expanding saturated modified supercritical solution through expansion paths (a) subsonic and (b) supersonic free jet region with pre-expansion condition 338.15 K and 200 bar (methanol 3 mole percentage)

According to Figure 4.9, the flow model gives a physical properties profile along the expansion path, capillary nozzle and expansion chamber of supercritical fluid with 3 mole percentage of methanol as a modified co-solvent. The pre-expansion temperature and pre-expansion pressure are 338.15 K, and 200 bar, respectively. The fluid velocity will increase continuously until it makes the higher number equal to unity at the exit of capillary nozzle for generating the supersonic condition. When the saturated solution is expanded to the supersonic region, the velocity is sharply increase along the Mach distance whiles the Mach number increases and then decreases at the expansion chamber distance 1.02 centimeters.

Figure 4.10 below represents the density profile of the modified supercritical fluid. The slightly decreasing of density profile along the capillary nozzle path results from adiabatic assumption. After the capillary exit, the density of fluid will drop abruptly due to the fact that the fluid temperature exchanges with the constant surrounding gas at a 298.15 K.

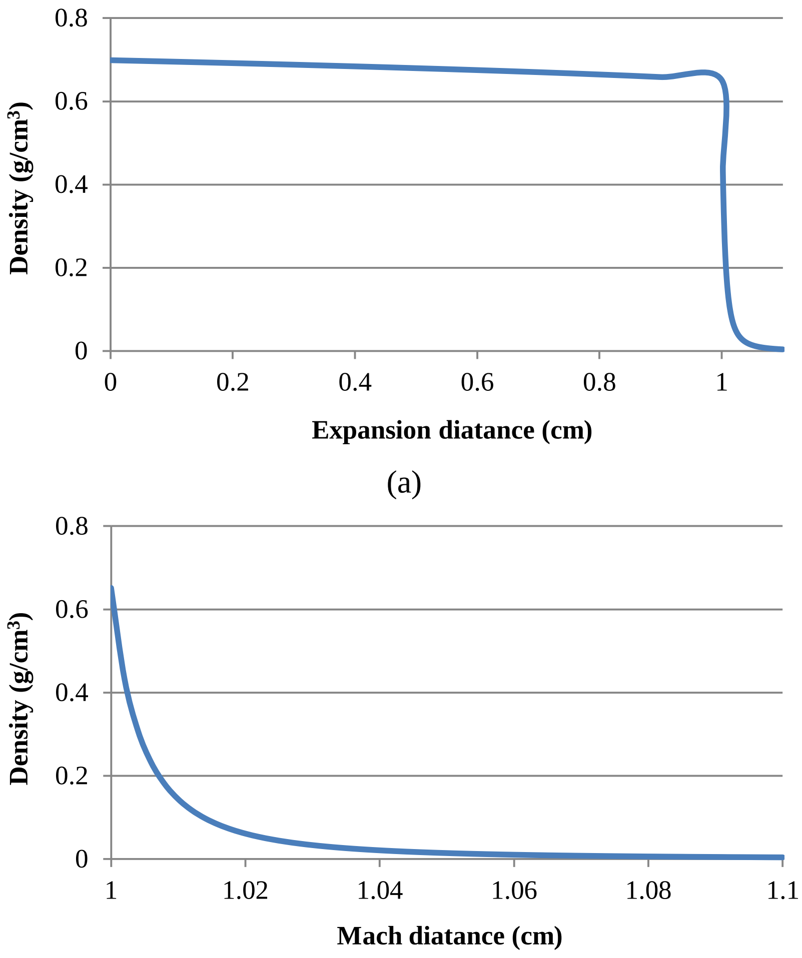

(a)

(b)

Figure 4.10 Calculated density profile (g/cm^3) correlated with expansion distance (cm) when expanding saturated modified supercritical solution through expansion paths (a) subsonic and (b) supersonic free jet region with pre-expansion condition 338.15 K and 200 bar (methanol 3 mole percentage)

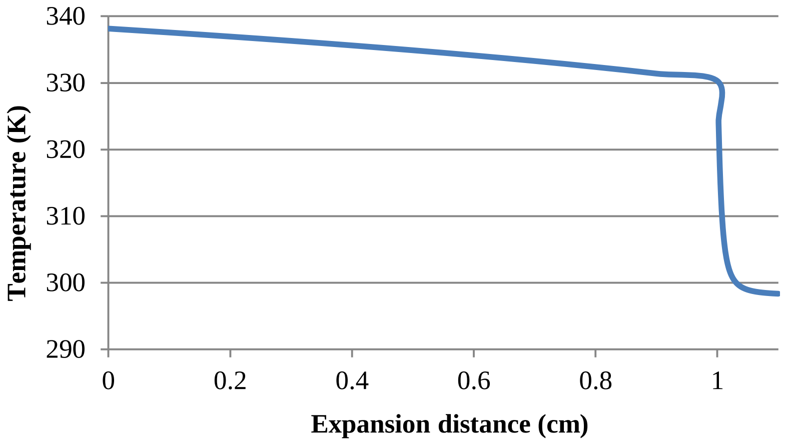

(a)

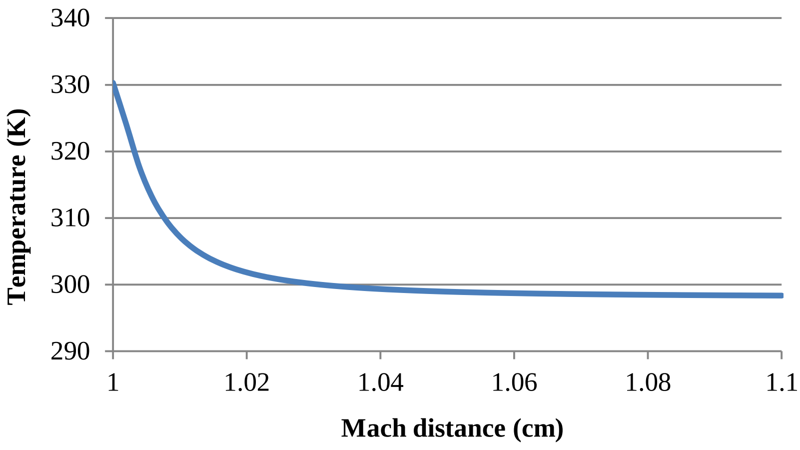

(b)

Figure 4.11 Calculated temperature profile (K) correlated with expansion distance (cm) when expanding saturated modified supercritical solution through expansion paths (a) subsonic and (b) supersonic free jet region with pre-expansion condition 338.15 K and 200 bar (methanol 3 mole percentage)

According to Figure 4.11, the temperature profile of modified supercritical fluid between carbon dioxide and 3 mole percentages methanol will decrease along with the capillary nozzle followed by a sharp drop trend to the supersonic free jet region. This phenomenon indicates that the reaction under capillary nozzle is endothermic and the heat of supercritical solvent will be transferred to the constant surrounding gas at a 298.15 K. As shown in this figure, the final fluid temperature is close to the surrounding temperature. Fluid temperature is the important effect causing the change in another physical profile pressure as shown in Figure 4.12 below.

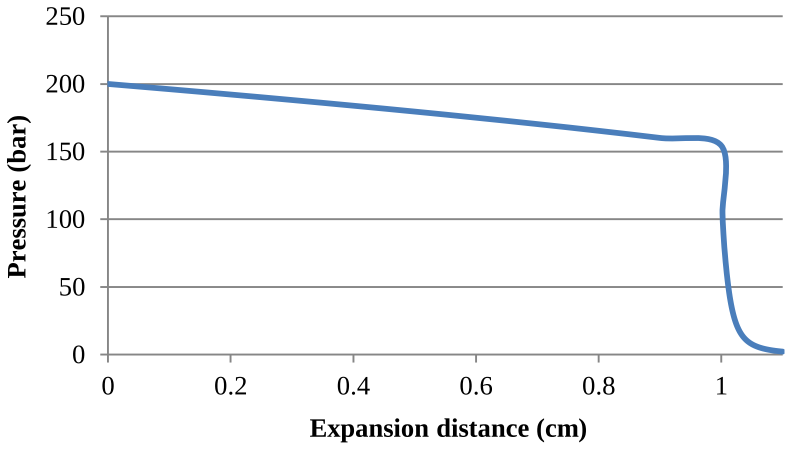

(a)

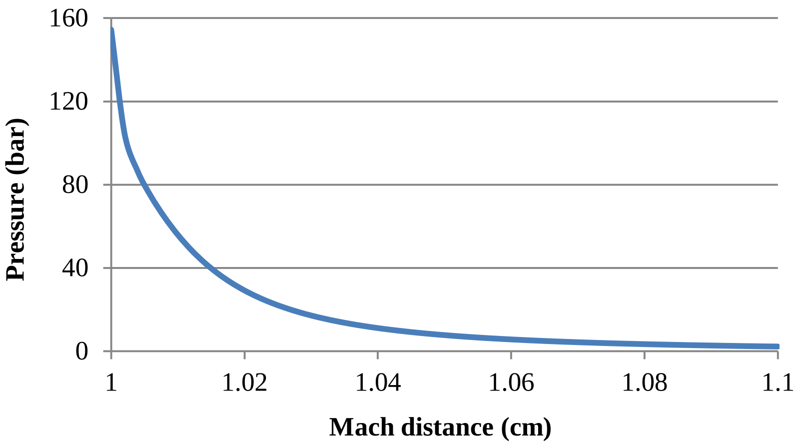

(b)

Figure 4.12 Calculated pressure profile (bar) correlated with expansion distance (cm) when expanding saturated modified supercritical solution through expansion paths (a) subsonic and (b) supersonic free jet region with pre-expansion condition 338.15 K and 200 bar (methanol 3 mole percentage)

Figure 4.12 represents the pressure profile of supercritical solvent between carbon dioxide and methanol along the expansion path including sub-sonic and supersonic free jet region. When the pressure of supercritical binary solvent is lower than 74.82 bar, the phase of supercritical fluid will change immediately at an expansion chamber distance 1.006 centometers.

In order to determine nucleation rate of DOX in supersonic free jet region, the driving force of this mechanism, supersaturation ratio, should be calculated. When the supersaturation ratio is higher than unity, the homogeneous nucleation rate of particle is assumed to start although the resident time is very short.

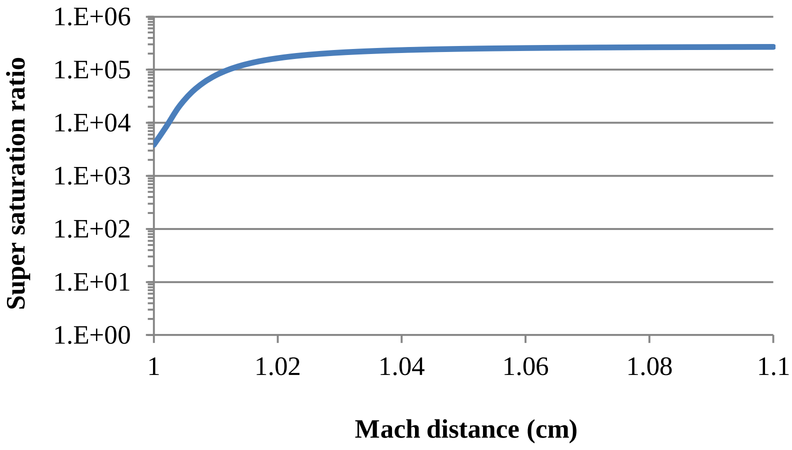

Figure 4.13 Calculated supersaturation ratio in supersonic free jet region correlated with expansion distance (cm) when expanding saturated modified supercritical solution through expansion path with pre-expansion condition 338.15 K and 200 bar (methanol 3 mole percentage)

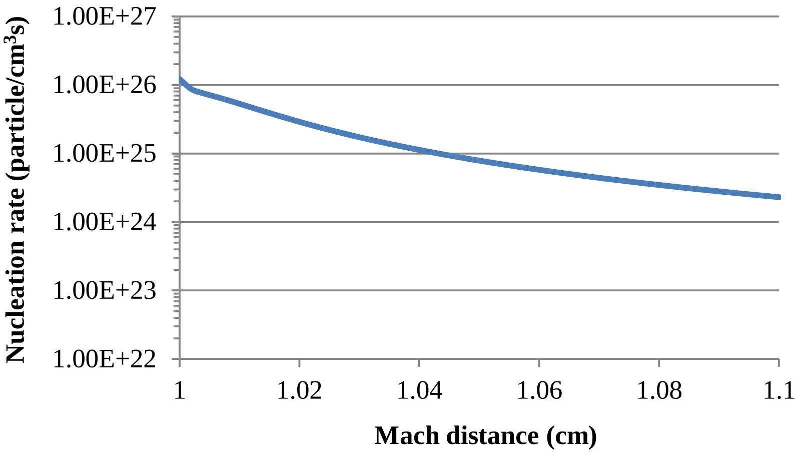

Figure 4.14 Calculated nucleation rate (particles/cm^{3}s) in supersonic free jet region correlated with expansion distance (cm) when expanding saturated modified supercritical solution through expansion path with pre-expansion condition 338.15 K and 200 bar (methanol 3 mole percentage)

Figure 4.13 - Figure 4.14 represent the calculated supersaturation ratio and nucleation rate of DOX in modified supercritical system with 3 mole percentage of methanol. As shown in Figure 4.14, the particle formation starts at the transition region from the end of sub-sonic region (capillary nozzle) to supersonic free jet region (expansion chamber). The result of flow model indicates that the range of nucleation rate along the Mach distance will drop continuously from 5 to 0.1 multiply with 10^{24} particles/cm^{3}s^1. Moreover, the supersaturation ratio will affect to number concentration of critical nuclei and critical radius of DOX in modified supercritical system as shown in Figure 4.15 and Figure 4.16 below.

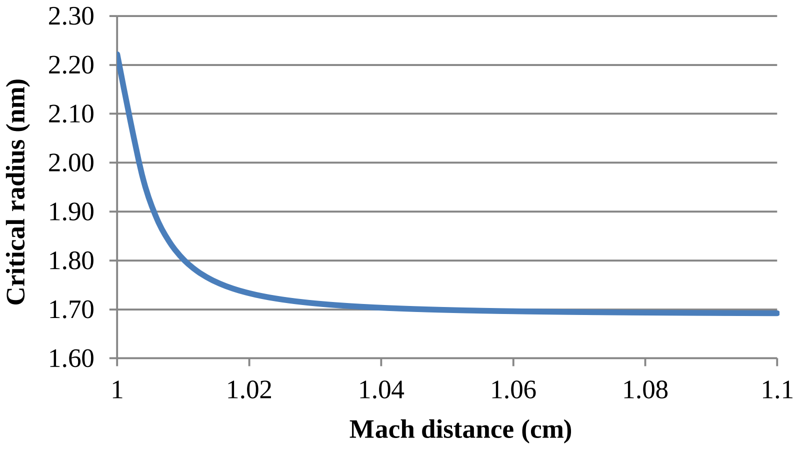

Figure 4.15 Calculated critical radius (nm) in supersonic free jet region correlated with expansion distance (cm) when expanding saturated modified supercritical solutionthrough expansion path with pre-expansion condition 338.15 K and 200 bar (methanol 3 mole percentage)

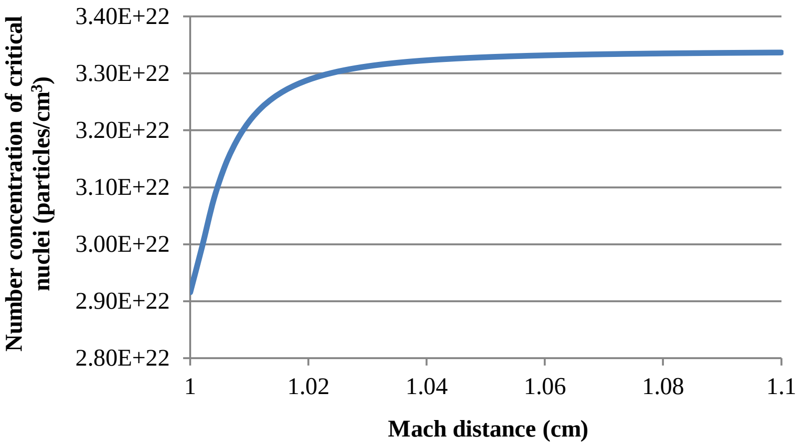

Figure 4.16 Calculated number concentration of critical nuclei (particles/cm^3) in supersonic free jet region correlated with expansion distance (cm) when expanding saturated modified supercritical solution through expansion path with pre-expansion condition 338.15 K and 200 bar (methanol 3 mole percentage)

The result indicate that the number of concentration of critical nuclei is about 10^{22} particles/cm^3 with the nanometer scale of particle approximately 1.7 nanometers, which is smaller than the original size. Both number concentration of critical nuclei and critical nuclei will be constant at the expansion chamber distance 1.02 centimeters which is the reverse point of supersaturation ratio. The increment of number concentration of critical nuclei results from the increase of expansion distance. Then the critical nuclei will be slightly decreased.

4.4 Sensitivity analysis

In this work; the effect of pre-expansion temperature, pre-expansion pressure, and mole percentage of adding methanol were investigated. The Rapid Expansion of Supercritical Solution (RESS) is necessary to perform a sensitivity analysis to evaluate the optimal condition. However, the range of adjustable parameters should be concerned for the limitation of equipment for safety operation. The valid ranges of adjustable operating parameter are as follows:

- The pre-expansion temperature: 333.15 – 343.15 K
- The pre-expansion pressure: 175 – 225 bar
- The mole percentage of methanol: 3 - 5 mole percentage

4.4.1 Pre-expansion temperature

Pre-expansion temperature is performed at 3 different temperatures (333.15, 338.15, and 343.15 K), which are higher than the extraction temperature in order to prevent phase changing and precipitation process in capillary nozzle (subsonic region). When the pre-expansion temperatures are varied, pre-expansion pressure and concentration of methanol in supercritical carbon dioxide is kept constantly as 200 bar and 3 mole percentage of methanol.

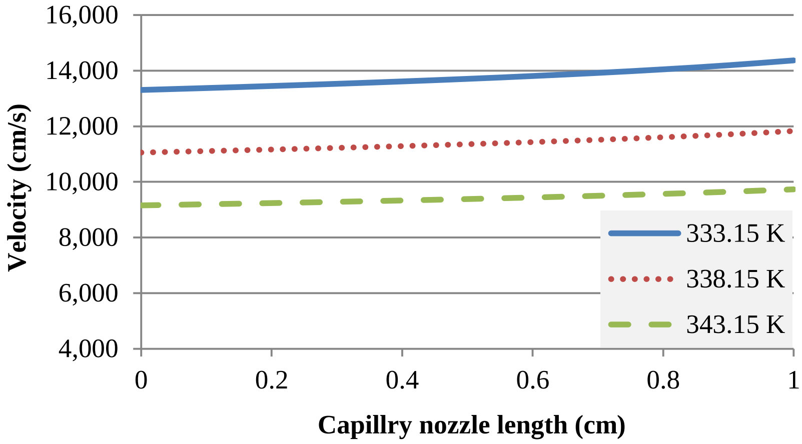

(a)

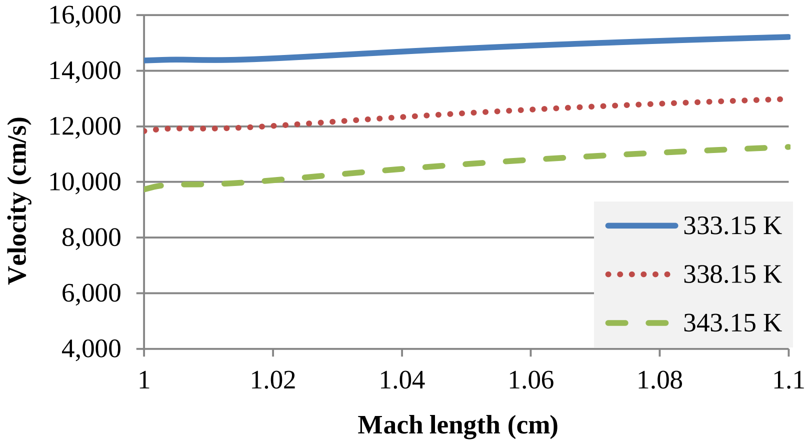

(b)

Figure 4.17 Velocity profile (cm/s) of modified saturated solution when expanding through (a) subsonic (b) supersonic free jet region correlated with expansion distance (cm) at various pre-expansion temperatures

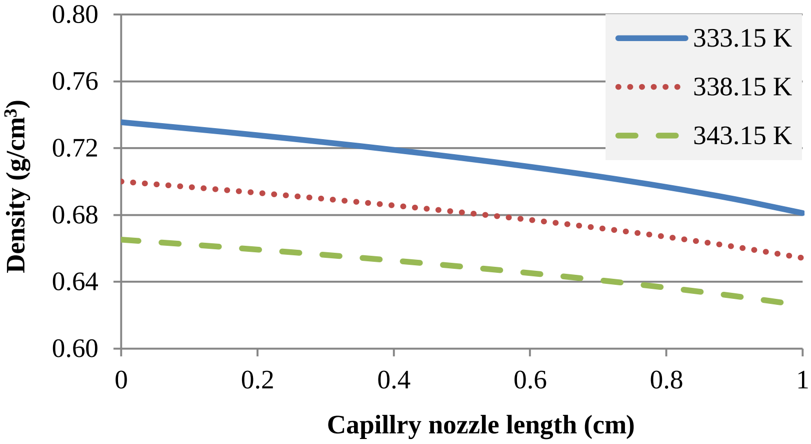

(a)

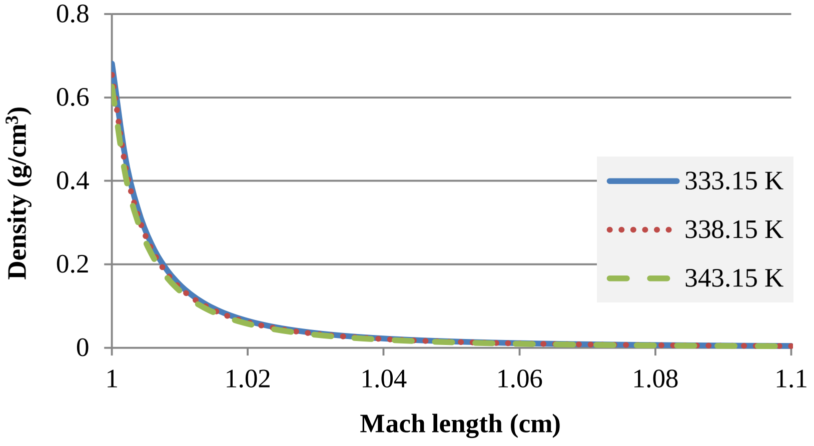

(b)

Figure 4.18 Density profile (g/cm^3) of modified saturated solution when expanding through (a) subsonic (b) supersonic free jet region correlated with expansion distance (cm) at various pre-expansion temperatures

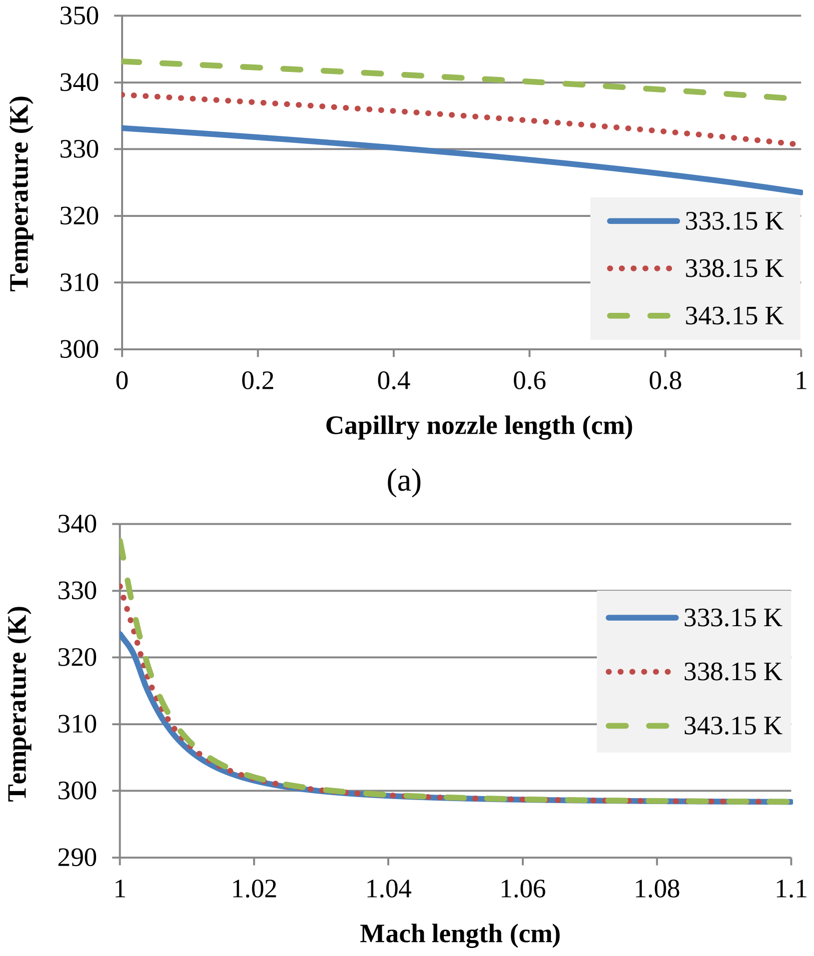

(a)

(b)

Figure 4.19 Temperature profile (K) of modified saturated solution when expanding through (a) subsonic (b) supersonic free jet region correlated with expansion distance (cm) at various pre-expansion temperatures

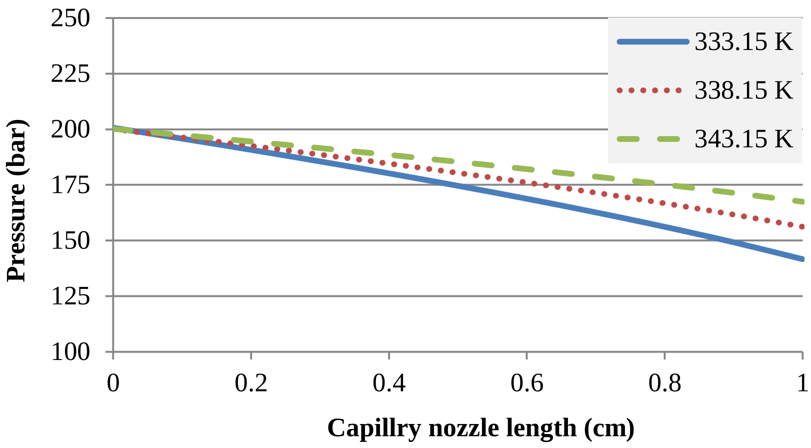

(a)

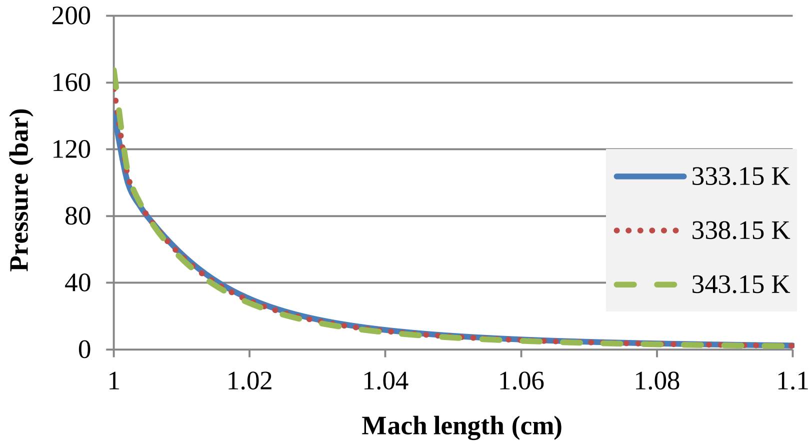

(b)

Figure 4.20 Pressure profile (bar) of modified saturated solution when expanding through (a) subsonic (b) supersonic free jet region correlated with expansion distance (cm) at various pre-expansion temperatures

According to Figures 4.17 – 4.20, velocity and density profile of supercritical fluid in expansion paths, sub-sonic (capillary nozzle) and supersonic free jet (expansion chamber) are inversely proportional to the pre-expansion temperature along the capillary nozzle. Due to the conservation of mass, the density shows an opposite behavior of fluid velocity profile (f the fluid density is decreased, the velocity should be increased). At this region every trend of pre-expansion temperature of supercritical fluid will slightly decrease; nevertheless, it is abruptly dropped from the end of capillary nozzle exit until the Mach distance reaches 1.02 centimeters. The fluid temperature will decrease until it closes to a constant environmental temperature at 298.15 K (condition of expansion chamber). Then, the fluid density will drop dramatically due to the effect of fluid temperature. In addition, the trend pressure profile of supercritical fluid is similar to the temperature effect in both regions. It can be summarized that the drop of supercritical temperature directly affects to the velocity, density, and pressure of both of capillary nozzle region and supersonic free jet region.

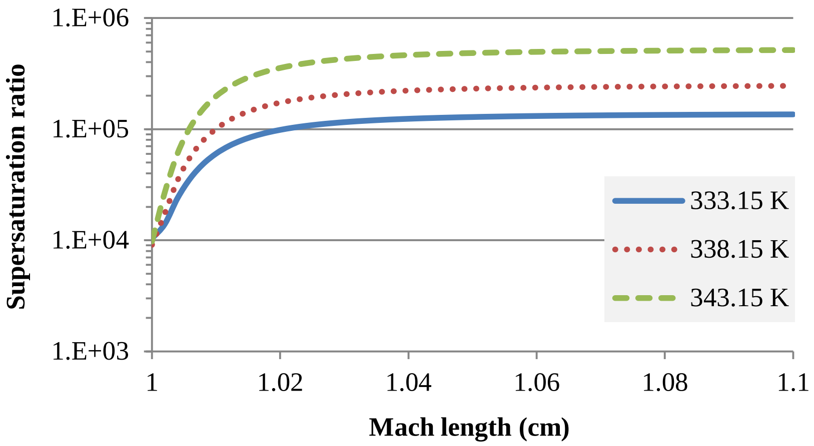

Figure 4.21 Supersaturation ratio in supersonic free jet region correlated with expansion distance (cm) at various pre-expansion temperatures

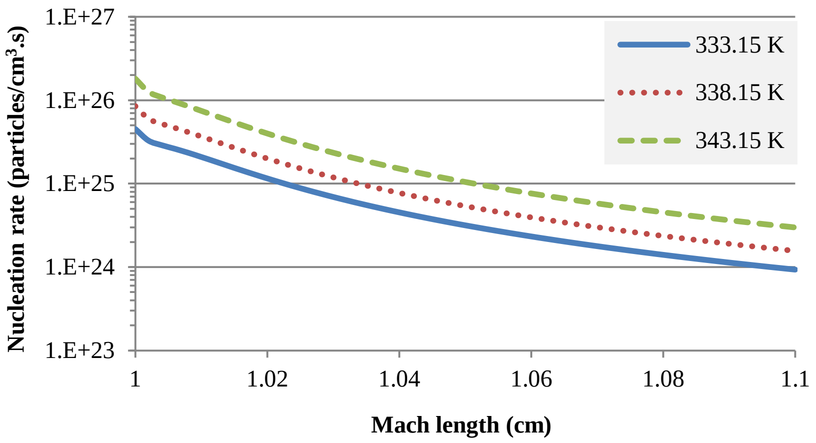

Figure 4.22 Nucleation rate (particles/cm^3s) in supersonic free jet region correlated with expansion distance (cm) at various pre-expansion temperatures

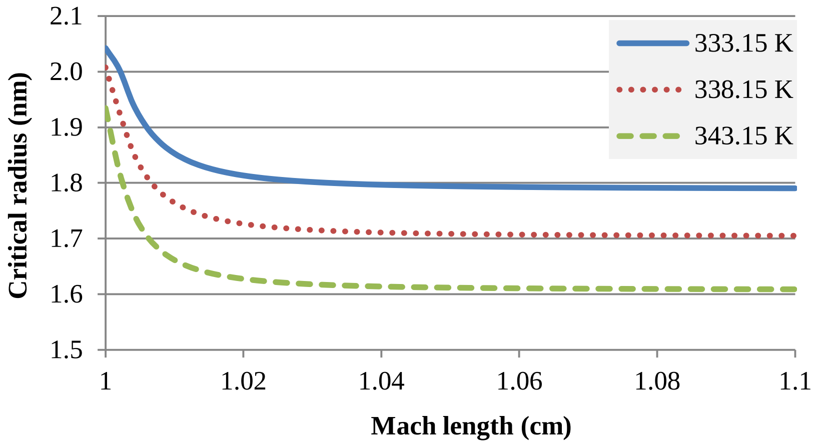

Figure 4.23 Critical radius (nm) in supersonic free jet region correlated with expansion distance (cm) at various pre-expansion temperatures

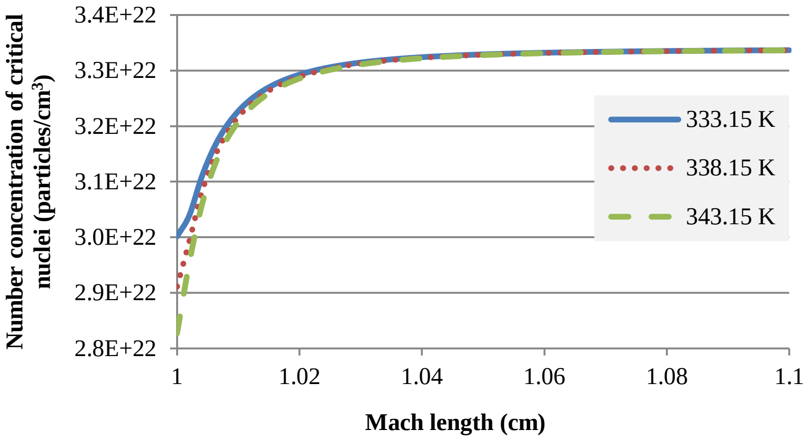

Figure 4.24 Number concentration of critical nuclei (particles/cm^3) in supersonic free jet region correlated with expansion distance (cm) at various pre-expansion temperatures

As shown in Figures 4.21 - 4.24, when pre-expansion temperature of supercritical fluid is increased, the supersaturation ratio along the supersonic free jet will increase and also causes nucleation rate of DOX to also increase. On the other hand, the value of supersaturation ratio is higher than unity before nozzle exit and, therefore, the particle formation earlier started inside the capillary nozzle for all pre-expansion temperature. The higher pre-expansion temperature is applied, the higher nucleation rate occurs.

Since the trend supersaturation ratio drop dramatically from the capillary nozzle exit until the Mach distance reaches to 1.02 centimeters, the critical radius and the number concentration of critical nuclei are similarly decreased and increased, respectively. The critical nucleus of DOX particle is inverse proportional with respect to the pre-expansion temperature. In addition, the results show that the variation of pre-expansion temperature range of 333.15 – 343.15 K does not affect the number of concentration of nuclei.

4.4.2 Pre-expansion pressure

The pre-expansion pressure was studied from 3 extraction pressures (175, 200, and 225 bar). When the pre-expansion pressure varies, the pre-expansion temperature and concentration of methanol in supercritical carbon dioxide are kept constantly as 338.15 K, and 3 mole percentage of methanol.

Velocity profile of the supercritical fluid slightly changes with pre-expansion pressure along two expansion paths, sub-sonic and supersonic free jet regions as represented in Figure 4.25 below. The higher value of pre-expansion pressure means the higher driving force of fluid flow in the capillary nozzle. At the transition region from the capillary nozzle exit to the expansion chamber, the velocity will reach the supersonic velocity condition with Mach number equals to unity.

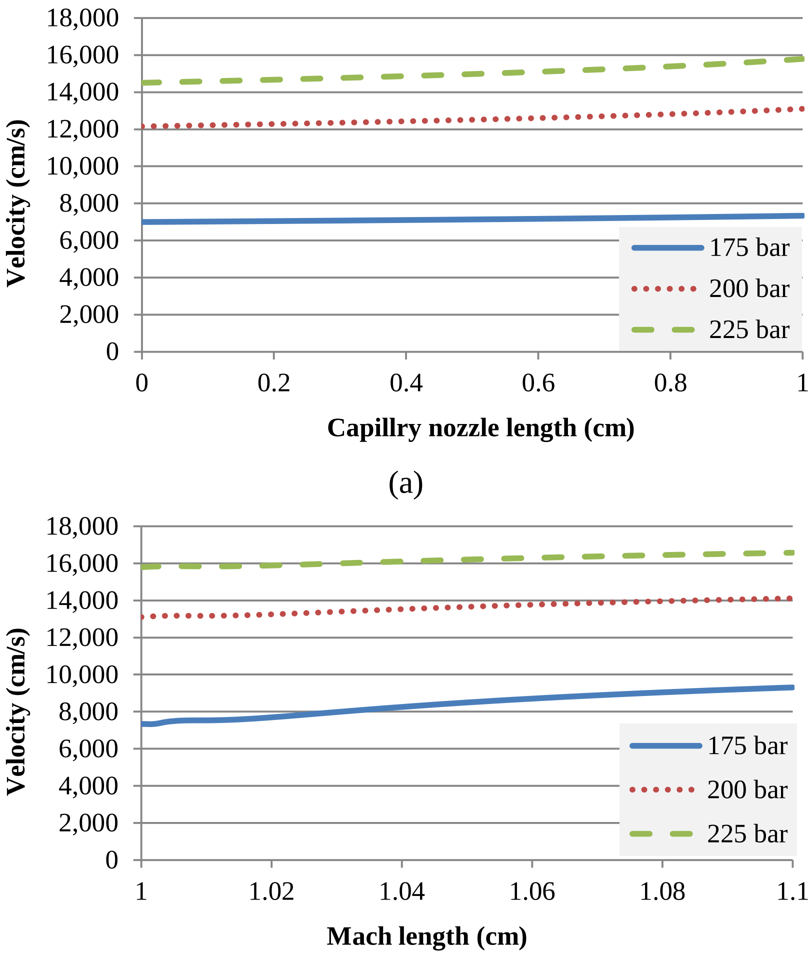

(a)

(b)

Figure 4.25 Velocity profile (cm/s) of modified saturated solution when expanding through (a) subsonic (b) supersonic free jet region correlated with expansion distance (cm) at various pre-expansion pressures

Figures 4.26 - 4.27 below represents the density and temperature profile of supercritical solvent along the two expansion paths, sub-sonic (capillary nozzle), and supersonic free jet (expansion chamber). As shown in Figure 4.26, the fluid density is directly proportional to the supercritical fluid temperature. Inside the capillary nozzle, the fluid density slightly decreases while the density dramatically drops at the expansion along the expansion chamber. The higher pre-expansion pressure is applied into saturated solution, the higher fluid density decreases and this will lead to more loss of solvating power.

Similarly, the supercritical fluid temperature will abruptly decrease in the pre-expansion pressure. Furthermore, at the transition region from nozzle exit to supersonic free jet, the fluid temperature abruptly drops from the capillary nozzle exit until the Mach distance reach 1.02 centimeters. The temperature will drop until the value close to a constant environmental expansion temperature at 298.15 K.

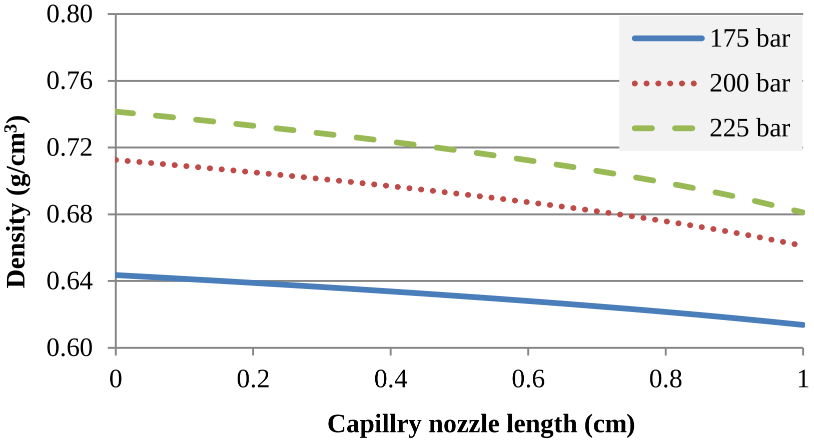

(a)

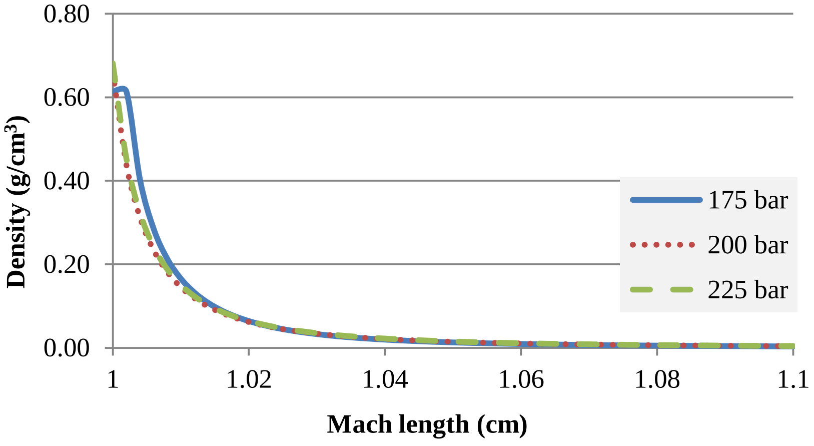

(b)

Figure 4.26 Density profile (g/cm^3) of modified saturated solution when expanding through (a) subsonic (b) supersonic free jet region correlated with expansion distance (cm) at various pre-expansion pressures

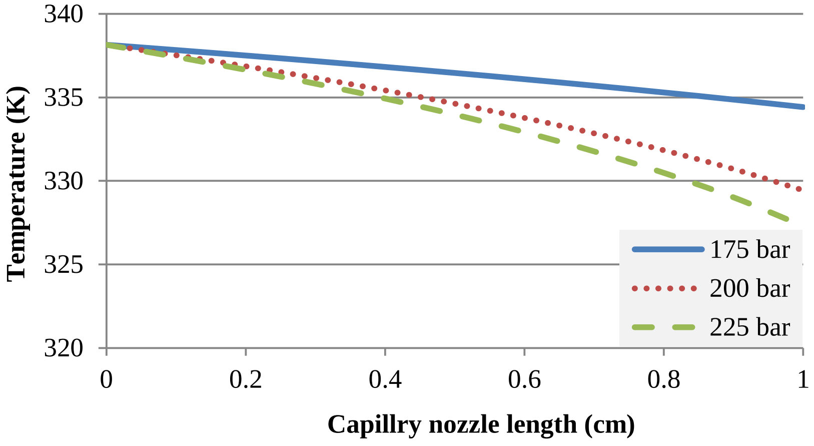

(a)

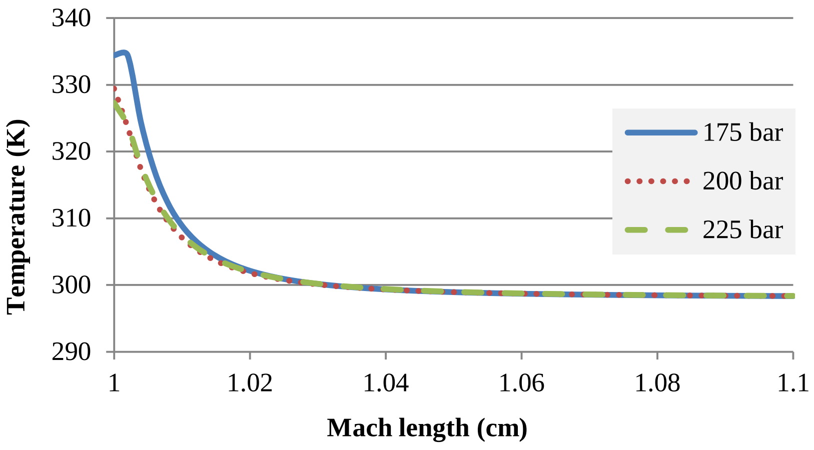

(b)

Figure 4.27 Temperature profile (K) of modified saturated solution when expanding through (a) subsonic (b) supersonic free jet region correlated with expansion distance (cm) at various pre-expansion pressures

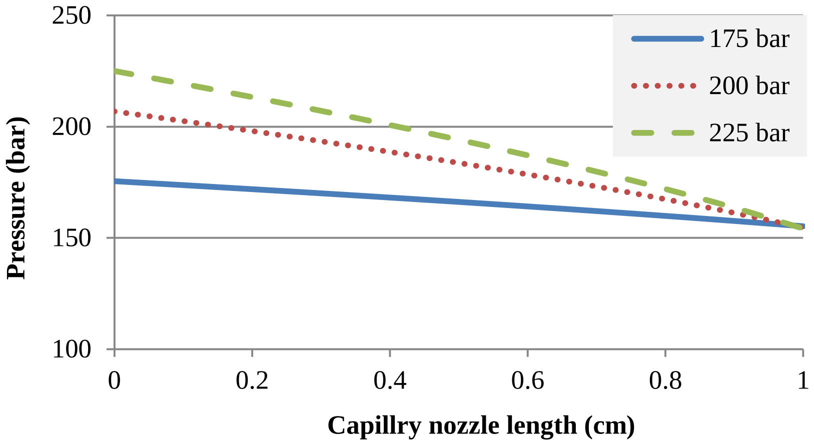

(a)

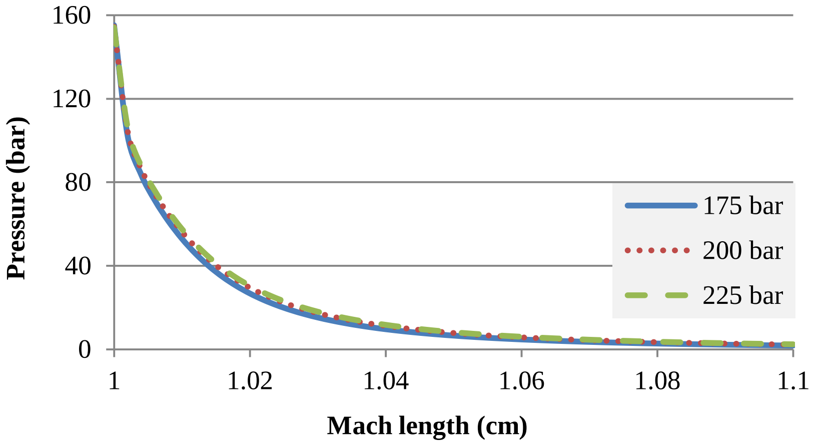

(b)

Figure 4.28 Pressure profile (bar) of modified saturated solution when expanding through (a) subsonic (b) supersonic free jet region correlated with expansion distance (cm) at various pre-expansion pressures

According to Figure 4.28, the pressure profile of supercritical solvent is directly proportional with the fluid temperature in both two expansion paths. In the capillary nozzle region, the fluid pressure will decrease to the pressure of 150 bar at the exit of capillary nozzle. Then the pressure will drop dramatically in the expansion chamber region from the capillary nozzle exit until the Mach distance reached 1.02 centimeters, which is similar to the trend of fluid temperature. The abrupt drop of the temperature and pressure in the supersonic free jet region results in the rapid decrease of the density at the different point at any pre-expansion pressure.

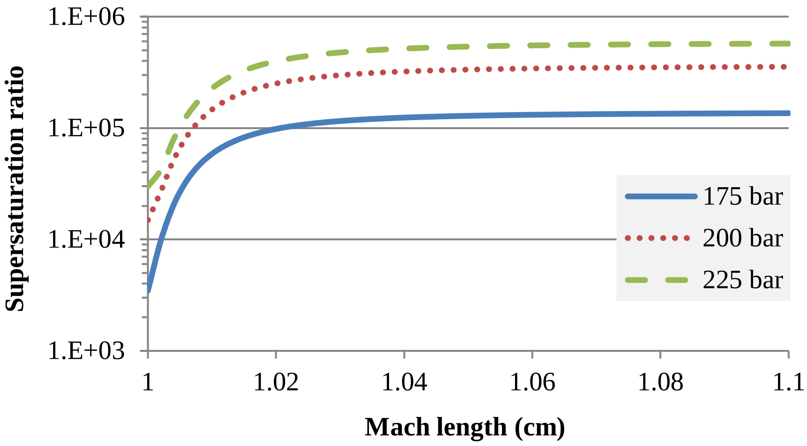

Figure 4.29 Supersaturation ratio in supersonic free jet region correlated with expansion distance (cm) at various pre-expansion pressures

Figures 4.29 represents the supersaturation ratio of saturated modified supercritical solution in supersonic free jet region for all pre-expansion pressure. The result shows that the supersaturation ratio is directly proportional with pre-expansion pressure. In addition, the increment of the supersaturation ratio will increasingly abrupt from the exit of capillary nozzle to 0.02 centimeters of Mach distance. After this point, the supersaturation ratio is quite maintained at a steady level. The supersaturation ratio is a driving force in the particle formation process. The more produced supersturation ratio, the more particles nucleate as shown in Figure 4.30 below. Therefore, the nucleation rate is directly proportional with respect to pre-expansion pressure that is similar to the supersaturation ratio. On the other hand, the nucleation rates would drop along the expansion chamber leading to the decrease of particle diameter. Moreover, the concentration of critical nuclei will increase from the effect of the supersaturation ratio. It can be concluded that the range of pre-expansion pressure 175 – 225 bar does not affect the number of concentration of nuclei.

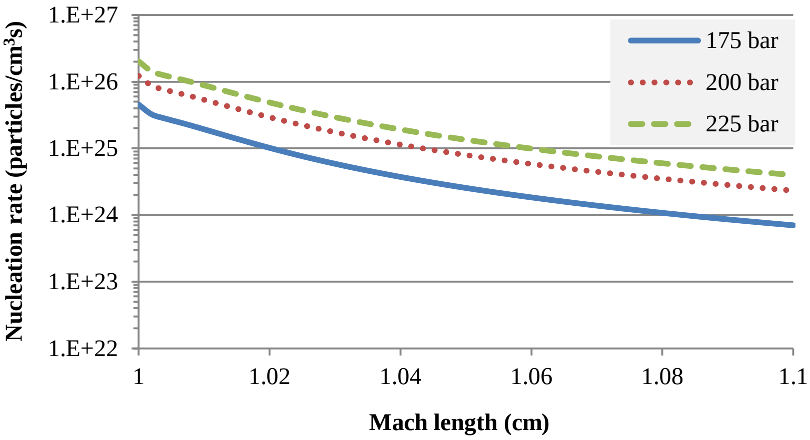

Figure 4.30 Nucleation rate (particles/cm^{3}s) in supersonic free jet region correlated with expansion distance (cm) at various pre-expansion pressures

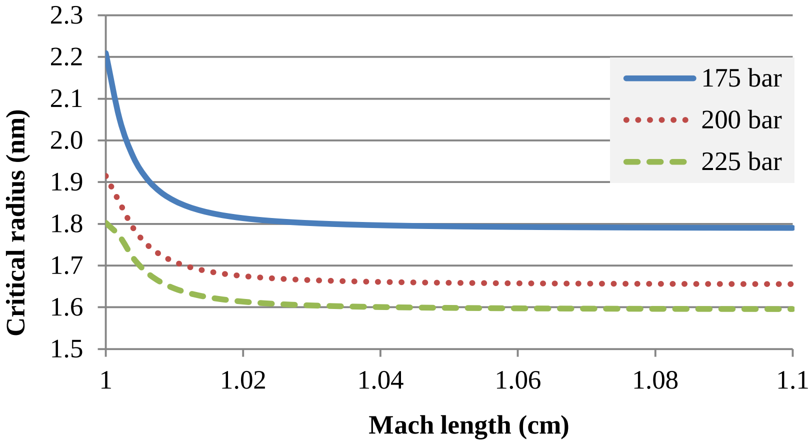

Figure 4.31 Critical radius (nm) in supersonic free jet region correlated with expansion distance (cm) at various pre-expansion pressures

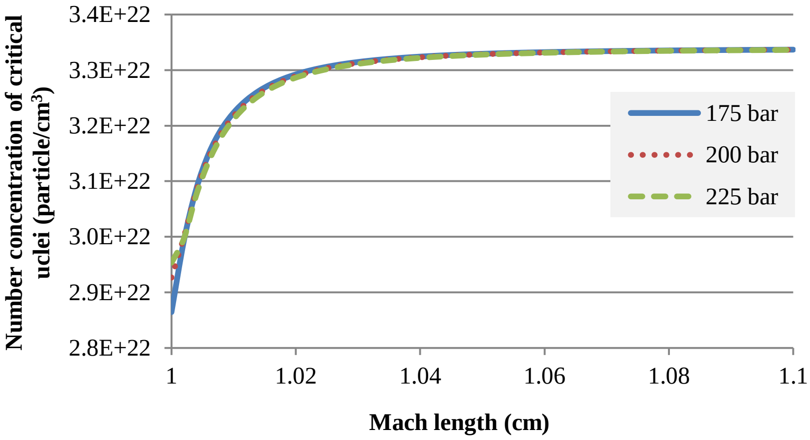

Figure 4.32 Number concentration of critical nuclei (particles/cm^3) in supersonic free jet region correlated with expansion distance (cm) at various pre-expansion pressures

4.4.3 Co-solvent concentration (methanol)

Effect of co-solvent concentration is studied at 3, 4, and 5 mole percentage of methanol. Pre-expansion temperature and pressure are kept constant as 338.15 K and 200 bar, respectively.

According to Figure 4.33 – 4.36, the velocity profile of supercritical fluid in both expansion paths, sub-sonic and supersonic free jet was inversely proportional with the co-solvent concentration. While the effect of co-solvent concentration does not affect the fluid density, temperature, and pressure profile. These physical properties will decrease along the capillary nozzle and then dramatically drop at the end of capillary nozzle to 0.02 centimeters of Mach distance.

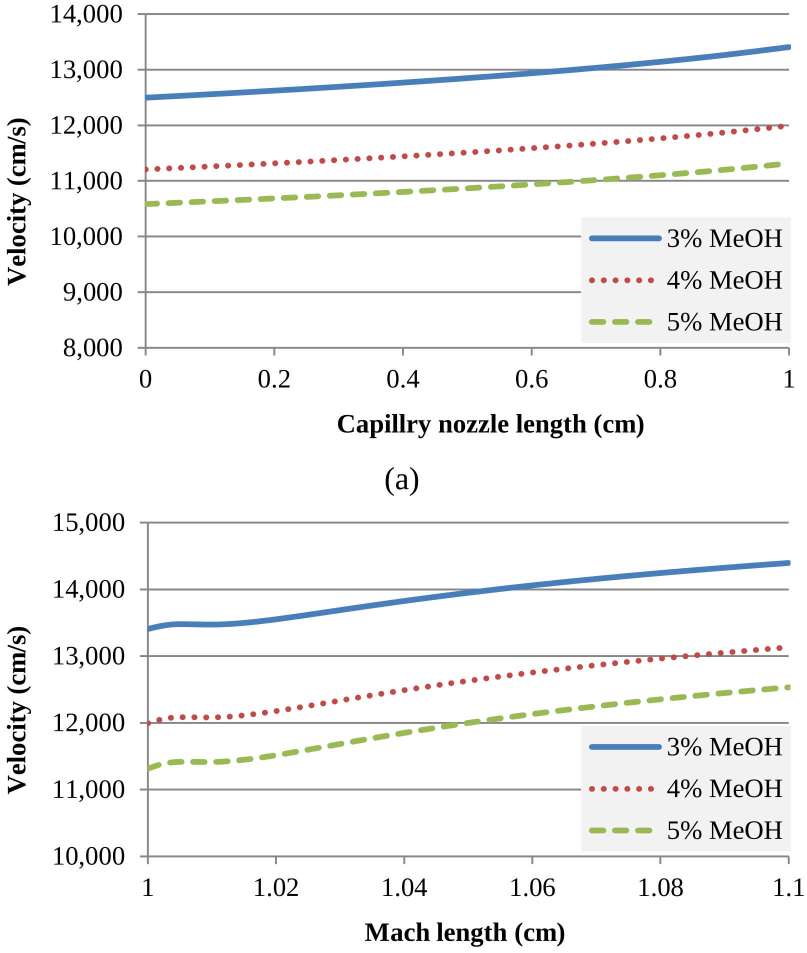

(a)

(b)

Figure 4.33 Velocity profile (cm/s) of modified saturated solution when expanding through (a) subsonic (b) supersonic free jet region correlated with expansion distance (cm) at various ratios of methanol modified co-solvent

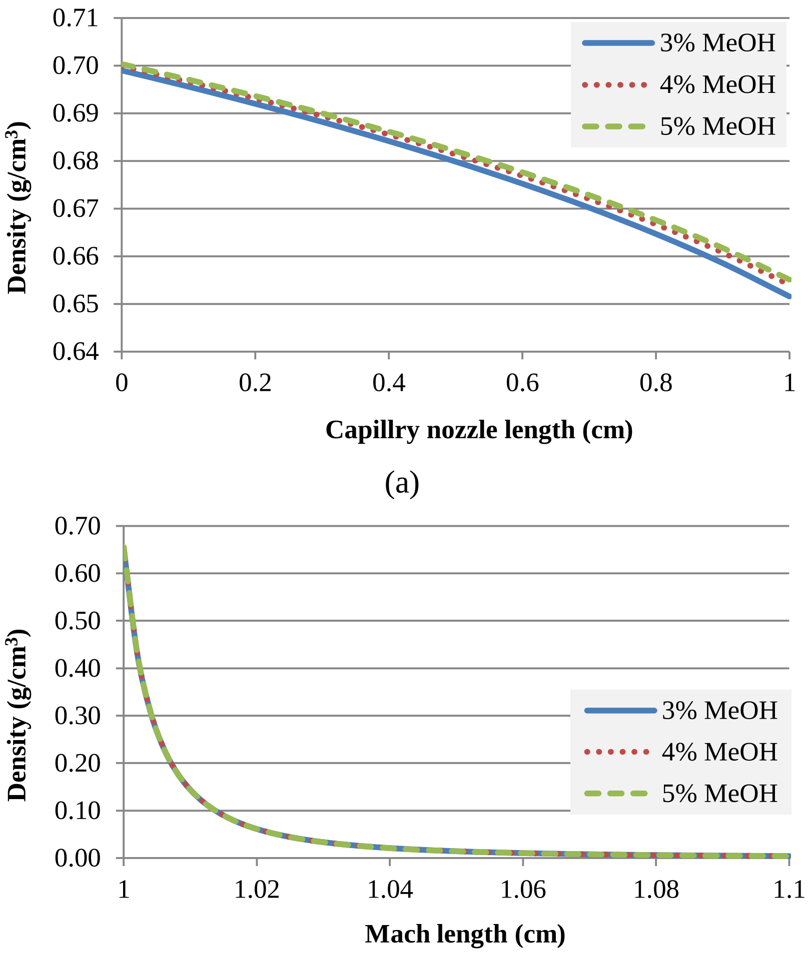

(a)

(b)

Figure 4.34 Density profile (g/cm^3) of modified saturated solution when expanding through (a) subsonic (b) supersonic free jet region correlated with expansion distance (cm) at various ratios of methanol modified co-solvent

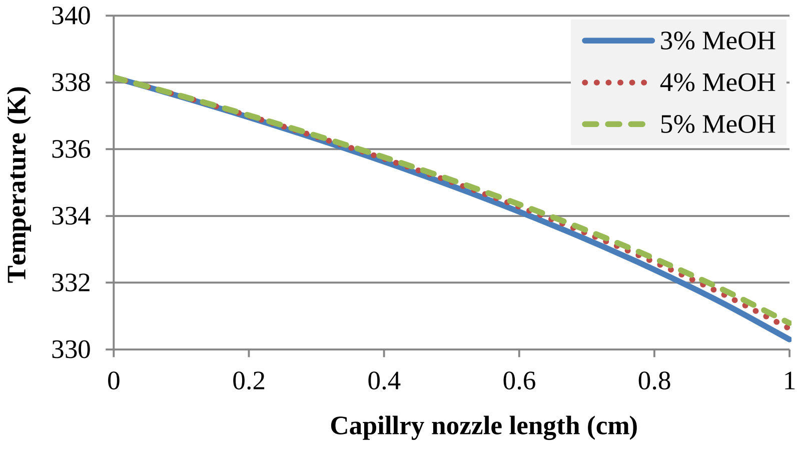

(a)

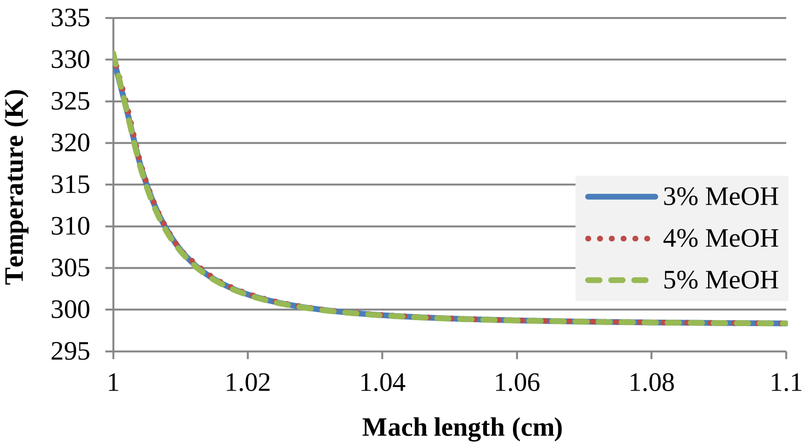

(b)

Figure 4.35 Temperature profile (K) of modified saturated solution when expanding through (a) subsonic (b) supersonic free jet region correlated with expansion distance (cm) at various ratios of methanol modified co-solvent

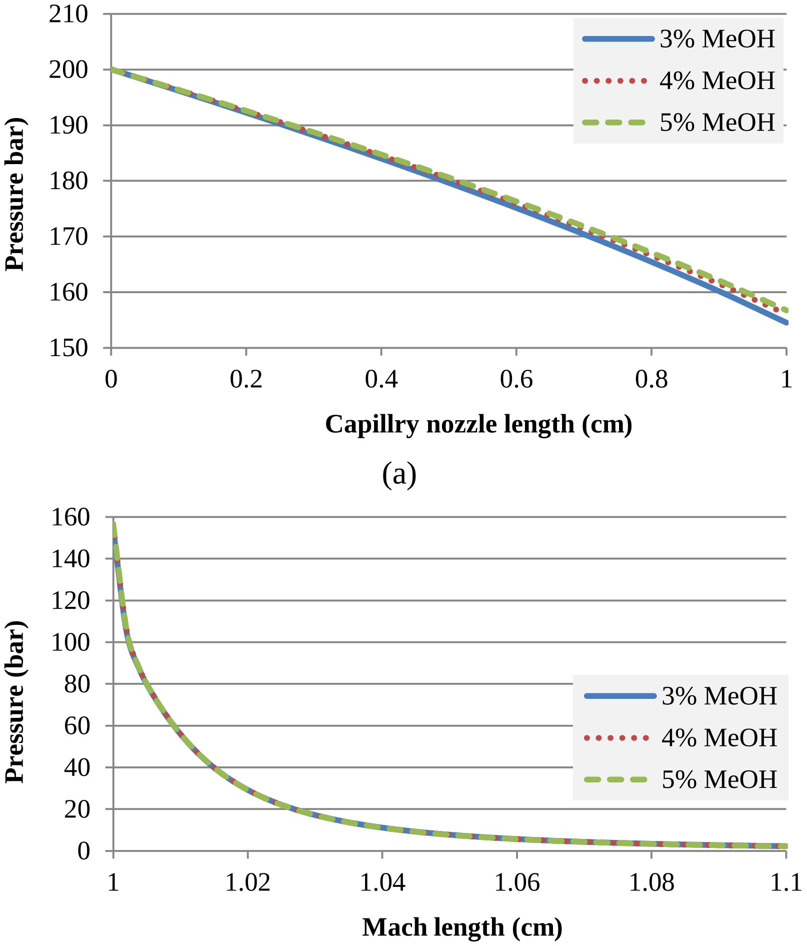

(a)

(b)

Figure 4.36 Pressure profile (bar) of modified saturated solution when expanding through (a) subsonic (b) supersonic free jet region correlated with expansion distance (cm) at various ratios of methanol modified co-solvent

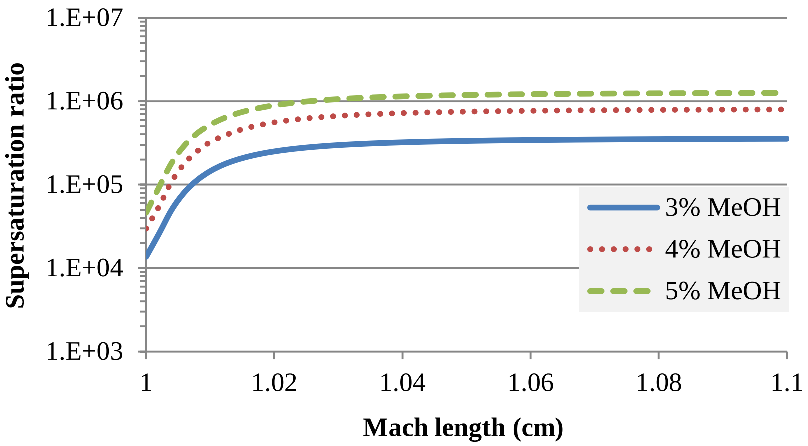

Figure 4.37 Supersaturation ratio in supersonic free jet region correlated with expansion distance (cm) at various ratios of methanol modified co-solvent

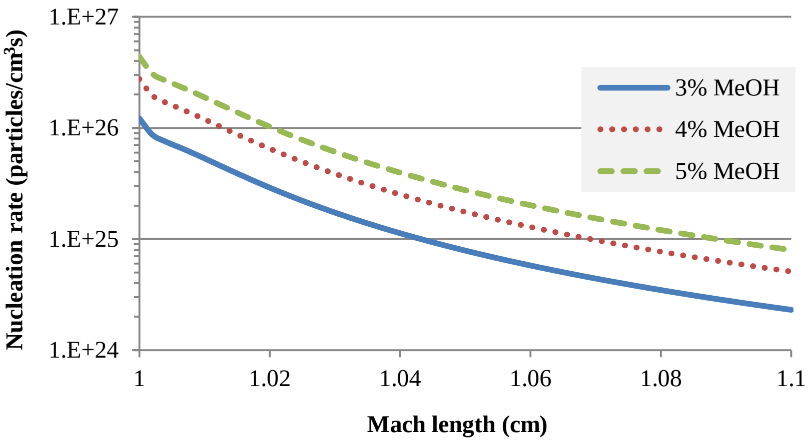

Figure 4.38 Nucleation rate (particles/cm^3s) in supersonic free jet region correlated with expansion distance (cm) at various ratios of methanol modified co-solvent

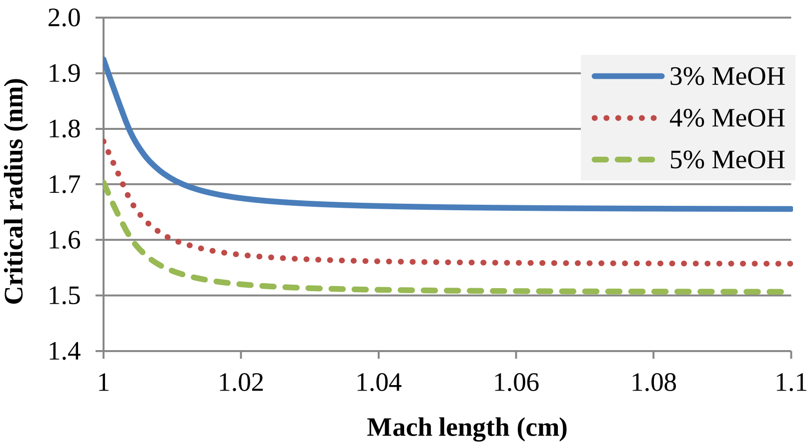

Figure 4.39 Critical radius (nm) in supersonic free jet region correlated with expansion distance (cm) at various ratios of methanol modified co-solvent

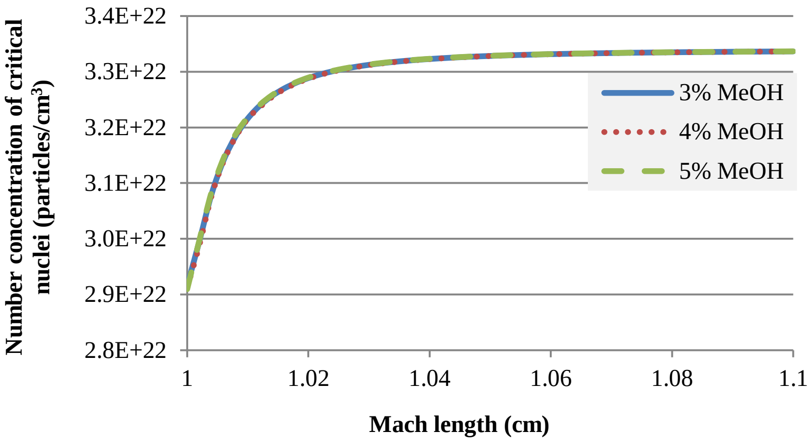

Figure 4.40 Number concentration of critical nuclei (particles/cm^3) in supersonic free jet region correlated with expansion distance (cm) at various ratio of methanol modified co-solvent

In contrast, the co-solvent concentration will affect the supersaturation ratio and nucleation the rate directly, as shown in Figures 4.37 - 4.38. The supersaturation ratio will abrupt and increase from the exit of capillary nozzle to the Mach distance, which is 0.02 centimeters away from the exit. For the nucleation rate, it will decrease along the expansion chamber. However, the effect of co-solvent concentration was inversely proportional with the critical radius of nucleated particle as shown in Figure 4.39. At least, the co-solvent concentration does not have an effect on the number concentration of critical nuclei like the two previous effects, pre-expansion temperature and pre-expansion pressure.

In conclusion, the results of sensitivity analysis of the 3 precipitation variables indicated that the model tends to predict the particle size following Retrograde behavior of the decrease in solubility upon isobaric heating. Increasing of pre-expansion condition result the decreasing of particle size.

CHAPTER 5 CONCLUSIONS AND RECOMMENDATIONS

5.1 Conclusions

The Rapid Expansion of Supercritical Solution (RESS) is studied to cover the solubility of Doxorubicin (DOX) in supercritical solvent and the particle formation after depressurizing saturated supercritical solvent. The results indicate that the solubility of DOX in non-polar pure supercritical carbon dioxide is quite low in the range of 10 times 10^{-11} to $\times 10^{-8}$ in mole fraction unit due to the complicated molecular structure, size, and polar functional group. Therefore, adding polar co-solvent into non-polar supercritical solvent will increase the solubility of solvent in supercritical phase. The solubility of DOX is determined at the extract temperature and pressure range of 308.15 – 323.15 K, and 80 – 300 bar due to the limitation of DOX degradation temperature and GCA-EoS model. These mole percentages of methanol (3, 4, and 5) are mixed into pure supercritical carbon dioxide as a modified co-solvent. The solubility will increase at least 2 to 20 times comparing with the pure supercritical carbon dioxide at the same extraction condition because of the effect of association between associating group in DOX molecule and hydroxyl group in methanol molecule. The hydroxyl group in methanol molecule will break down the interaction of the molecular force and the hydrogen bonding.

In the participating part, the physical properties profile, velocity, density, temperature, and pressure of fluid are investigated along two expansion paths which were nozzle region and supersonic free jet region. As the low solubility of solid solute in modified supercritical fluid was very low, the flow model will be specified only at the properties of solvent in vapor phase. Furthermore, the assumptions of these two regions are the flows which are steady, one-dimensional, and adiabatic. At the nozzle exit, the Mach number, the ratio of fluid velocity and sound velocity is equal to unity. The results of this section indicate that the temperature, the pressure, and the density profile in nozzle region are continuously reduced while the velocity profile is continuously increased along the nozzle distance. After the nozzle exit, the saturated solvent with solid solute is sent to supersonic free jet region which is limited by the Mach distance. The Mach distance is calculated from the expression between pre- and post-expansion pressure. The physical properties profiles, the temperature and the pressure are sharp drops resulting from the decrease of density in this region. On the other hand, the velocity profile will sharply increase. The decrease of fluid temperature is the cause of high super saturation ratio, and nucleation rate that tends to decrease the critical nuclei size and increase the number concentration of critical nucleus. The results of mild condition (318 K, 200 bar, and 3 percentage mole of methanol) indicate that the nucleation rate of DOX is about 10^{24} particles/cm^3s whereas the number of concentration of critical nuclei is about 10^{22} particles/cm^3 with the nanometer scale of particle at approximately 1.7 nanometer is generated, which that is smaller than the original size.

In addition, sensitivity analysis of pre-expansion pressures in the range of 175 - 225 bar, pre-expansion temperatures in the range of 333.15 - 343.15 K, and mole percentage of methanol in the range of 3 – 5 are investigated. The results indicate that the model trends to predict the particle size following Retrograde behavior showing a decrease in solubility upon isobaric heating. Increasing the pre-expansion temperature and pre-expansion pressure results the decrease of particle size.

Moreover, the effect of mole percentage of methanol in the system is more significant than the effect of temperature and pressure. The smallest particle size can generate the critical radius of nuclei about 1.5 nanometer by the RESS under, 338.15 K, 200 bar and 5 mole percentage of methanol condition.

5.2 Recommendations

5.2.1 The experimental of DOX in Rapid Expansion of Supercritical Solution (RESS) in both of supercritical solvent between pure and modified co-solvent are required to compare with this modeling result.

5.2.2 The other Equation of State should be studied and used to predict the equilibrium mole fraction in order to compare with Group Contribution with Association Equation of State (GCA-EoS).

5.2.3 The recent estimation of critical properties method should be studied to validate with the widely used group contribution method of Marrero and Gani.

5.2.4 The complex assumption of flow model such as two-dimension, non-adiabatic, and viscid should be considered in the further work.

5.2.5 The phenomena after the Mach disk, for example condensation and coagulation rate, should be investigated.

5.2.6 The other sensitivity variables such as nozzle length, nozzle diameter, etc. should be investigated to prove the effect of the product characteristics.

REFERENCES

[1] Perrut, M., **Supercritical fluid applications in the pharmaceutical industry** [online], Available: http://www.iptonline.com/articles/public/IPTNINE118NoPrint.pdf, [2011, May 3].

[2] King, M.B. and Bott, T.R., 1993, **Extraction of Natural Products Using Near-Critical Solvents**, Blackie Academic & Professional, pp. 34.

[3] Brunner, G., 1994, **Gas Extraction: An Introduction to Fundamentals of Supercritical Fluids and the Application to Separation Processes,** Steinkopff, pp. 43.

[4] Fornari, T., 2007, "Revision and summary of the group contribution equation of state parameter table: Application to edible oil constituents", **Journal of Fluid Phase Equilibria**, Vol. 262, No. 1-2, pp. 187–188.

[5] Ferreira, O., Eugenia, A.M. and Esteban, A.B., 2005, "Application of the GCA-EoS model to the supercritical processing of fatty oil derivatives", **Journal of Food Engineering**, Vol. 70, No. 4, pp. 579-587.

[6] Turk, M., 1999, "Formation of small organic particles by RESS: experimental and theoretical investigations", **Journal of Supercritical Fluids**, Vol. 15, No. 1, pp. 79-89.

[7] **Doxorubicin** [online], Available: http://en.wikipedia.org/wiki/Doxorubicin, [2011, Nov 15].

[8] Phonktummaruk, K., 2010, **Group Contribution Equation of state for Rapid expansion Super critical of Doxorubicin**, Master of Engineering, Chemical Engineering, Faculty of Engineering, King Mongkut's University of Technology Thonburi, Thailand, pp.24-25.

[9] Cai, S., Thati, S., Bagby, T.R, Diab, H.M., Davies, N.M., Cohen, M.S. and Forresta, M.L.,2010, "Localized doxorubicin chemotherapy with a biopolymeric nano carrier improves survival and reduces toxicity in xenografts of human breast cancer", **Journal of Controlled Release,** Vol. 146, No. 2, pp. 212–218.

[10] The American Society of Health-System Pharmacists, Inc., **Doxorubicin** [online], Available: http://www.nlm.nih.gov/medlineplus/druginfo/meds/a682221.html, [2011, May 3].

[11] Rizvi, S.S.H., Benado, A.L., Zollweg, J.A. and Daniels, J.A., 1986, "Supercritical fluid extraction: Fundamental principles and modeling methods", **Food Technology**, Vol. 40, pp. 55-65.

[12] Palmer, M.V. and Ting, S.S.T., 1995, “Applications for supercritical fluid technology in food processing”, **Journal of Food chemistry,** Vol. 52, No.4, pp. 345-352.

[13] **Supercritical fluid extraction** [online], Available: http://www.cyberlipid.org/extract/extr0008.htm, [2011, May 4].

[14] Tonthubthimthong, P., 2002, **Supercritical Extraction – A Comprehensive Experimental and Modeling Study**, Master of Engineering, Chemical Engineering, Faculty of Engineering, King Mongkut’s University of Technology Thonburi, Thailand, pp.1-33.

[15] **Supercritical fluid extraction of Natural products** [online], Available: http://www.andrew.cmu.edu/user/jitkangl/SFE/Supercritical%20Fluid%20Extraction%20of%20Natural%20Product.htm, [2011, May 4].

[16] McHugh, A.M. and Krukonis, J.V., 2004, **Supercritical Fluid Extraction: Principle and Practice**, Butterworth-Heinemann, pp. 1.

[17] Hitchen, S.M. and Dean, J.R., 1993, **Properties of Supercritical Fluids**, Blackie Academic and Professional, Glasgow, pp.1-11.

[18] Charoenchaitrakool, M., 2001, **Enhancing Dissolution Rates of Poorly Water-Soluble Drugs using Dense Gas Technology**, Philosophy of Engineering thesis, Chemical Engineering, Faculty of Engineering, University of New South Wales, Australia, pp.1-139.

[19] Kopcak, U., and Mohamed, R.S., 2005, “Caffeine solubility in supercritical carbon dioxide/co-solvent mixtures”, **Journal of Supercritical Fluids**, Vol. 34, No. 2, pp. 209–214.

[20] Tian, Y.L., Chen, L., Li, M.W. and Fu, H.F., 2003, “Calculation of Gas-Liquid Critical Curves for Carbon Dioxide-1-Alkanol Binary Systems”, **Journal of Physical Chemistry**, Vol. 107, pp. 3076-3080.

[21] Marrero, J. and Gani, R., 2001, “Group-contribution based estimation of pure component properties”, **Journal of Fluid Phase Equilibria**, Vol. 183–184, pp. 183–208.

[22] Soria, T.M., Sanchez, F.A., Pereda, S. and Bottini, S.B., 2010, “Modeling alcohol water hydrocarbon mixtures with the group contribution with association equation of state GCA-EoS”, **Journal of Fluid Phase Equilibria**, Vol. 296, pp. 116-124.

[23] Gros, H.P., Bottini, S. and Brignole, E. A., 1996, “A Group Contribution Equation of State for associating mixtures”, **Journal of Fluid Phase Equilibria**, Vol. 116, pp. 537–544.

[24] Jung, J. and Perrut, M., 2001, “Particle design using supercritical fluids: Literature and patent survey”, **Journal of Supercritical Fluids**, Vol. 20, No.3, pp. 179–219.

[25] Ginosar, D.M., Swank, D.S., McMurtrey, R.D. and Carmack, W.J., “Flow-Field Studies of the RESS Process”, **Proceedings of the 5th International Symposium on Supercritical Fluids**

[26] Kwauk, X. and Debenedetti, G.P., 1993, “Mathematical modeling of aerosol formation by Rapid Expansion of Supercritical Solution in a converging nozzle”, **Journal of Aerosol Science**, Vol. 24, No. 4, pp. 445-469.

[27] Lele, K.A. and Shine, D.A., 1992, “Morphology of Polymers Precipitated from a Supercritical Solvent”, **AIChE Journal**, Vol. 38, No. 5, pp.742-752.

[28] Chafera, A. and Bernaa, A., 2005, “Solubility of solid carnosic in supercritical CO_2 with ethanol as a co-solvent”**, Journal of Supercritical Fluids**, Vol. 34, pp. 323–329.

[29] Lyman, J.W., Reehl, F.W. and Rosenblatt, H.D., 1982**, Handbook of Chemical Property Estimation Methods**, American Chemical Society.

[30] **Joback method** [online], Available: http://en.wikipedia.org/wiki/Joback_method, [2011, Nov 15].

[31] **Carbon dioxide: Hazardous Substances Data Bank (HSDB**) [Online], Available: http://toxnet.nlm.nih.gov/cgi-bin/sis/search/f?./temp/~Rl1QjK:1, [2011, August 28].

[32] **Methanol: Hazardous Substances Data Bank (HSDB)** [Online], Available: http://toxnet.nlm.nih.gov/cgi-bin/sis/search/f?./temp/~BldJwp:1, [2011, August 28].

[33] Sanchez A.F., Mohammadi, H.A., Andreatta, A., Pereda, S., Brignole, E. and Richon, D., 2009, “Phase Behavior Modeling of Alkyl Amine Hydrocarbon and Alkyl Amine Alcohol Systems Using a Group Contribution Associating Equation of State”, **Industrial and Engineering Chemistry Research**, Vol. 48, pp. 7705-7712.

[34] Ferreira, O., Brignole A.E. and Macedo, A.E., 2004, “Modelling of phase equilibria for associating mixture using an equation of state”, **Journal of Chemical Thermodynamic**, Vol. 36, pp. 1105-1107.

[35] Helfgen, B., Hils, P., Holzknecht, Ch., Turk, M. and Schaber, K., 2001, “Simulation of particle formation during the rapid expansion of supercritical solutions”, **Journal of Aerosol Science**, Vol. 32, pp. 295-319.

[36] Hirunsit, P., Huang, Z., Srinophakun, T., Charoenchaitrakool, M. and Kawi, S., 2005, “Particle formation of ibuprofen–supercritical CO_2 system from rapid expansion of supercritical solutions (RESS): A mathematical model”, **Powder Technology**, Vol. 154, pp. 83-94.

[37] Platzer, B. and Maurer, G., 1993, “Application of a generalized Bender equation of state to the description of vapour-liquid equilibria in binary systems”, **Journal of Fluid Phase Equilibria**, Vol. 84, pp. 79-110.

[38] Yaws, L.C., 1996, **Handbook of Thermodynamic Diagrams, Volume 1: Organic Compounds C_1 to C_4**, Gulf Public Company.

[39] Sandler, I.S., 1989, **Chemical and Engineering Thermodynamics**, 3rd edition, John Wiley & Sons Wiley, New York.

APPENDIX A COMPARISON OF ESTMATION METHOD

In order to estimate the solubility of Doxorubicin (DOX) in supercritical co-solvent between carbon dioxide and methanol, thermodynamic properties of DOX like normal boiling point, critical temperature and pressure are necessary. Due to the highly complicated and toxic of DOX, thus it is hardly to measure the experimental data. This is the obstacle of this works as a result the estimation method from mathematical model is concerned.

The group-contribution methods such as Lyderson, Joback and Reid, Lyman et al., Horvath, and Marrero and Gani method have been widely used [21]. These methods provide the advantage of quick estimates without requiring substantial computational resources. However, some methods have a limitation of applicability due to the simplification and complication of molecular structure represented in the system. In this work, two widely used method, Joback and Reid [30], and Marrero and Gani [21] method are selected to estimate the thermodynamic properties of DOX. Comparing the two methods and select the suitable one for entire estimation of this work.

As the reason that is given in Chapter 4, normal melting point is the referent data for comparing the two methods of estimation.

A.1 Estimation of thermodynamic properties of Doxorubicin (DOX) by using method of Marrero and Gani [21]

The method of Marrero and Gani is performed in 3 levels. The first level will specify a set of simple groups that allows to describing a large variety of complex organic compounds. On the other hand, the first level is intended to deal with the classification among isomer, while the last two levels involves the better description along substituent group on aromatic or cycloaliphatic compound, and complex heterocyclic or polyfunctional acyclic compound for the second and the third level, respectively.

From the highly poly-functional group substitute on the aromatic and heterocyclic rings in the molecular structure of DOX, entire 3 levels of estimation are necessary. The property-estimation model is followed the equation (2.1) as mentioned in Chapter 2. Moreover, the simple function of the target property x on the left hand side of that equation, $f(x)$ is shown in Table 2.6, while the adjustable parameters is shown in Table 2.7. All of the mentioned equation and parameters are listed in Table A.1.

Table A.1 The property function, group contribution term and adjustable parameter of normal melting point estimation

Simple function **$f(x)$**	**Group Contribution term**	**Adjustable parameter (T_{m0}) (K)**
$exp(T_m/T_{m0})$	$\sum_i N_i T_{m1i} + \sum_j M_j T_{m2j} + \sum_k O_k T_{m3k}$	147.450

According to Table A.1, the 3 symbols T_{m1i}, T_{m2j}, and T_{m3k} represent the contributions of normal melting point property for the first, second, and third-order of estimation, while T_m is the target normal melting point estimation value.

The procedure of 3 levels of estimation is shown in Table A.2 – A.3 below.

Table A.2 First level group of estimation by using method of Marrero and Gani [21]

First-order groups	**T_{m1i} (K)**	**Occurrences in DOX (*Ni*)**	**Contribution**
1. CH_3	0.6953	2	1.3906
2. CH_2	0.2515	1	0.2515
3. aCH	0.5860	3	1.7580
4. aC fused with non-aromatic sub-ring	1.2065	6	7.2390
5. OH	2.7888	3	8.3664
6. aC-OH	5.1473	2	10.2946
7. CCO	1.0638	1	1.0638
8. CH-O	0.2461	1	0.2461
9. aC-O	1.3045	1	1.3045
10. $CH-NH_2$ (except above)	3.3478	1	3.3478
11. CH_2 (cyclic)	0.5699	3	1.7097
12. CH (cyclic)	0.0335	3	0.1005
13. O (cyclic)	1.3828	1	1.3828
14. CO (cyclic)	3.2119	2	6.4238
	$\sum_i N_i T_{m1i}$		**44.8791**

Table A.3 Second level group of estimation by using method of Marrero and Gani [21]

Second-order groups	**T_{m2i} (K)**	**Occurrences in DOX (*Ni*)**	**Contribution**
1. CH_2OH	-0.3489	1	-0.3489
2. $CH_{cyc}-CH_3$	-0.1326	1	-0.1326
3. $CH_{cyc}-OH$	1.3691	1	1.3691
4. $CH_{cyc}-O-$	-0.3978	2	-0.7956
5. $C_{cyc}-OH$	0.7334	1	0.7334
6. AROMRINGs1s4	0.9840	1	0.9840
	$\sum_i N_i T_{m2i}$		**1.8094**

Table A.4 Third level group of estimation by using method of Marrero and Gani [21]

Third-order groups	T_{m3i} (K)	Occurrences in DOX (Ni)	Contribution
1. aC-CHn,cyc (fused rings)	-0.5640	2	-1.1280
2. aC-CO-aC	-1.0394	2	-2.0788
$\sum_i N_i T_{m3i}$			**-3.2068**

According to Table A.2 – A.4, the contribution is the product between estimation levels of any groups of type *i*, and occurrences times in molecule of DOX. The summation of 3 level of estimation is approximately 43.4817 K, which will be the right hand side of estimated equation in Table A.1. Normally, this value is used to calculate normal melting point of DOX by using the exponential term of adjustable parameter, (T_{m0}) for the left hand side of equation. Finally, estimated normal melting point is about 556.23 K.

A.2 Estimation of thermodynamic properties of Doxorubicin (DOX) by using Joback and Reid (1984)

The method of Joback and Reid (1984) is an extension of the Lyderson method. Moreover, the Joback and Reid method will extend the range of supported properties, create the new parameters and modify slightly the formulas of the old Lyderson method.

This model will estimate the normal melting point following the simplest form of, by summing up the group contribution equation below:

$$T_m = 122.5 + \sum_i G_i \tag{A.1}$$

where G_i, denote a group contribution, that counts for each single variable group. The procedure of estimation is shown in Table A.5.

Table A.5 Estimation of normal melting point of method of Joback and Reid [30]

Groups	T_m (K)	**Number of groups in DOX**	**Contribution**
Non-ring groups			
$-CH_3$	-5.10	2	-10.20
$-CH_2$	11.27	1	11.27
Ring groups			
$-CH_2-$	7.75	3	23.25
>CH-	19.88	5	99.40
>C<	60.15	1	60.15
=CH-	8.13	3	24.39
=C<	37.02	9	333.18
Oxygen group			
-OH (alcohol)	44.45	3	133.35
-OH (phenol)	82.83	2	165.66
-O- (non-ring)	22.23	2	44.46
-O- (ring)	23.05	1	23.05
>C=O (non-ring)	61.20	1	61.20
>C=O (ring)	75.97	2	151.94
Nitrogen group			
$-NH_2$	66.89	1	66.89
	$\sum_i G_i$		**1,187.99**

From the data in Table A.5, the summation of group contribution product, which represents the estimated normal melting point of DOX, is approximately about 1,188 K. Following the Equation A.1, this group contribution estimated value must be sum up with the adjustable parameter, first term of the right hand side of equation. After that, the estimated melting point is about 1,309.00 K.

APPENDIX B VALIDATION OF ESTIMTION PROPERTIES BETWEEN PREVIUOS AND THIS WORK

As mention in Chapter 3, critical properties of Doxorubicin (DOX) are the most important parameters for predicting the solubility of DOX in supercritical systems, pure carbon dioxide and modified co-solvent. According to the validation of previous work, Phongtummaruk [8], the normal melting point is also used as a referent data by using the method of Marerro and Gani, the more accuracy method due to Appendix A. The detail of estimation is shown in the following 3 levels below.

B.1 First level of estimation

At the first level of estimation, DOX molecule has to be defined as a set of simple functional groups of organic compounds as described in Figure B.1 (a) and (b). The differences of simple functional groups from the previous work are divided into 4 important points as follows.

(1) Firstly, the second (CH_2) and the thirteenth groups (O cyclic) represented in Figure B.1 (a) are recently defined in this work while the previous are not.

(2) Secondly, the sixth group (CCO) of previous work will be rearranged into two simple functional groups in this work due to the meaning of the CCO as a straight chain structure. The new rearranged groups consist of the fourth (aC fused with non-aromatic sub-ring) and fourteenth (CO cyclic) which are quite accuracy than the previous work defined as illustrated in Figure B.1 (b).

(3) Thirdly, the seventh group (C-O) of previous work has to be re-defined as CH-O, the eighth functional group of this work as shown in Figure B.1 (a) and (b), respectively. There is not the simple functional group for defining the C in cyclic bond with oxygen atom. Therefore, the CH-O is the most suitable functional group for this situation.

(4) The last one, the straight chain of amine group (the ninth group of previous work) is re-defined as $CH-NH_2$ in cyclic as shown in the tenth group of Figure B.1 (b).

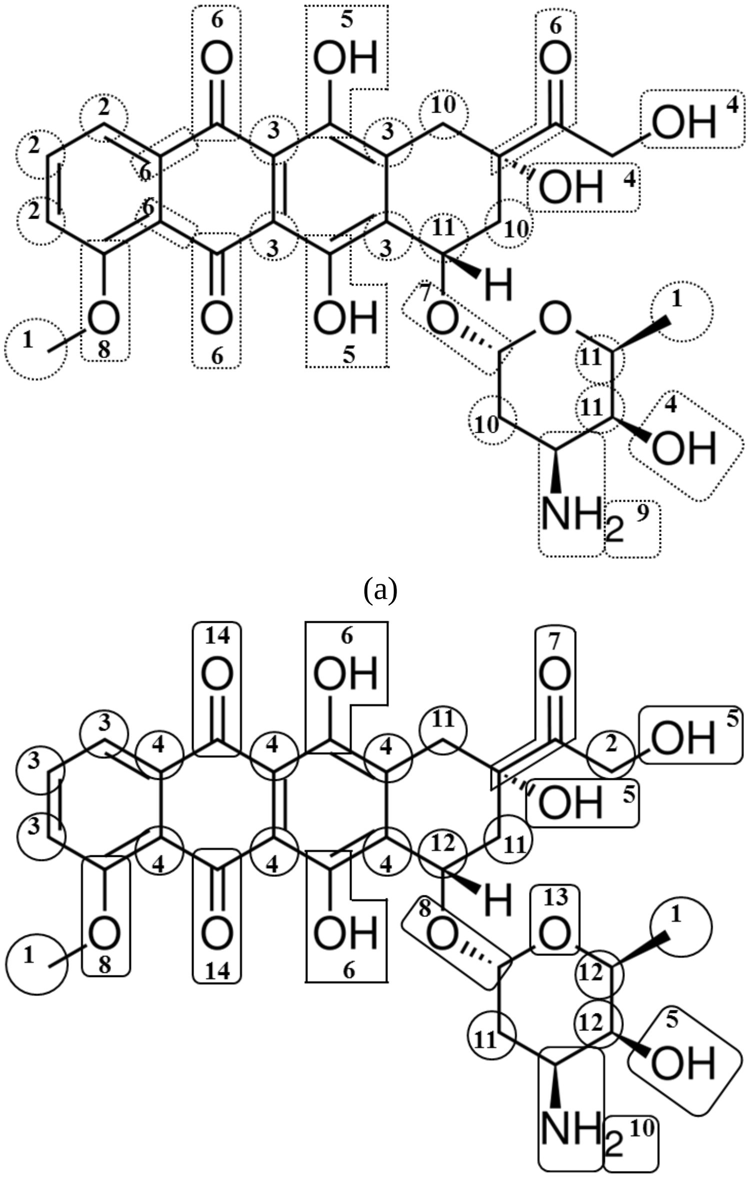

(a)

(b)

Figure B.1 Defined simple functional groups in first level of estimation of DOX molecule (a) previous work of Phongtummaruk and (b) this work

Table B.1 Group contribution parameters of first level of estimation of the previous work of Phongtummaruk [8]

First-order groups	T_{m1i} **(K)**	**Occurrences in DOX molecule (N_i)**	**Contribution**
1. CH_3	0.6953	2	1.3906
2. aCH	0.5860	3	0.7580
3. aC fused with non-aromatic sub-ring	1.2065	4	4.8260
4. OH	2.7888	3	8.3664
5. aC-OH	5.1473	2	10.2946
6. CCO	1.0638	3	3.1914
7. C-O	-0.4446	1	-0.4446
8. aC-O	1.3045	1	1.3045
9. $CH\text{-}NH_2$	30.8394	1	30.8394
10. CH_2 (cyclic)	0.5699	3	1.7097
11. CH (cyclic)	0.0335	3	0.1005
12. C (cyclic)	0.1695	1	1.1695
			63.5060

Table B.2 Group contribution parameters of first level of estimation of this work

First-order groups	T_{m1i} **(K)**	**Occurrences in DOX molecule (N_i)**	**Contribution**
1. CH_3	0.6953	2	1.3906
2. CH_2	0.2515	1	0.2515
3. aCH	0.5860	3	1.7580
4. aC fused with non-aromatic sub-ring	1.2065	6	7.2390
5. OH	2.7888	3	8.3664
6. aC-OH	5.1473	2	10.2946
7. CCO	1.0638	1	1.0638
8. CH-O	0.2461	1	0.2461
9. aC-O	1.3045	1	1.3045
10. $CH\text{-}NH_2$ (cyclic)	3.3478	1	3.3478
11. CH_2 (cyclic)	0.5699	3	1.7097
12. CH (cyclic)	0.0335	3	0.1005
13. O (cyclic)	1.3828	1	1.3828
14. CO (cyclic)	3.2119	2	6.4238
			44.8791

B.2 Second level of estimation

The second level is used for identifying polyfunctional compounds, polar or nonpolar compounds, and also aromatic or cycloaliphatic compounds with only one ring and several substituents.

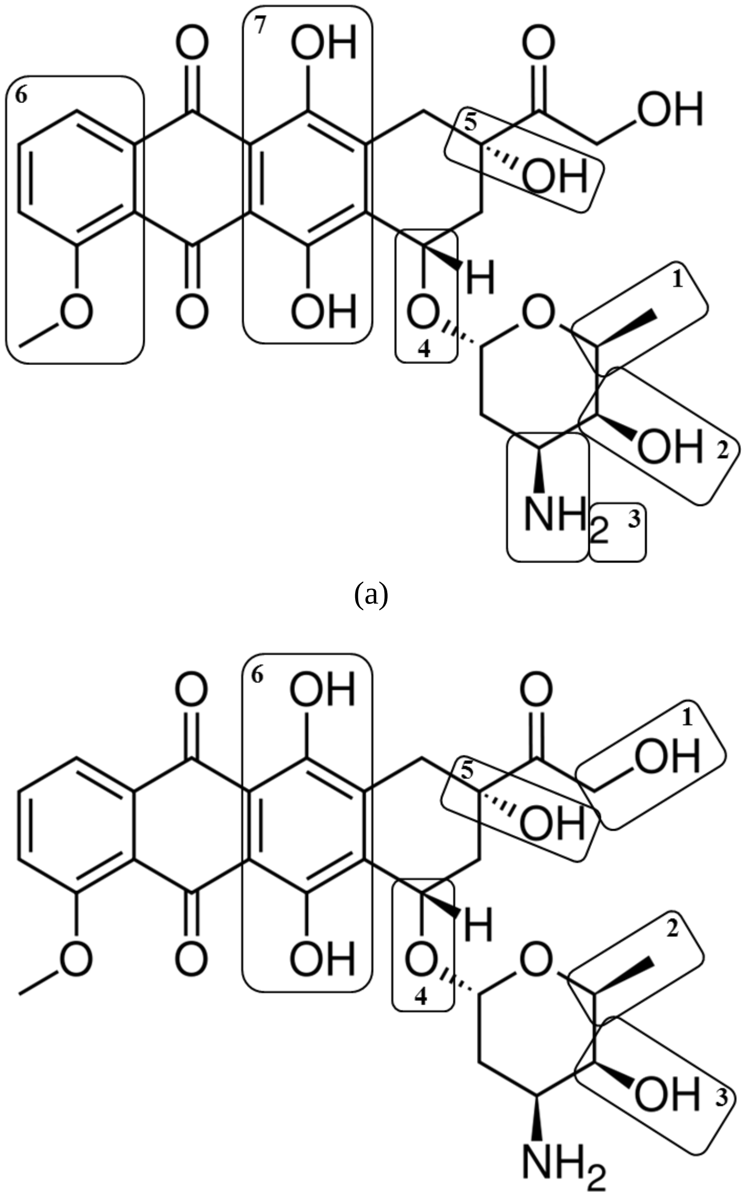

Figure B.2 Defined polyfunctional groups in second level of estimation of DOX molecule (a) previous work of Phongtummaruk and (b) this work

Table B.3 Group contribution parameters of second level of estimation of the previous work of Phongtummaruk

Second-order groups	T_{m2i} **(K)**	**Occurrences in DOX molecule (N_i)**	**Contribution**
1. CH_{cyc}-CH_3	-0.1326	1	-0.1326
2. CH_{cyc}-OH	1.3691	1	1.3691
3. CH_{cyc}-NH_2	1.5069	1	1.5069
4. CH_{cyc}-O-	-0.3978	1	-0.3978
5. C_{cyc}-OH	0.7334	1	0.7334
6. AROMRINGs1s2s3	-0.2762	1	-0.2762
7. AROMRINGs1s4	1.7722	1	1.7722
			4.2261

Table B.4 Group contribution parameters of second level of estimation of this work

Second-order groups	T_{m2i} **(K)**	**Occurrences in DOX molecule (N_i)**	**Contribution**
1. CH_2OH	-0.3489	1	-0.3489
2. CH_{cyc}-CH_3	-0.1326	1	-0.1326
3. CH_{cyc}-OH	1.3691	1	1.3691
4. CH_{cyc}-O-	-0.3978	2	-0.7956
5. C_{cyc}-OH	0.7334	1	0.7334
6. AROMRINGs1s4	0.9840	1	0.9840
			1.8094

According to Figure B.2 (a) and (b), there are the important 3 different points between this work and previous work as follows:

(1) Due to the non-defined CH_2 group in the first level of previous work as described in the previous topic, therefore polyfuctional group of primary alcohol (CH_2OH) is defined as the first group of this work.

(2) According to the fourth difference in first level of estimation between the previous work and this work, third group (CH_{cyc}-NH_2) in the previous work is not necessary to defined in this work.

(3) The meaning of AROMRINGs1s2s3 is 3 substituents along aromatic ring. Then, the sixth group defined in previous work fails to define. However, this group completely defined as methyl phenyl ether (aC-O) in the eighth group of previous work at first level of estimation. On the other hand, this work defined the secondary butyl ether (CH-O) instead of the methyl phenyl ether (aC-O) group which is less accuracy comparing to the previous defined.

B.3 Third level of estimation

Since, the second-order groups are unable to provide a good representation of compounds containing more than one ring in some cases as well as. The third level is required to allow a better description of these types of compounds.

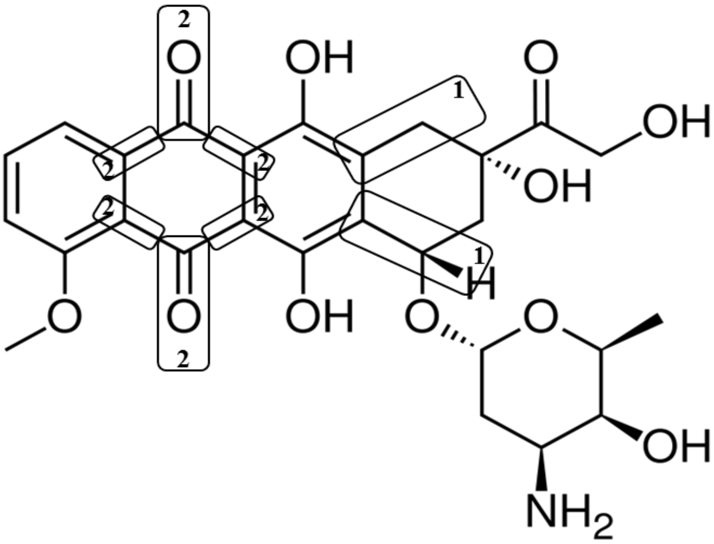

Figure B.3 Defined in polycyclic groups in third level of estimation of DOX molecule in this work

Table B.5 Group contribution parameters of third level of estimation of this work

Third-order groups	**T_{m3i} (K)**	**Occurrences in DOX molecule (N_i)**	**Contribution**
1. aCH-CH$_{n,cyc}$	-0.5640	2	-1.1280
2. aC-CO-aC	-1.0394	2	-2.0788
			-3.2068

This level is well-defined in this work only for indicating bonding of polycyclic compound. As can be seen in the second level of estimation, substituents groups are specified in both chain and cyclic part. Two chains of cyclic consisting of aCH-CH$_{n,cyc}$ and aC-CO-aC are defined.

APPENDIX C PARAMETERS ESTIMATION

C.1 Estimation of normal boiling point and critical properties of DOX by using method of Marrero and Gani [21]

The procedure of calculating, normal boiling point, critical temperature, and critical pressure, is same as the estimating the normal melting point in section A.1. By the way, the function of target property x on the left hand side of the equation (2.17), $f(x)$ and adjustable parameters are list in Table C.1.

Table C.1 The property function, group contribution term and adjustable parameter of normal boiling point, critical temperature, and critical pressure estimation

Properties	**Simple function** ***f(x)***	**Group Contribution term**	**Adjustable parameter**
Normal boiling point (T_b)	$exp(T_b/T_{b0})$	$\sum_i N_i T_{b1i} + \sum_j M_j T_{b2j} + \sum_k O_k T_{b3k}$	T_{b0} = 222.543 K
Critical temperature (T_c)	$exp(T_c/T_{c0})$	$\sum_i N_i T_{c1i} + \sum_j M_j T_{c2j} + \sum_k O_k T_{c3k}$	T_c = 231.239 K
Critical pressure (P_c)	$(P_c-P_{c1})^{-0.5}-P_{c2}$	$\sum_i N_i P_{c1i} + \sum_j M_j P_{c2j} + \sum_k O_k P_{c3k}$	P_{c1} = 5.9827 bar P_{c2} = 0.108998 bar$^{-0.5}$

The procedure of 3 levels of estimation is shown in Table C.2 – C.4 below.

Table C.2 First level group of estimation normal boiling point critical temperature, and critical pressure by method of Marrero and Gani [21]

First-order groups	**Occurrences in DOX (*Ni*)**	T_{b1i} **(K)**	T_{c1i} **(K)**	P_{c1i} **(bar)**
1. CH_3	2	0.8491	1.7506	0.018615
2. CH_2	1	0.7141	1.3327	0.013547
3. aCH	3	0.8365	2.0337	0.007260
4. aC fused with non-aromatic sub-ring	6	1.1995	3.1058	0.006512
5. OH	3	2.5670	5.2188	-0.005401
6. aC-OH	2	3.3205	9.3472	-0.008788
7. CCO	1	1.7287	0	0
8. CH-O	1	0.8924	0.7889	0.014487
9. aC-O	1	1.8522	3.6588	0.005115
10. CH-NH_2 (cyclic)	1	2.0315	4.2847	0.130490
11. CH_2 (cyclic)	3	0.8234	1.8815	0.009884
12. CH (cyclic)	3	0.5946	1.1020	0.007596
13. O (cyclic)	1	1.0245	2.7409	-0.000387
14. CO (cyclic)	2	2.8793	12.6396	-0.000207

Table C.3 Second level group of estimation normal boiling point, critical temperature, and critical pressure by method of Marrero and Gani [21]

Second-order groups	**Occurrences in DOX (*Ni*)**	T_{b2i} **(K)**	T_{c2i} **(K)**	P_{c2i} **(bar)**
1. CH_2OH	1	-0.2825	-0.6768	0.000246
2. CH_{cyc}-CH_3	1	-0.1210	-0.1233	0.000779
3. CH_{cyc}-OH	1	-0.3179	0.8973	0.004640
4. CH_{cyc}-O-	2	-0.2787	0	0
5. C_{cyc}-OH	1	-0.6775	-2.1303	-0.004683
6. AROMRINGs1s4	1	0.1007	0.0803	0.000467

Table C.4 Third level group of estimation normal boiling point, critical temperature, and critical pressure by using method of Marrero and Gani [21]

Third-order groups	**Occurrences in DOX (*Ni*)**	T_{b3i} **(K)**	T_{c3i} **(K)**	P_{c3i} **(bar)**
aC-CHn,cyc (fused rings)	2	-0.1736	0.5060	-0.003746
aC-CO-aC	2	1.0171	-0.2678	-0.001837

Table C.5 Estimated normal boiling point, critical temperature, and critical pressure by using method of Marrero and Gani [21]

Estimation Level	**Summation of each group contribution properties**		
	Normal boiling point (T_b)	**Critical temperature (T_c)**	**Critical pressure (P_c)**
First	44.0027	109.6236	0.2796
Second	-1.8556	-1.9528	0.0014
Third	-1.6870	0.4764	-0.0112
Total	43.8341 K	108.1472 K	0.2699 bar
Estimation value	841.30 K	1,083.01 K	12.95 bar

Tables C.2 – C.4 show the group-contribution of type *i*, and number of times in DOX molecule, while Table C.5 represents the summation of product between the two mention values for each level of estimation. Moreover, the Table C.5 also represents the summation of each estimation level of all properties, which are 43.8341 K, 108.1472 K, and 0.2699 bars for normal boiling point, critical temperature, and critical pressure, respectively. These estimation values will be the right hand side, while the simple function including the adjustable parameter for each property is the other side of equation. Then, the estimated value of normal boiling point, critical temperature, and critical pressure will be computed. The values are 841.30 K, 108.01 K, and 12.95 bars, respectively.

C.2 Molar volume

The solid density of DOX is calculated by the method of Lyman [29] as shown in Equation C.1. Calculated crystal volume of a single molecule (V_S), a summation of atomic volume (V_i), are shown and listed in Table C.6.

$$\rho_s = 1.66 \frac{MW}{V_s} \tag{C.1}$$

where ρ_s denotes solid density (g/cm^3), MW is molecular weight of DOX molecule, and V_s is the calculated crystal volume of a single molecule ($\dot{A}^3$/molecule).

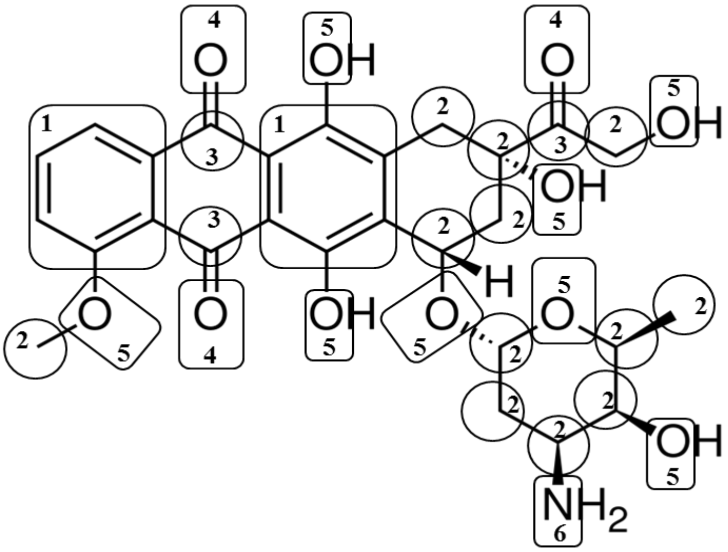

Figure C.1 Estimation of molar volume of pure solid base on Lyman method

Table C.6 Simple group, number of each group in DOX molecule, and volume increment (ΔV) for estimating solid density based on Lyman method

Groups	Occurrences in DOX molecule (*Ni*)	V_i ($\dot{A}^3$)	V_s ($\dot{A}^3$/molecule)
1. C benzene ring	2	75.2	150.4
2. >C<	12	15.3	183.6
3. =C<	3	13.7	41.1
4. =O	3	11	33
5. -O-	8	9.2	73.6
6. –N<	1	7.2	7.2
7. Hydrogen	29	6.9	200.1
			689

C.3 Vapor pressure

The vapor pressure is estimated according to these following equations [29]:

$$lnP_s^{sub} = \frac{\Delta H_{vb}}{\Delta z_b RT_b}\left[1 - \frac{\left(3 - 2T_{\rho b}\right)^m}{T_{\rho b}} - 2m\left(3 - 2T_{\rho b}\right)^{m-1} lnT_{\upsilon b}\right] \qquad \text{(C.2)}$$

$$\frac{\Delta H_{vb}}{T_b} = K_F\left(8.75 + RlnT_b\right) \qquad \text{(C.3)}$$

$$T_{\rho b} = \frac{T}{T_b} \qquad \text{(C.4)}$$

where P_s^{sub} is vapor pressure (atm), ΔH_{vb} denotes heat vaporization at the normal boiling point (cal/mol), Δz_b is compressibility factor at the normal boiling point, R is gas constant, T_b represents temperature of the normal boiling point (K) obtained from Group Contribution base estimate method of Marerro and Gani [21], T is temperature (K), and K_F is the constant for aromatic hydrogen bond systems.

Steps for vapor pressure estimation

1. Obtain T_b (K) from the experimental data or estimation method
2. Obtain K_F (assume K_F equals to 1.06 for DOX)
3. Set m as a constant value following these cases:

   For liquids

   m equals to 1.09

   For solid

   if $T_{\rho b} > 0.6$ m equals to 0.36

   if $0.5 > T_{\rho b} > 0.6$ m equals to 0.8

   if $T_{\rho b} < 0.5$ m equals to 1.19
4. Calculate $\frac{\Delta H_{vb}}{T_b}$ from Equation C.3 (R is set to be 1.987 cal/mol.K)
5. Assume Δz_b to be 0.97
6. Calculate and take anti-log to obtain the vapor pressure, P_s^{sub}, from Equation C.2

C.4 Liquid density

The liquid density of DOX is calculated by the method of Grain [27] as shown in Equation C.5. The Schroeder volume increments (V_b) are listed in Table C.7 below.

$$\rho_L = MW \frac{1}{V_b}\left(3-2\frac{T}{T_b}\right)^n \tag{C.5}$$

which ρ_L denotes liquid density (g/mL), MW is molecular weight of DOX, V_b is incremental values for estimating molar volume by Schroeder's method (cm^3/g), T represents temperature (K), T_b is temperature of the normal boiling point (K) obtained from Group Contribution base estimate method of Marerro and Gani [21], and n is number of mole depending on chemical class (DOX is assigned as other organics which n equals to 0.31).

Table C.7 Molecular feature, number of each feature in DOX molecule, and incremental values (V_b) for estimating molar volume based on Schroeder's method

Molecular feature	**Occurrences in DOX molecule (*Ni*)**	**V_b (cm^3/g)**	**Summation**
Atom			
1. C	27	7	189
2. H	29	7	203
3. N	1	7	7
4. O	7	11	77
Ring	5	-7	-35
Double bonds	9	7	63
			504

C.5 Surface tension

Surface tension can be estimated by Grain's method [27] as shown in Equation C.6.

$$\sigma = \left[\frac{P(1+k)}{V_b}\left(3-2\frac{T}{T_b}\right)^n\right]^4 \tag{C.6}$$

Where σ represents surface tension (dynes/cm), P is Parachor presented by Quayle, V_b denotes molar volume at the normal melting point (cm^3/mol), T represents temperature (K). DOX is assigned to class of other organic, therefore, k and n equals to 0 and 0.31, respectively.

Quayle presented a comprehensive review of methods for estimating the Parachor and devised one that is suitable for a wide variety of organic compound as shown in Table C.8 below.

Table C.8 Simple groups for Parachoe estimation, number of each group in DOX molecule, and Parachor incremental for estimating molar volume based on Schroeder's method

Molecular feature	**Occurrences in DOX molecule (*Ni*)**	**V_b (cm^3/g)**	**Summation**
1. C	27	9	243
2. H	23	15.5	356.5
3. H-OH	5	10	50
4. H-NH	1	12.5	12.5
5. N	1	17.5	17.5
6. O	11	19.8	217.8
7. Double bond	7	19.1	133.7
8. 6 member rings	5	0.8	4
Position in benzene ring			0
9. Ortho-meta	3	2.6	7.8
10. Ortho-para	1	2.9	2.9
			1,045.7

CURRICULUM VITAE

NAME	Miss Ploypetch Prissawong
DATE OF BIRTH	12 May 1987
EDUCATIONAL RECORD	
HIGH SCHOOL	High School Graduation Mahavajiravudh School, 2006
BACHELOR’S DEGREE	Bachelor of Engineering (Chemical Engineering) King Mongkut’s University of Technology Thonburi 2009
MASTER’S DEGREE	Master of Engineering (Chemical Engineering) King Mongkut’s University of Technology Thonburi, 2011